

Air Force Institute of Technology

**AFIT Scholar**

---

Theses and Dissertations

Student Graduate Works

---

3-3-2004

## Structural Design and Analysis of a Rigidizable Space Shuttle Experiment

Raymond G. Holstein III

Follow this and additional works at: <https://scholar.afit.edu/etd>



Part of the [Dynamics and Dynamical Systems Commons](#), and the [Structures and Materials Commons](#)

---

### Recommended Citation

Holstein, Raymond G. III, "Structural Design and Analysis of a Rigidizable Space Shuttle Experiment" (2004). *Theses and Dissertations*. 3926.  
<https://scholar.afit.edu/etd/3926>

This Thesis is brought to you for free and open access by the Student Graduate Works at AFIT Scholar. It has been accepted for inclusion in Theses and Dissertations by an authorized administrator of AFIT Scholar. For more information, please contact [AFIT.ENWL.Repository@us.af.mil](mailto:AFIT.ENWL.Repository@us.af.mil).



**STRUCTURAL DESIGN AND ANALYSIS OF A RIGIDIZABLE SPACE  
SHUTTLE EXPERIMENT**

THESIS

Raymond G Holstein III, Captain, USAF  
AFIT/GAE/ENY/04-M08

**DEPARTMENT OF THE AIR FORCE  
AIR UNIVERSITY**

**AIR FORCE INSTITUTE OF TECHNOLOGY**

**Wright-Patterson Air Force Base, Ohio**

APPROVED FOR PUBLIC RELEASE; DISTRIBUTION UNLIMITED

The views expressed in this thesis are those of the author and do not reflect the official policy or position of the United States Air Force, Department of Defense, or the United States Government.

AFIT/GAE/ENY/04-M08

**STRUCTURAL DESIGN AND ANALYSIS OF A RIGIDIZABLE SPACE  
SHUTTLE EXPERIMENT**

**THESIS**

Presented to the Faculty

Department of Aeronautics and Astronautics

Graduate School of Engineering and Management

Air Force Institute of Technology

Air University

Air Education and Training Command

In Partial Fulfillment of the Requirements for the  
Degree of Master of Science in Aeronautical Engineering

Raymond G Holstein III, BSE

Captain, USAF

March 2004

APPROVED FOR PUBLIC RELEASE; DISTRIBUTION UNLIMITED

**STRUCTURAL DESIGN AND ANALYSIS OF A RIGIDIZABLE SPACE  
SHUTTLE EXPERIMENT**

Raymond G Holstein III, BSE  
Captain, USAF

Approved:

Signed  
\_\_\_\_\_  
Prof. Anthony N. Palazotto (Chairman)

03Mar04  
\_\_\_\_\_  
date

Signed  
\_\_\_\_\_  
Major Richard G. Cobb (Member)

03Mar04  
\_\_\_\_\_  
date

Signed  
\_\_\_\_\_  
Prof. Richard A. Raines (Member)

03Mar04  
\_\_\_\_\_  
date

## **Abstract**

AFIT is in the process of designing a Space Shuttle experiment designated as the Rigidized Inflatable Get-Away-Special Experiment (RIGEX) to study the effects of microgravity on the deployment of rigidizable composite structures. Once in space, the experiment will inflate and rigidize three composite structures and perform a vibration analysis on each by exciting the tubes using piezoelectric patches and collecting data via an accelerometer.

This paper presents the structural and vibration analysis of the RIGEX assembly and inflatable composite tubes using ABAQUS Finite Element Analysis (FEA) software. Comparison of the analysis has been carried out with Eigenvalue/Eigenvector experimentation by means of ping testing. This FEA analysis has been used to verify the natural frequency and structural integrity of the RIGEX support assemblies. The ABAQUS FEA results correlated to within 20% of experimental values.

## **Acknowledgements**

I would like to express my sincere appreciation to my thesis advisor, Dr Anthony Palazotto, for his patience, guidance, and cool demeanor throughout this project. I would also like to thank Major Richard Cobb for his assistance in the lab and his indispensable insight into vibration analysis. What can I say about Dr Jacques? If it wasn't for his encouragement and leadership, I would not have made it this far. Thanks goes out to the folks at the AFIT model shop for all the time and effort they put into getting "one more modification" onto the structure. I would also like to express my appreciation to Mark Haney, for his willingness to answer an endless stream of ABAQUS modeling questions and for always being there to offer recommendations and guidance.

Additionally, I could not have made it through this project without the support of my friends, namely Brian Lutz, my colleagues, Steve Lindemuth and David Moody, and my family, but especially my wife for her patience and understanding. Thank you all for your support and encouragement; it has been the difference in this endeavor.

Raymond G. Holstein

## Table of Contents

	Page
Abstract .....	iv
Acknowledgements .....	v
List of Figures .....	viii
List of Tables .....	xi
I: Introduction .....	1
Background .....	1
Scope of Project .....	3
RIGEX Background .....	4
Research Objectives .....	5
Methodology .....	6
Assumptions .....	7
Summary of Thesis .....	8
II: Literature review .....	9
Overview .....	9
Finite Element Method .....	10
ABAQUS Software .....	12
ABAQUS Applications .....	15
Previous Research on Inflatable Tube Vibration and Modal Testing .....	18
Dynamic Analysis of Beams .....	19
NASA Get Away Special Experiments .....	24
Payload Considerations .....	26
Design and Testing Requirements .....	26
Summary .....	28
III: Experiment Methodology .....	30
Overview .....	30
Structural Design Considerations .....	31
ABAQUS Vibration Modeling and Simulation .....	33
Rigidized Tube Model .....	33
Quarter Structure Model .....	39
Full Structure Model .....	43
Dynamic Stress Analysis on Full Model .....	48
Design and Manufacturing .....	49
IV: Results and Discussion .....	52



	Page
Overview .....	52
ABAQUS Vibration Results .....	52
Rigidized Tube Model Results.....	53
Quarter Structure Model Results .....	65
Full Structure Model Results .....	70
Dynamic Stress Analysis of the Full Structure .....	80
V: Conclusions and Recommendations .....	89
ABAQUS Frequency Evaluation.....	89
ABAQUS Stress Evaluation .....	90
Recommendations .....	91
Appendix A. Fundamental Frequency Calculations .....	93
Appendix B. RIGEX Structural Drawings.....	94
B.1 Eleven-Inch Plate .....	94
B.2 Thirteen-Inch Plate .....	95
B.3 Bottom Plate .....	96
B.4 Top Plate.....	97
B.5 Top Plate (Camera Mount Hole Detail) .....	98
B.6 Battery Plate .....	99
Appendix C. Additional Tube Models .....	100
C.1 Tube with two bolt boundary condition.....	100
C.2 Tube with 35 gram accelerometer.....	102
Appendix D. Ping Test Results .....	104
D.1 Ping Test Results for Rigidized Tube .....	104
D.2 Ping Test Results for Quarter Structure .....	106
D.3 Ping Test Results for Full Structure (Empty) .....	107
Bibliography.....	108
Vita.....	111

## List of Figures

	Page
Figure 1. Inflatable Antenna Experiment .....	2
Figure 2. RIGEX Shuttle Integration.....	4
Figure 3. RIGEX Preliminary Design.....	5
Figure 4. FEM Mesh.....	11
Figure 5. Pitch-Hinge Assembly.....	16
Figure 6. FUSE Collimator .....	17
Figure 7. Linear Spring Constants .....	21
Figure 8. Cantilever Beam with Mass on Free End .....	22
Figure 9. GAS Experiment Configuration.....	25
Figure 10. Experiment Mounting Plate.....	32
Figure 11. Inflatable Tubes .....	35
Figure 12. ABAQUS Tube Construction.....	36
Figure 13. ABAQUS Continuum Elements .....	37
Figure 14. Tube with Simply Supported Boundary Condition.....	38
Figure 15. Tube with Clamped Boundary Condition.....	38
Figure 16. Quarter Structure Model and Actual Quarter Structure .....	39
Figure 17. Quarter Structure Mounting Configuration to EMP.....	40
Figure 18. ABAQUS Bending Mode 1 for Quarter Structure .....	41
Figure 19. Accelerometer Tip Location on Quarter Structure .....	42
Figure 20. Accelerometer mid span location on quarter structure .....	42
Figure 21. RIGEX Structure .....	44

	Page
Figure 22. ABAQUS representation of RIGEX Structure .....	45
Figure 23. Laser Vibrometer and Meshed Plates .....	46
Figure 24. Ping Test Hammer Location.....	47
Figure 25. Ping Test Hammer.....	47
Figure 26. Bumper Assembly .....	51
Figure 27. ABAQUS Beam Model.....	54
Figure 28. 1 <sup>st</sup> Bending Mode of the Beam Model .....	55
Figure 29. 1 <sup>st</sup> Bending Mode of the Beam Model about Axis 2 .....	56
Figure 30. 2 <sup>nd</sup> Bending Mode of the Beam Model about Axis 2 .....	57
Figure 31. 2 <sup>nd</sup> Bending Mode of the Beam Model about Axis 3 .....	58
Figure 32. Coarse and Fine Mesh for 1 <sup>st</sup> Bending Mode of Tube Model.....	60
Figure 33. Coarse and Fine Mesh for 1 <sup>st</sup> Bending Mode of Tube Model about Axis 1 ...	61
Figure 34. Coarse and Fine Mesh for 2 <sup>nd</sup> Bending Mode of Tube Model about Axis 2...	62
Figure 35. Coarse and Fine Mesh for 2 <sup>nd</sup> Bending Mode of Tube Model about Axis 1 ...	63
Figure 36. Coarse and Fine Mesh for Mode 1 of Quarter Structure .....	66
Figure 37. Coarse and Fine Mesh for Mode 2 of Quarter Structure .....	67
Figure 38. Coarse and Fine Mesh for Mode 3 of Quarter Structure .....	68
Figure 39. Three-Dimensional ABAQUS Full Structure Model.....	71
Figure 40. Mode 1 for the Two-Dimensional Model of the RIGEX Structure.....	73
Figure 41. Mode 2 for the Two-Dimensional Model of the RIGEX Structure.....	74
Figure 42. Mode 1 for the Three-Dimensional Model of the RIGEX Structure.....	75
Figure 43. Mode 2 for the Three-Dimensional Model of the RIGEX Structure.....	76

Figure 44. Mode 1 for the Massed Three-Dimensional Model of the RIGEX Structure .	77
Figure 45. Mode 2 for the Massed Three-Dimensional Model of the RIGEX Structure .	78
Figure 46. 15G Loading on Two-Dimensional Model .....	81
Figure 47. Deformed Structure under 15G Load .....	82
Figure 48. Worst Case Loading for 15G Load .....	83
Figure 49. Detail 1 of Worst Case Loading for 15G Load .....	84
Figure 50. Detail 2 of Worst Case Loading for 15G Load .....	85
Figure 51. Worst Case Loading for 20G Load .....	86
Figure 52. Detail 1 of Worst Case Loading for 20G Load .....	86
Figure 53. Detail 2 of Worst Case Loading for 20G Load .....	87
Figure 54. Detail 3 of Worst Case Loading for 20G Load .....	87

## List of Tables

Table	Page
Table 1. Principal GAS Constraints .....	7
Table 2. Inflatable Tube Properties.....	19
Table 3. Fundamental Frequency Formulas.....	24
Table 4. Preliminary Weight Analysis .....	26
Table 5. GAS Structural Verification Requirements .....	27
Table 6. GAS Structural Verification Testing .....	28
Table 7. Results of the Beam and Three-Dimensional Tube Model.....	64
Table 8. Results of the Quarter Structure Frequency Analysis.....	69
Table 9. Results of the Full Structure Frequency Analysis .....	79
Table 10. Stress Analysis Results .....	88

# STRUCTURAL DESIGN AND ANALYSIS OF A RIGIDIZABLE SPACE SHUTTLE EXPERIMENT

## **I: Introduction**

### **Background**

In an effort to deploy larger and more complicated space assets, the DoD NASA and the commercial sector have begun research to develop a more practical, reliable and inexpensive method of inserting these assets into orbit. Inflatable structures offer substantial weight savings over conventional mechanical structures, and would require approximately 1/10 of the payload volume of a traditional structure for antenna reflectors (11). Substantial reductions in both volume and weight allows for smaller launch vehicles, which translates to marked savings in launch cost.

Inflatable technology has been neglected in the past. Lack of funding and interest have kept the technology in its infancy; however, the enormous potential benefits in cost, weight and volume savings have renewed research in this area. Inflatables also allow for optics on a scale not possible with traditional structures. Rigidizable inflatable structures are not required to maintain internal pressure because they become rigid after inflation. As a result, inflatable rigidizables have an advantage over pure inflatables because if they are pierced by micro meteors or collide with orbiting debris, they will not deflate and thus can be considered a more robust structural member. Figure 1 shows the deployment of the Inflatable Antenna Experiment (IAE) in space.

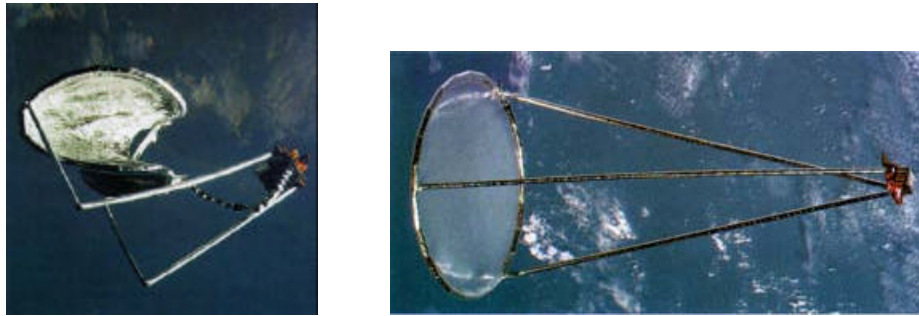


Figure 1. Inflatable Antenna Experiment

Inflatables can be used for many different applications in the space environment including: sunshades for space telescopes, precision booms, optical telescope mirrors, planetary rovers, and extremely light weight solar cells, to name a few. Space-based platforms requiring large aperture sizes, such as those systems employed by the Intelligence Surveillance and Reconnaissance (ISR) community stand to benefit greatly from inflatable technology. The performance of these systems has been limited by the substantial size and weight of their rigid mirrors and associated supporting structure, all of which must conform to the payload capabilities of the launch platform.

Rigidized Inflatable Get-Away-Special Experiment (RIGEX) is designed to develop a correlation between ground based testing of inflatable rigidizable structures with data collected on inflatables deployed under the temperature, pressure and micro-gravity conditions of space. While the effects of temperature and pressure can be studied on the ground, there is no means for effectively measuring the effects of micro gravity, not to mention the simultaneous combination of all three on deployment and rigidization of the tubes. A better understanding of the effects these elements play on the deployment

of inflatable structures will provide valuable insight into the design of future inflatable rigidizable structures.

### **Scope of Project**

The goal of the RIGEX Inflatable Get-Away-Special (GAS) Experiment is to validate ground tests of the deployment, rigidization and vibration analysis of a collapsible inflatable tube in the space environment. The RIGEX GAS Experiment will be mounted in a canister inside the space shuttle cargo bay. When the shuttle is in orbit, the GAS Experiment will be exposed to the vacuum, temperature and micro gravity of space throughout the heating, deployment, rigidization and vibration analysis.

The goal of this thesis is to provide a structural analysis through the use of ABAQUS Finite Element Modeling for the design, manufacturing and testing of the RIGEX support assembly. Furthermore, the analysis is compared to vibrational frequency structural response. The RIGEX structural assembly will be modeled based on the preliminary design of John D. DiSebastian III (10) from August 2000 through March 2001 and Thomas G. Single (26) from August 2001 through March 2002, with the goal of reducing the overall structural weight by 10 percent, maintaining NASA GAS structural safety requirements and providing for the accommodations of all necessary experimental components.



## RIGEX Background

The groundwork for RIGEX began in 2001, with the preliminary design of a project capable of safely delivering an experiment into space aboard the shuttle (10). Once in orbit, it would collect data on the inflation, rigidization and modal analysis of compact composite tubes. Follow-on work focused on ground testing of the composite tubes using beam theory to predict natural frequencies and mode shapes of the rigidized tubes (26). This effort encountered difficulties due to limitations in simple beam theory. Figure 2 shows how RIGEX will be integrated on the space shuttle, and Figure 3 depicts the preliminary design of the RIGEX structure and experiment assemblies.



Figure 2. RIGEX Shuttle Integration

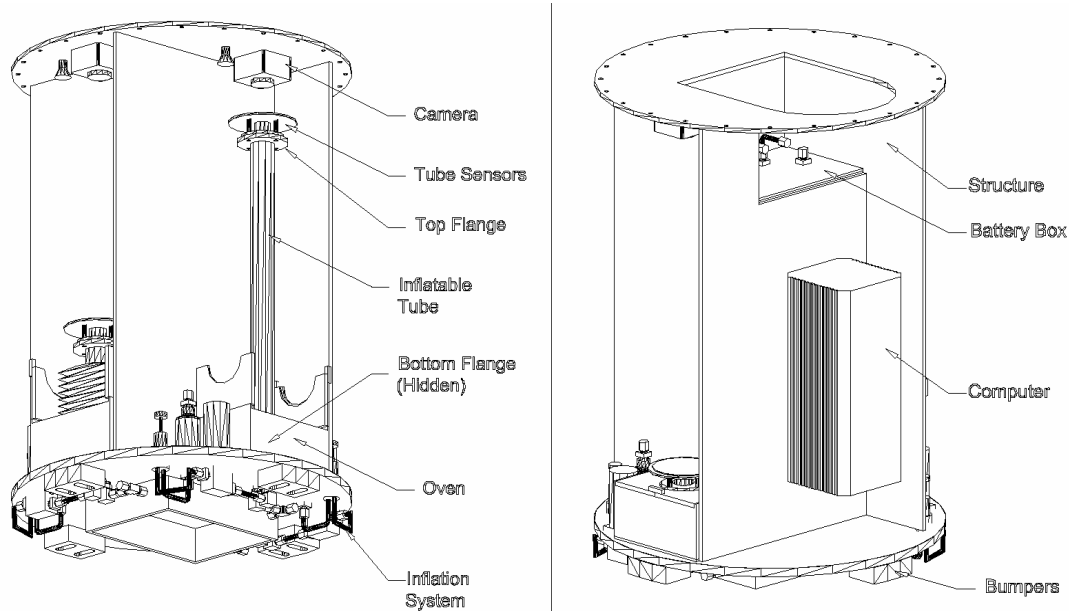


Figure 3. RIGEX Preliminary Design (10)

In 2002, research was done to improve the design of the ovens, which are used to heat the tubes before inflation. The latest work done on RIGEX was performed in 2003 by Thomas Philley (25), who conducted tests on the heating and inflation of the tubes in a scaled-down test structure. Philley also conducted vibration tests on the rigidized tubes to characterize their first three natural frequencies and mode shapes with various types of boundary conditions applied to the tubes.

## Research Objectives

The overall mission objective of the RIGEX is:

*To verify and validate ground testing of inflation and rigidization methods for inflatable space structures against a zero-gravity environment.*

The specific objective of this research effort is to produce an accurate Finite Element representation of the RIGEX support structure for the purpose of manufacturing and testing a flight-worthy article capable of housing the RIGEX experimental components. The Finite Element model will be used to verify the natural frequency of the structure and to determine structural loading on the support assembly, representative of the loads to be encountered at shuttle lift-off and landing.

## **Methodology**

In order to build an accurate Finite Element Model (FEM) of the overall RIGEX support structure, we want to first construct a three dimensional deformable model of an inflated and rigidized tube assembly for which we have experimental vibration test results from a previous thesis (25 and 26). The purpose of this model is two-fold, first it will provide a good training tool for modeling a simple structure and secondly the results should give an indication of how well ABAQUS frequency analysis results correlate with test results previously obtained and characterize the tubes material properties. The second step in obtaining an accurate FEM of the RIGEX structure will be to construct an accurate ABAQUS model of the quarter structure which was manufactured for ground testing of a single tube inflation system. Once modeled, a frequency analysis can be performed on the quarter model and the results compared to ping tests on the existing structure. Finally the entire structure will be modeled in ABAQUS and both frequency and stress analysis simulations run to verify NASA structural safety requirements have been meet.

## Assumptions

The primary design constraints for a GAS experiment are defined in the Shuttle Small Payloads Project Office (SSPPO) experimenter's handbook (23). These requirements must be met in order to allow for experiment integration into the NASA GAS canister. Table 1 contains a list of the principal experiment constraints.

Table 1. Principal GAS Constraints (10)		
Constraint	Limit	Imposed by:
Weight	200 lbs	NASA
Size	19.75 inches (diameter)	NASA
	28.25 inches (height)	NASA
Payload Volume	5 cubic feet	NASA

In addition to these overall limitations on experiment size and weight, experimenters are required to conduct additional structural verification of the experiment support structure in accordance with NASA requirements:

Structure materials used in the construction of the primary load bearing assembly, as well as structural fasteners, are of primary concern in regards to stress corrosion cracking; therefore, these materials must meet NASA requirements. Materials listed in Table 1 of MSFC-SPEC-522 are in full compliance with NSTS 1700.7, Safety Policy and Requirements for Payloads Using the Space Transportation System.

The following assumptions will be used in the development of the structural design and modeling of the RIGEX structure: clamp constraint for back of Experiment Mounting Plate (EMP) to simulate experiment connection to GAS canister, experimental components modeled as rigid masses of approximate dimension, structural plates are tied at nodes to represent welds of aluminum plates, and composite material modeled as

isotropic for modeling purposes. Fracture control will not be considered because we will not be employing a motorized door assembly equipped GAS canister.

## **Summary of Thesis**

In the subsequent chapters, the design and fabrication of the RIGEX support assembly as well as the Finite Element Modeling and testing is presented. Chapter 2 gives a brief outline of Finite element theory with respect to ABAQUS and outlines some of the analysis applications for which ABAQUS has been used. Procedures for building the finite element models and testing the results are discussed in Chapter 3. Chapter 4 presents the results of the FE analysis and compares them to experimental test values. The first models will be made on the inflatable rigidizable tube and the quarter test structure to validate the ABAQUS model and assumptions followed by the analysis on the full support structure. Finally, conclusions and recommendations for future work are presented in Chapter 5.

## **II: Literature review**

### **Overview**

Inflatable structures are light, compact deployable structures that come in two varieties, rigidizable and purely inflatable. The difference in the two is that the purely inflatable requires internal pressure to maintain the rigidity of the structures, where the inflatable rigidizable requires heat to change the material properties of the two to make the tube pliable for inflation, but once inflated and solidified it requires no external means to maintain its shape.

Previous work has been done to model the rigidized inflatable tubes using classical beam theory and modal analysis. Since the inflatable tubes are a composite structure composed of a carbon fiber tube with aluminum flanges inserted into each end, the tube cannot be considered homogeneous and is therefore more difficult to model.

The Finite Element Method is used to determine the static and dynamic behavior of complex geometries and assemblies by breaking them down into small elements and employing computers to solve for variance in a field parameter across the element. There are many different brands of Finite Element software currently on the market. ABAQUS is a widely employed Finite Element software tool that combines the flexibility and power of Finite Element Analysis with the ease of modeling using a built-in job preprocessor.

## **Finite Element Method**

In 1943, R. Courant wrote a paper on the torsional rigidity of a hollow shaft in which he broke it up into small triangles and interpolated the stress function across each triangle from net points (nodes) across the shaft (7, p10). Courant suggested that the method might be suited to solving a wide variety of problems. Today, Finite Element Analysis is indeed employed in many fields from heat transfer and stress analysis to fluid dynamics and the study of electromagnetic fields, to mention a few.

Why use Finite Element Analysis? Classical stress and vibration analysis techniques can solve simple beam and plate structures quite handily. As the geometries of structures become more complex, these methods are no longer sufficient for developing accurate models of their behavior. Finite element analysis tackles these sophisticated parts and geometries by breaking them down into more manageable pieces, and then applying the processing power of a computer to grind out the solutions (6).

The Finite Element Method (FEM) or Finite Element Analysis (FEA) is a numerical method for solving partial differential equations. This method by which complex physical problems, whose field distribution such as deformation is characterized by differential or integral equations, are broken down into small finite elements and then solved numerically across the entity. Finite elements are small pieces of the overall structure connected to each other at points called nodes. The collections of finite elements throughout the part to be modeled are called a Finite Element Mesh. An example of a Finite Element Method mesh is depicted below in Figure 4.

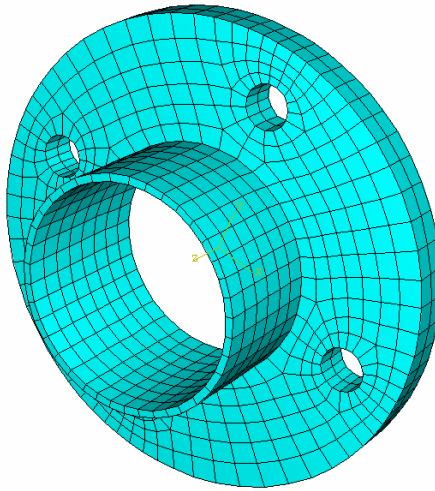


Figure 4. FEM Mesh

Each finite element allows a simple distribution of the field variable across the element. The distribution could be linear or quadratic, but will generally not be as complicated as the actual distribution in the region occupied by the particular finite element. The field variable, such as deformation, is then approximated across the entire object to obtain a solution. For this reason Finite Element Analysis (FEA) cannot be counted on to return an exact solution to the physical problem. However, the Finite Element approximation can be made more and more accurate by reducing the size of each element and thus increasing the total number of elements in the model. Although as the number of elements increases, so does the time it takes for the computer software to converge to an answer.

FEA can be employed for solving both static problems such as beam bending, and dynamic problems like vibration in structures and crash analysis (12). Before obtaining solutions to all of these problems, they must first be modeled correctly. Software programs such as ABAQUS/CAE (Complete ABAQUS Environment) can be beneficial



in helping to input the parameters needed to fully specify the model. First, the geometry of the part must be laid out; this is basically a three-dimensional representation of the object or objects to be examined. Followed by inputting the material properties of the parts, the loads and boundary conditions acting on the structure are loaded into the model. Finally, the types of elements to be used in dividing up the structure can be called out and the parts meshed. ABAQUS will take all of the information entered in the CAE module and construct the matrices that describe the behavior of each element. The software then takes all of these element matrices and combines them to form the finite element matrix for the entire structure, and solves it for the requested field values. The results are then graphically displayed in the visualization module.

## **ABAQUS Software**

The ABAQUS software suite is based on the Finite Element Method, and is composed of two main analysis modules: ABAQUS/Standard for solving linear and non-linear static, dynamic and thermal problems, and ABAQUS/Explicit for solving short transient events and highly non-linear problems such as impact and blast dynamics (17). ABAQUS/CAE (Complete ABAQUS Environment) allows for preprocessing and post processing of the analysis problem, and is the interface with both ABAQUS/Standard and ABAQUS/Explicit. The model of the problem to be solved is created in a (Computer Aided Design) CAD-like environment within CAE where individual modules are used to specify the geometry of parts and assemblies, material properties, analysis type, element types, boundary conditions, and applied loadings. Once the model is built,

ABAQUS/CAE hands the model off to either ABAQUS/Standard or Explicit, which processes the job in the background. All of this can be monitored in CAE, which also allows for the visualization of the results once the job is complete.

ABAQUS/Standard is the muscle behind the Finite Element Method (FEM) static and dynamic analysis. For the study of dynamic problems, ABAQUS solves the following eigenvalue problem to determine the natural frequencies of the model structure:

$$[ [K] - \omega^2 [M] ] \{ \phi \} = \{ 0 \} \quad (1)$$

The eigenvalues and mode shapes describe the free vibration of the structure. ABAQUS provides two eigensolvers for frequency extraction, Lanczos eigensolver and subspace iteration eigensolver. Lanczos method is generally faster when determining a large number of eigenmodes in a system with many degrees of freedom. Subspace iteration can be faster for systems with a small number of eigenmodes (i.e. less than twenty); however, it also requires more memory than the Lanczos method.

For static models, ABAQUS/Standard solves the total equilibrium equations at each node, where

$$\{P\} - [K]\{u\} = 0 \quad (2)$$

in which P is the externally applied forces, K represents the stiffness matrix, and u the nodal displacements. ABAQUS solves this matrix equation iteratively using the Newton-Raphson iteration method, and for static problems it requires one iteration and increment.

Some Finite Element software programs limit the user to triangle and tetrahedral elements for two and three-dimensional model Finite Element mesh creations. While this does not impact the overall solution to the problem, it can significantly increase the

amount of time it takes the program to converge to that solution. The ABAQUS/CAE (Complete ABAQUS Environment) software includes an extensive library of finite elements for use in a wide variety of applications in one, two and three dimensions. There are one-dimensional line type elements that include beam, truss and connector elements, two-dimensional quadrilateral and triangular type elements such as shell and membrane elements, and three-dimensional hexahedral, wedge and tetrahedral continuum elements. All of these elements come with linear and quadratic interpolation schemes, and the continuum elements allow for either full or reduced integrations across the element. These element types are available in the CAE module, which also color codes regions in the model to inform the user which elements are available for meshing in the designated regions. This flexibility in element selection provides the user with the tools necessary to model a given problem in the most efficient manner possible.

ABAQUS/CAE also provides a graphical means for establishing boundary conditions on the given model. Boundary conditions can be established on the surface of the part or at nodes, by selection on-screen and then using the dialogue box to constrain the degrees of freedom necessary to achieve the condition you are trying to simulate. Another useful feature in ABAQUS/CAE is in its ability to join parts together to form complex assemblies. Two parts can be joined at the shared nodes along their surfaces; this is called tying and is especially useful in creating a seamless union between parts. Tying lines up the nodes where the two parts come together and fixes them to one another so that forces and displacements can be transmitted from one part to the other, without having to go through the laborious process of manually trying to line up the meshes between the two parts. ABAQUS/CAE also provides a simple method for dividing parts

up and defining the size of the elements that will comprise the meshes for the parts. This procedure is called seeding and can be accomplished by either selecting the part and specifying an increment for the size of each element, or by selecting an edge of the part and inputting the number of elements desired along the edge. Once the seeding is specified for the part, it can be meshed and ABAQUS will try to accommodate the seeding specified by the user. Seeding makes refining a mesh a much easier prospect than having to re-specify the locations of every node for each part.

ABAQUS/FEA software is both powerful and versatile, capable of handling linear and non-linear static and dynamic analysis problems involving complex geometries. ABAQUS/CAE provides the interface that allows the user to harness this power without spending excessive amounts of time building the model and preparing it for analysis.

### **ABAQUS Applications**

ABAQUS Finite Element Analysis (FEA) software is widely used in industry and research as a tool for modeling and simulation of the dynamic and static behavior of complex parts, geometries and assemblies. The use of ABAQUS and other FEA software has begun to find its way into industry over the past decade. This transition was made possible by advances in personal computer processing capability and the introduction of a user friendly software interface to guide the user through the setup of the analysis to visualization of the results. ABAQUS has found application in industry from the aerospace community and automotive industry to civil engineering and the analysis of railroad trusses, to biomedical manufacturing and the manufacture of prosthetic devices

to include breast implants. Boeing aerospace used ABAQUS in the redesign of the pitch-hinge assembly for its CH-47 Chinook helicopter. Engineers at Boeing ran thermal-friction testing of the redesigned bearing on ABAQUS to predict wear on the new design. The analysis allowed the engineers to spot flaws in the design before they reached prototype, and allowed for substantial cost saving brought about by reducing the amount of testing and redesign required (28). Figure 5 depicts the pitch-hinge assembly that is used to mount the propeller blades to the CH-47.



Figure 5. Pitch-Hinge Assembly (28)

ABAQUS also allows parts created on other Computer Aided Design (CAD) programs to be imported into an assembly and then meshed individually. Once contact is established between the parts, the analysis is ready to be run. This procedure allows

meshing of large assemblies of parts without the time consuming process of lining up the nodes of the individual part meshes. John Hopkins has used ABAQUS in the development of the primary mirror for the Far Ultraviolet Spectroscopic Explorer (FUSE) collimator. ABAQUS was used to determine stress in the mirror mount and distortion in the mirror due to back supports. Figure 6 depicts the FUSE collimator.



Figure 6. FUSE Collimator (13)

In a study sponsored by Rolls Royce jet engines, ABAQUS was used in a finite element torsional buckling analysis for jet engine drive shafts. In an effort to produce torque transmitting shafts that are smaller and lighter in weight, thin-walled drive shafts are required to increase engine efficiency and performance; however, as the wall thickness decreases they become more susceptible to torsional collapse. A method was desired to predict buckling in new shaft designs, which could be used for the certification of the shaft design without extensive and expensive testing. Research to date was based on either analytical or semi-empirical formulation, but was limited in its ability to adequately model the complex features of modern shaft design such as the air and oil

distribution features within the real shaft. The ABAQUS model produced results that were in good agreement with tests run against actual shafts. The model has since been adopted by Rolls Royce for use in development of future jet engines and could show considerable cost savings over existing shaft certification testing (21).

### **Previous Research on Inflatable Tube Vibration and Modal Testing**

Single's thesis (26) presented the first work on developing a model for analyzing the modal properties of the Rigidized Inflatable Get-Away-Special Experiment (RIGEX) rigidized inflatable tubes. He began his analysis using a modified Euler Bernoulli Beam theory to determine the natural frequencies and damping ratios for the tubes. He then compared these results to vibration testing performed on tubes using both shaker table and Piezoelectric Transducer (PZT) to excite the beams. This study of the tube vibration characteristics was built upon by Philley (25) in 2003, when he performed testing on the RIGEX tubes using the logarithmic decrement and half power methods to determine the natural frequencies and damping ratios for the tubes. Philley conducted several vibration tests on the tubes, actuating them with PZTs and collecting data with a laser vibrometer and again using an accelerometer mounted on the top flange. During these tests, the boundary conditions were varied to determine what effect this might have on the frequency response of the tubes. The result of the testing showed the first and second bending modes of the tube to be around 62 and 660 Hz respectively.

## Dynamic Analysis of Beams

In producing the ABAQUS Finite Element Model of the 20-inch inflatable composite tube, dimensions and material properties for the individual components were drawn from Single's thesis (26). He notes that due to the proprietary nature of the material used in the construction of the beams, not all of the material properties are known. One of the principal properties required for producing an accurate Finite Element Model in ABAQUS is Young's Modulus. The value for Young's Modulus given in Table 2 was converted to psi (24511 psi) for use in the ABAQUS model. This was found to be much too low to provide a reasonable value for the fundamental natural frequency of the rigidized tube assembly. Unable to obtain the true material properties for the composite tube, Young's Modulus was back-calculated using the fundamental frequency formula and experimental results for the fundamental bending mode of the tube (4).

Table 2. Inflatable Tube Properties (26)

Property Description	Value	Units
Aluminum Base Flange Mass	74.02	grams
Aluminum Tip Flange Mass	74.6	grams
Beam Material Thickness (H)	0.015	inches
Young's Modulus (E)	9.5E(6)	lbf/in <sup>2</sup>
	1.69E(8)	N/m <sup>2</sup>
Moment of Inertia (I)	8.275E(-9)	m <sup>4</sup>
Material Density (?)	8.64307E(2)	kg/m <sup>3</sup>

The fundamental frequency formula will be used to back-calculate a more realistic value for Young's Modulus of the composite tube, based on experimental results for the first natural frequency of the rigidized tube mounted to a table. The natural frequency of a single degree-of-freedom system can be determined by considering the



total energy of the system in motion. The kinetic energy of the body is given by

$$KE = \frac{1}{2}mv^2 \text{ where } x = A\sin \omega t \text{ and } v = \omega A \cos \omega t \text{ represent the displacement and}$$

velocity of the body in simple harmonic motion.  $A$  and  $A\omega$  represent the maximum displacement and velocities, respectively. Thus, when the displacement  $x$  is zero the velocity  $v$  is at its maximum and so is the value of the kinetic energy

$$KE_{\max} = \frac{1}{2}m(\omega A)^2 \quad (3)$$

Considering the potential energy of the system, which is given by the relation

$$PE = \frac{1}{2}kx^2 \quad (4)$$

where  $k$  is the linear spring constant.  $PE$  obtains its maximum value when  $x = A$  and the velocity  $v = 0$ .

$$PE_{\max} = \frac{1}{2}kA^2 \quad (5)$$

Since the energy of the system is conserved  $KE_{\max} = PE_{\max}$  or

$$\frac{1}{2}m(\omega A)^2 = \frac{1}{2}kA^2 \quad (6)$$

$$\omega = \sqrt{\frac{k}{m}} \quad (7)$$

$$\text{where } \omega = 2\pi f \quad (8)$$

$$f = .159\sqrt{\frac{k}{m}} \quad (9)$$

where  $f$  is the fundamental natural frequency,  $k$  is the linear spring constant and  $m$  is the mass supported at the free end of the beam. Spring constants for the beam can be

calculated from formulas based on boundary conditions and beam geometry, where  $k$  is highly dependant on the type of boundary condition applied at the fixed end of the beam. Several values of  $k$  are depicted in Figure 7.

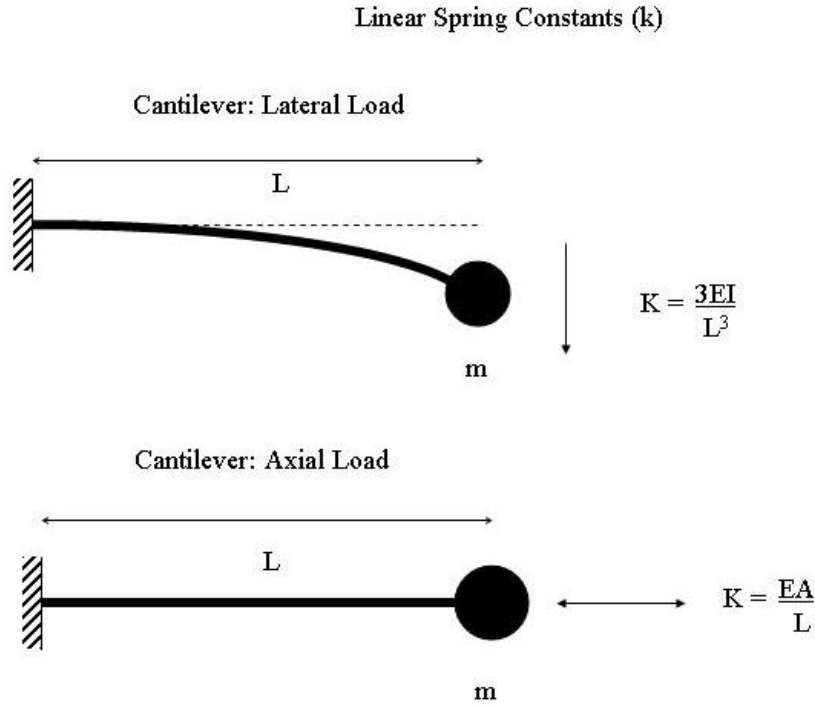


Figure 7. Linear Spring Constants (4)

Now consider a uniform cantilever beam of mass,  $m_b$ , with flexural rigidity  $EI$  and length  $L$ , with the same point mass attached at the free end. Again, the vibrating structure will be modeled as a single degree of freedom system and will yield only the first or lowest natural frequency. The beam, or spring as it is being modeled in this case, can no longer be considered massless and must be accounted for in calculation. The formula for the fundamental frequency can be obtained by using an approximate energy method and

considering a portion of the beams effective distributed mass to lumped in with that of the point mass attached to the end of the beam. Under these conditions, the only force that acts to deflect the beam during vibration is the concentrated inertia force at the tip of the beam. It is therefore assumed that the deflection curve of the vibrating beam is the same as the deflection curve of the statically loaded beam with the mass concentrated at the tip. This approximation is known as Rayleigh's energy method for estimating the fundamental frequency, and should lead to an approximation at least as high as the actual fundamental natural frequency (20:63).

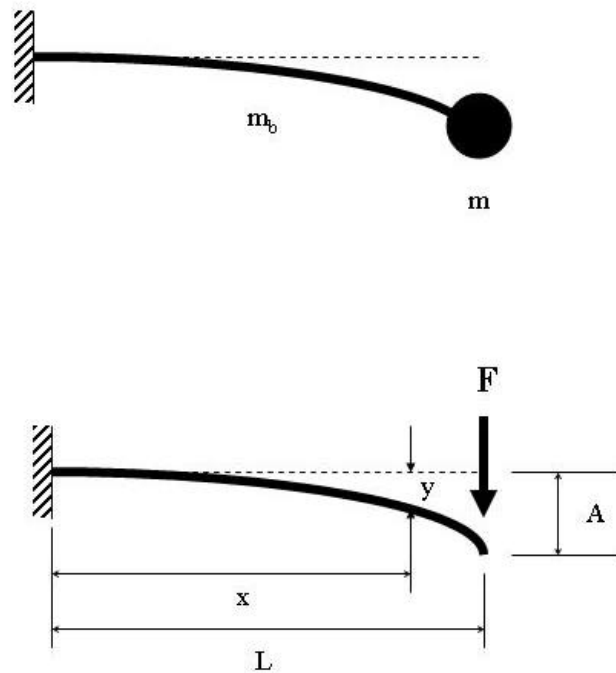


Figure 8. Cantilever Beam with Mass on Free End (4)

From Figure 8 we see that the maximum displacement of the beam tip is  $A$  due to the application of the force  $F$ . The applied force  $F$  is equal to the linear spring constant from

Figure 7 (for an end loaded cantilever beam in bending),  $k = \frac{3EI}{L^3}$  times the displacement

A. The potential energy of the beam is equal to the amount of work done by the tip force

to deflect the beam, where  $PE = \frac{1}{2}Fd = \frac{1}{2}FA$  or  $PE = \frac{1}{2}kA^2$  and the maximum  $PE$  of

the beam is

$$PE_{\max} = \frac{1}{2}kA^2 \text{ or } PE_{\max} = \frac{3EIA^2}{2L^3} \quad (10)$$

The amplitude of displacement at an arbitrary location  $x$  along the beam measured from the clamped end is given by

$$y_{\max} = \frac{F}{EI} \left( \frac{Lx^2}{2} - \frac{x^3}{6} \right) = \frac{3A}{L^3} \left( \frac{Lx^2}{2} - \frac{x^3}{6} \right) \quad (11)$$

The harmonic amplitude at  $x$  is given by  $y = y_{\max} \cos \omega t$  and the velocity is

$$\frac{dy}{dt} = y_{\max} \cdot \omega \sin \omega t = \frac{3x^2L - x^3}{2L^3} \cdot \omega A \sin \omega t \quad (12)$$

The maximum kinetic energy due to the motion of the point mass and the distributed mass of the beam is

$$KE_{\max} = \frac{m(\omega A)^2}{2} + \left( \frac{m_b}{2L} \right) \int_0^L \left( \frac{3x^2L - x^3}{2L^3} \cdot \omega A \right)^2 dx \quad (13)$$

yielding

$$KE_{\max} = \frac{1}{2} (\omega A)^2 \left( m + \frac{33}{140} m_b \right) \quad (14)$$

Setting the maximum potential and kinetic energies equal to one another and solving for the frequency  $f$ , we obtain

$$f = .159 \sqrt{\frac{3EI}{L^3(m + .235m_b)}} \quad (15)$$

Rayleigh's energy method can be used in a similar fashion to produce a fundamental frequency formula for a single degree of freedom system under axial loading. The results are summed up in Table 3, which illustrates how the fundamental frequency for bending and axial are calculated.

$$f = .159 \sqrt{\frac{k}{(m + \mathbf{a}m_b)}} \quad (16)$$

Table 3. Fundamental Frequency Formulas (4)

	<b><i>k</i></b>	<b><i>a</i></b>
Axial Vibration	EA/L	1/3
Lateral Vibration	EI/L <sup>3</sup>	1/4

where  $m$  = lumped mass  
 $m_b$  = beam mass  
 $\mathbf{k}$  = spring constant  
 $\mathbf{a}$  = parameter

## NASA Get Away Special Experiments

In the mid-seventies, NASA commenced the Get-Away-Special (GAS) Program to provide the general scientific community with an inexpensive means in which they could access space with their experiments. The GAS canisters come in two varieties, one being small (2.5 cu ft) which can accommodate 60 to 100 lbs of customer payload, and the other being a 5 cu ft canister capable of accommodating an experiment up to 200 lbs. Figure 9 shows an exploded view of the GAS can.

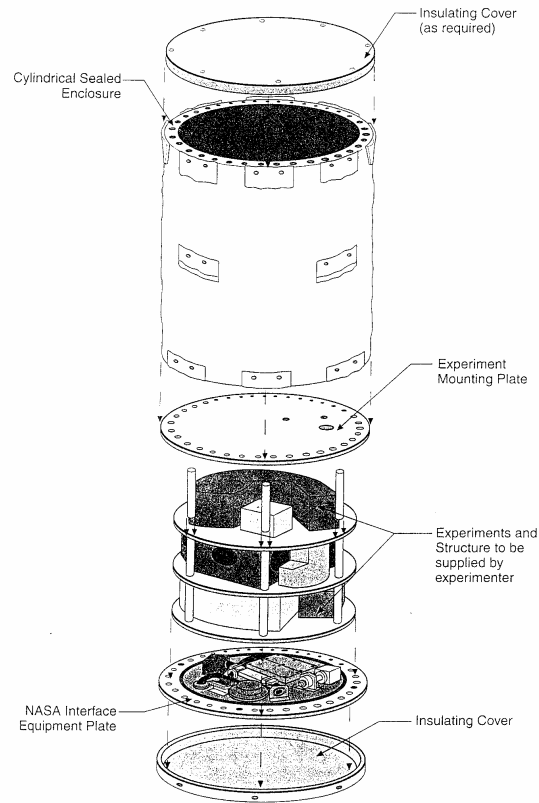


Figure 9. GAS Experiment Configuration (23)

GAS payload canisters are mounted in various locations within the payload of the space shuttle. Up to twelve canisters can be mounted at a time on a bridge assembly, depicted earlier in Figure 2.

GAS canister experiments must be completely self-contained and autonomous. The only interface allowed between the experiments and the shuttle are three on-off controls, operated by the space shuttle crew. It is the responsibility of each experimenter to provide heating, data handling and electrical power for their particular payload.

## Payload Considerations

The RIGEX preliminary design called for a total of 196.2 lbs of support structure and experimental components, all of which had to be organized into the 19.75” diameter by 28.25” cylindrical area. Table 4 illustrates the weight breakdown for the RIGEX preliminary design. In addition, to accomplish the operational goals of the RIGEX experiment, the system must be able to survive the effects of take-off and have the components retain the capability of fulfilling their intended functions.

Table 4. Preliminary Weight Analysis (10)

Item	Weight	Quantity	Total
Structure	58.24	1	58.24
Battery Cell	6.60	8	52.80
Battery Box	18.60	1	18.60
Computer	7.75	1	7.75
Sensors	2.48	1	2.48
Heaters	1.00	5	5.00
Oven	4.25	3	12.75
Inflatables	2.50	3	7.50
Inflation System	5.25	3	15.75
Video	0.75	3	2.25
Wiring	10.00	1	10.00
<i>TOTAL</i>			<i>193.12</i>

## Design and Testing Requirements

The experiment structural assembly must be designed to mount to an Experiment Mounting Plate (EMP) that is provided by NASA. Under structural verification, there are two basic requirements for GAS experiment support structures:

- 1) The structure must withstand flight limit loads of 10 g's in the X, Y, and Z axes with an ultimate factor of safety of 2.0 when verified by analysis only or*

*an ultimate factor of safety of 1.5 when verified by test to a yield factor of safety of 1.25. The structure must also exhibit positive margins of safety under these loads. The loads must be combined using the X, Y, and Z loads in the worst case loading conditions (this means combining compression, tension, bending, and shear stresses).*

- 2) *The fundamental frequency of the experiment support structure about any axis must be greater than or equal to 35 Hz. This can be verified by analysis or test. (22, B1-3)*

These requirements are summarized in Table 5.

Table 5. GAS Structural Verification Requirements (23)

Structural Loads	Factors of Safety		
	Verification Method	FS on Yield	FS on ULT
Structural design accelerations shall be +/-10.0 G's  in each coordinate axis applied simultaneously.	Analysis & Test *	1.25	1.5
	Analysis Only	1.5	2
* Test Factor = 1.25			

GAS experimenters are given the option of verifying structural integrity through analysis or testing. However if testing is used for verification, then the testing must be supported by analysis. The structural verification of the loading and frequency requirements above can be accomplished through classical techniques or through the use of Finite Element Analysis. If the analysis only option is selected for structural analysis, the applied load analysis must consider margins of safety on yield and ultimate strength of 1.5 and 2.0, respectively.

If testing is used to verify the structure, then the analysis must still be conducted but the factors of safety for yield and ultimate strength are reduced to 1.25 and 1.5 times



the flight limit loads. The testing must then be conducted to verify that the structure can sustain the applied loads. Test set-up and procedure must be documented, and results must verify that the structural flight requirements have been met. Acceptable tests for structural verification are summed up in Table 6.

Table 6. GAS Structural Verification Testing (22)

<b>Static Loads Test</b>
The static loads test is sometimes referred to as a "pull test" and consists of loading or pulling the structure to 1.25 times the flight limit loads. The experimenter can monitor the experiment support structure response using strain gages or other methods. The static test results are then correlated to determine if the stress and strain match those predicted by analysis.
<b>Sine Burst Test</b>
The sine burst test is a low frequency(< 20 Hz) sine test for 5 cycles at 100% of the test loads. The test load that should be applied is 17.7 g's in each of the three axes. This test load includes the required factor of safety (1.5) for the test. Again, the results should match the predicted values determined by analysis.
<b>Sine Sweep Test</b>
The sine sweep test is used to verify the experiment structure fundamental frequency. A harmonic vibration can be created by a vibration table or other method, and the vibration should be forced at the 1/4 g, 1/2 g, or 1 g level. A sine function vibration sweep from 20 Hz to 200 Hz is applied and the associated test result plots are used to determine the resonant frequency.
<b>Random Vibration Test</b>
The random vibration test verifies workmanship and results are not acceptable for structural verification. The GAS experimenter is not required to conduct a random vibration test but may desire to conduct such a test for confidence purposes. Appropriate levels may be found in the GAS Experimenter Handbook.

## Summary

The Finite Element Method was developed to simplify the analysis of complex structures and geometries. Recent advances in computer technology have allowed software such as ABAQUS to be employed on a much wider scale. This software

presents users with a more tractable means of employing the Finite Element Method to model static and dynamic problems, which are beyond the scope of analytical methods.

Also discussed in this chapter were previous efforts to analyze the vibrational characteristics of RIGEX tubes and vibrational techniques for determining natural frequencies of beams. These techniques will be used to verify the ABAQUS Finite Element Model of the RIGEX tubes and to help establish more reasonable values of its material properties.

Finally, RIGEX design considerations were reviewed, and criteria for the design and testing of the RIGEX structural assembly were presented. The next chapter will address the structural frequency and stress modeling in ABAQUS/FEA.

### **III: Experiment Methodology**

#### **Overview**

Due to the fact that a GAS experiment hazard could potentially jeopardize the astronauts, space shuttle or ground facilities, NASA requires that all payloads conform to the requirements set forth in “Safety Policy and Requirements for Payloads Using the Space Transportation System (STS),” NHB 1700.7B (23). The “GAS Experimenter’s Guide to the STS Safety Review Process and Data Package Preparation” (22) provides further details on specific structural test and analysis requirements for GAS experiment safety verification.

Finite Element Analysis (FEA) was selected from the list of approved analytical structural verification methods, and can be used for both the structural and fundamental frequency verification requirements. Due to the lack of a slip table for the shaker table, FEA alone will be used for structural verification of flight limit loads and determination of the structural fundamental frequency. The structural design of the support structure will be accomplished through the use of PRO-Engineer for the design and fabrication of the structure, and then ABAQUS will then be used to perform frequency and stress analysis on a Finite Element model of the support structure imported from PRO-Engineer.

During the design of the full structure, ABAQUS models will be constructed from existing components, namely the inflated tube assembly and quarter test structure used in Philley’s thesis (25), to verify frequency analysis modeling in using ABAQUS/FEA.

Finally, ping testing and experimental results from previous thesis will be conducted to verify the results of ABAQUS frequency analysis.

### **Structural Design Considerations**

The RIGEX preliminary design was used as a baseline for the structure, owing to the fact that it was capable of accommodating all of the experimental components, allowed for the inflation of the tubes and was within weight and volume limitations imposed by the GAS payload program. The integration of the RIGEX structure into the GAS canister was another consideration in the design. NASA provides GAS experimenters with an Experiment Mounting Plate (EMP) which is the interface between the GAS can and the users experiment. This EMP is a 5/8 inch thick, 22.678 inch diameter aluminum plate with 45 mounting holes arranged for experiments to be attached. The experimenter is responsible for designing their experiment to mate up with the EMP, while keeping at least one purge port on the EMP unobstructed. NASA provided an EMP as depicted in Figure 10.

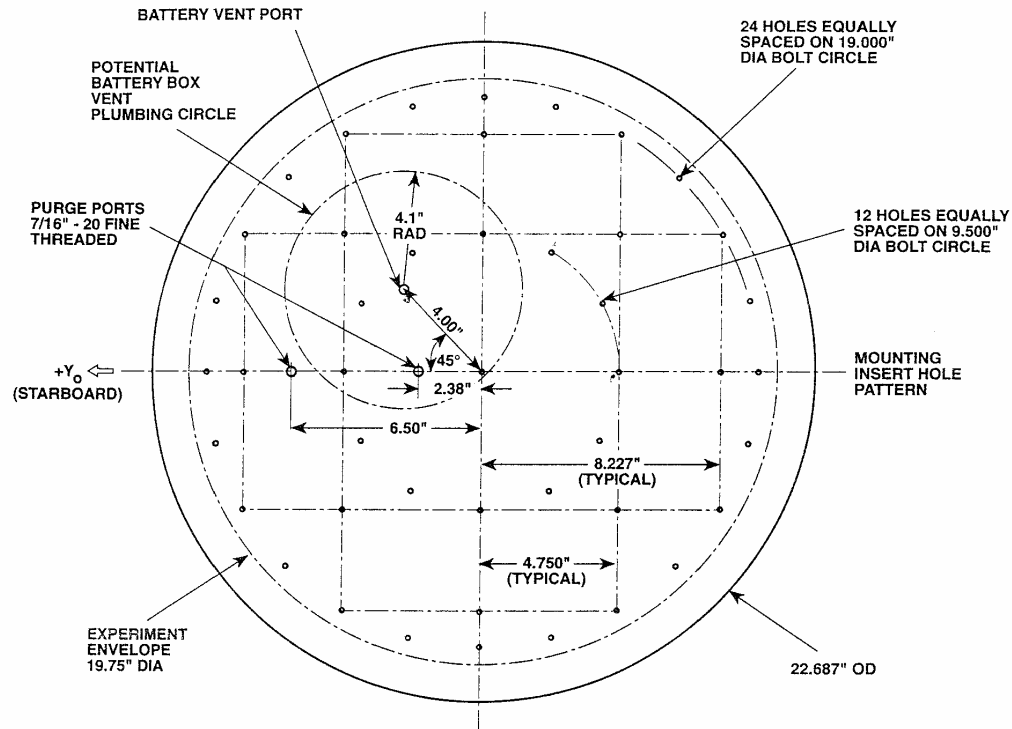


Figure 10. Experiment Mounting Plate (22)

Before the RIGEX support structure design could be analyzed, a structural material acceptable to NASA had to be selected for its construction. The structural material selection had to be balanced between the NASA requirements for providing protection against Stress Corrosion Cracking and those of material strength to support the flight loads imposed at take off and landing. Structure manufacturing also plays a part in the material selection, where machinability and weldability must also be considered. Once a material is selected for the structure a Finite Element Analysis (FEA) model can be constructed in ABAQUS, and the analysis can begin to determine if the structure meets the requirements laid out in the “GAS Experimenters Guide to the STS Safety Review Process and Data Package Preparation”.

Bumpers are required to provide later support for the free end of the structure, so that if the structure deflects enough to contact the wall of the GAS canister it will not cause damage to the canister. These are required unless the experimenter can prove through analysis that the structure will not contact the GAS canister.

### **ABAQUS Vibration Modeling and Simulation**

ABAQUS Vibration modeling and simulation will be conducted by modeling the rigidized tube assembly in ABAQUS/CAE and running a frequency extraction procedure in ABAQUS using the Lanczos solver to determine the eigenvalues and mode shapes of the tube. The first and second bending mode will be determined in this fashion and compared to experimental values. When an accurate tube model has been produced and verified, the more complicated quarter structure can be modeled and its natural frequency determined in a similar manner as the tube. Since the quarter test structure has no supporting vibration test data, the structure will be modified for mounting on the Experiment Mounting Plate (EMP) and a ping test will be conducted to verify the fundamental frequency. Finally, the full RIGEX structural assembly will be modeled in ABAQUS and a frequency analysis run to determine its vibration characteristics. The structure will again be mounted to the EMP and ping tested to verify the results of the ABAQUS analysis.

### **Rigidized Tube Model**

The RIGEX rigidized tube assembly is composed of three components, a composite rigidized tube and two aluminum end flanges. For the model, the composite

tube will be modeled as an isotropic material. The material properties for the composite tube, specifically Young's Modulus (E), will have to be estimated for reasons mentioned in the Introduction. This can be accomplished by using experimental results for the tubes natural frequency in bending and the Fundamental Frequency Equation to back-solve for Young's Modulus. Once the material properties are available, two models of the tube will be constructed to compare the results of using beam and continuum elements. Beam elements will be used to get a rough idea regarding the validity of the continuum element model once it is produced, and should match closely to analytic beam theory results. The beam element model should also be easier to set up, and since it's a one-dimensional representation it should require much less computational time to solve.

Since the composite tube closely resembles a pipe, that is the beam element that will be used to produce the model. The Pipe element represents a thin wall cross-section, which provides good results as long as the wall thickness is less than 1/10th the cross-section dimension of the beam. In the case of the composite tube, the ratio is 1/100th (where the wall thickness is 0.015 inches and the cross-sectional diameter is 1.5 inches) and definitely falls into the realm of where acceptable results should be obtained. Figure 11 shows a representation of the actual composite tube.

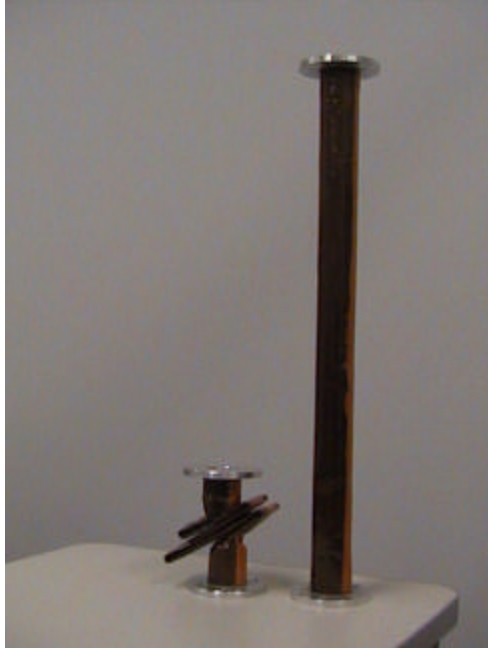


Figure 11. Inflatable Tubes

Following the beam element analysis, a tube model will be constructed using continuum hexahedral elements (linear and quadratic). Continuum elements are more general type elements used for modeling general three-dimensional parts and assemblies. Continuum elements come in three basic types: hexahedral (hex), wedge or tetrahedron (tets). They are assigned based on the particular geometry of the assembly being meshed, and applicable meshing schemes are available due to the user created partitioning. It is generally preferable to use a structured meshing technique with hex elements because they are more computationally efficient than the tets or wedges, but in some cases part geometries do not lend themselves to a structured mesh and free or swept meshing must be used with wedges and tets, respectively. The final descriptor of the element will be whether it uses a linear or quadratic interpolation to determine the variance in the displacements between the nodes. Comparison will be made between the performance of



the lineal hex elements (C3D8R) and the quadratic hex elements (C3D20R), both of which are six Degree of Freedom (DOF) elements (three translation and three rotation).

Figure 12 depicts the elements used in the construction of the continuum element tube.

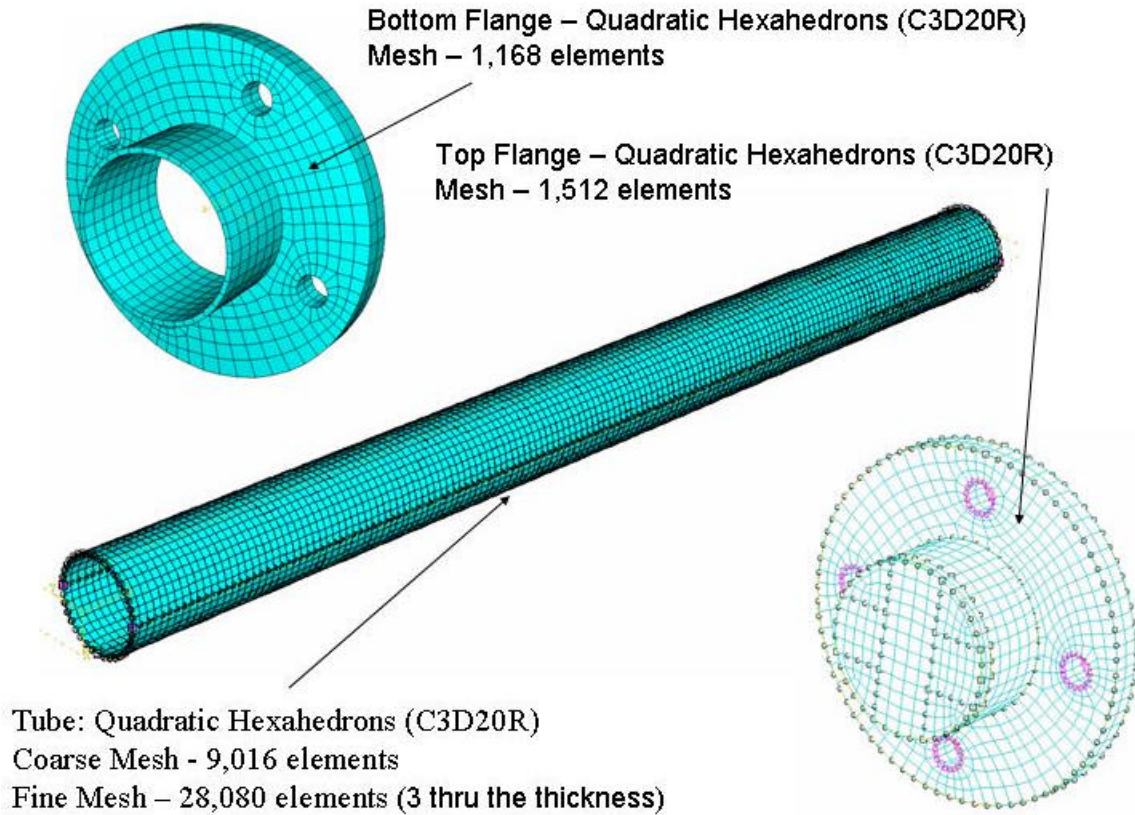


Figure 12. ABAQUS Tube Construction

### ABAQUS Continuum Elements

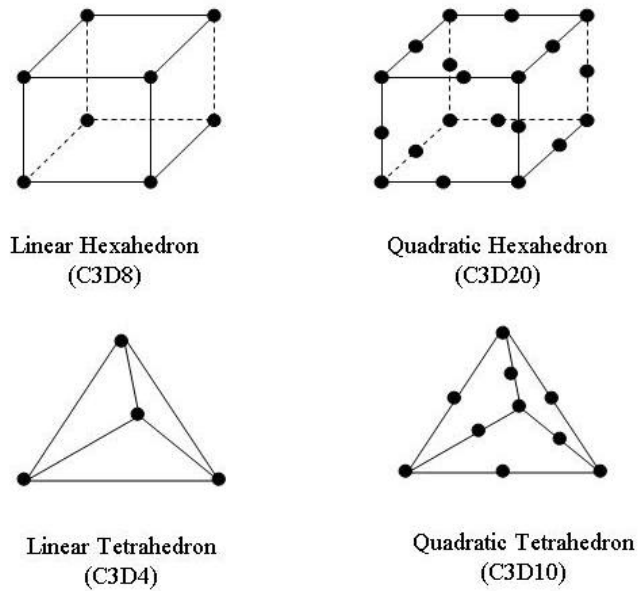


Figure 13. ABAQUS Continuum Elements (16)

The results will also be compared to the previous test results obtained for the composite tube assembly and by ping testing with a modified boundary condition. Figure 13 shows the boundary conditions used for previous vibration testing. This setup more closely resembles a simply constrained cantilever beam than a clamped beam, due to the fact that the base is only attached to the table with two bolts instead of four along the perimeter of the bottom flange. This was a result of the base flange holes not matching up with the holes on the table top. To examine the difference the boundary conditions had on the frequency analysis, an aluminum plate was constructed that provided four mounting holes for the bottom flange and eight holes for mounting the plate to the table. This can be seen in Figure 14 and Figure 15.

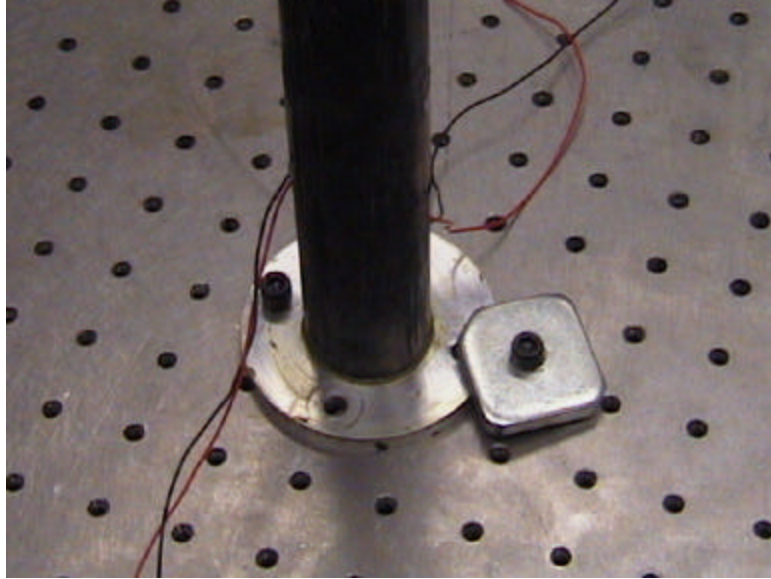


Figure 14. Tube with Simply Supported Boundary Condition

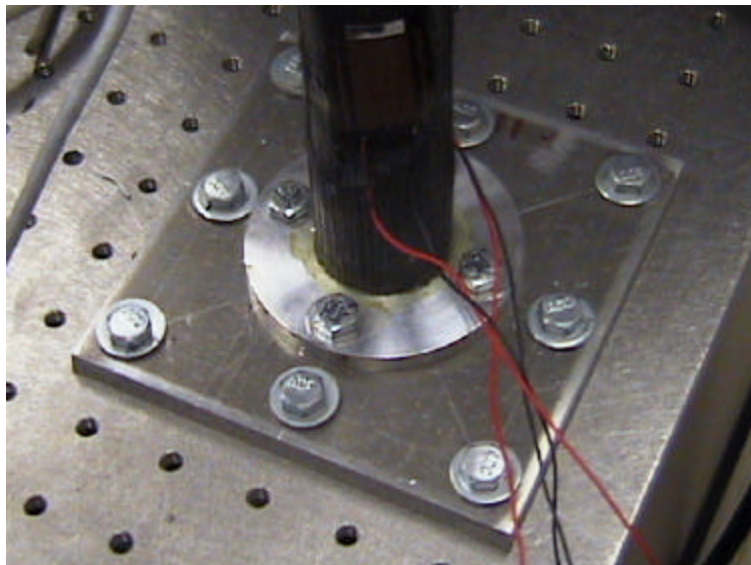


Figure 15. Tube with Clamped Boundary Condition

The Ping test was carried out by attaching an accelerometer to the top flange and the hammer was used to strike the base of the tube near the bottom flange. The data was collected and saved for processing in MATLAB.

### **Quarter Structure Model**

Having the quarter structure test model on-hand provides the ability to test the frequency analysis capabilities of ABAQUS on a more complicated assembly. The quarter structure will be modeled using continuum hex elements. In this model, the quarter structure will be modeled as a single aluminum part and attached to a modeled Experiment Mounting Plate (EMP). The quarter structure is actually an assembly of four plates, two long narrow plates forming an L shape are capped on each end by quarter circle-end plates, all are screwed together along their edges. Figure 16 depicts the quarter structure and the ABAQUS representation of the quarter structure.

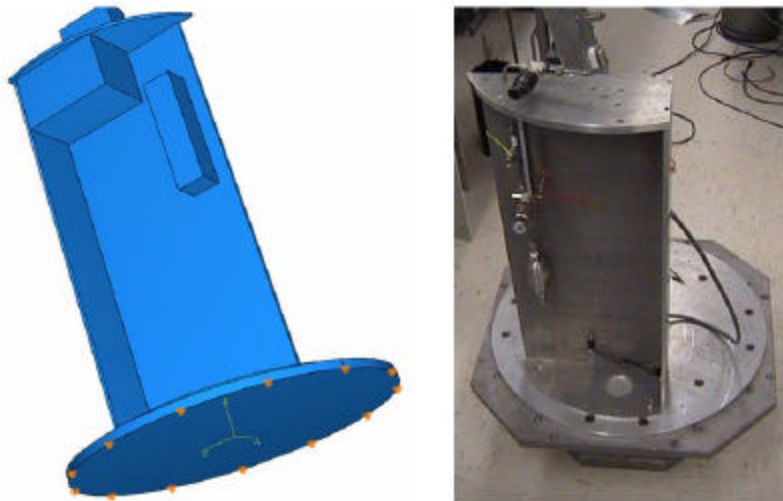


Figure 16. Quarter Structure Model and Actual Quarter Structure

This should produce a model that is slightly stiffer than the actual structure. Additionally, the oven and inflation system will have to be modeled and attached to the assembly. Material properties of these subsystems will be based on the weight assigned to them in the weight breakdown sheet of Disebastian's thesis (10). In essence, the experimental components will act as point masses for frequency determination of the structure. The connection between the structure and the EMP will be modeled by tying the nodes of the two surfaces together. This should provide for a reasonable boundary condition, considering the bolting scheme for attaching the two parts together. The bolting pattern for connecting the quarter structure to the EMP is detailed in Figure 17.

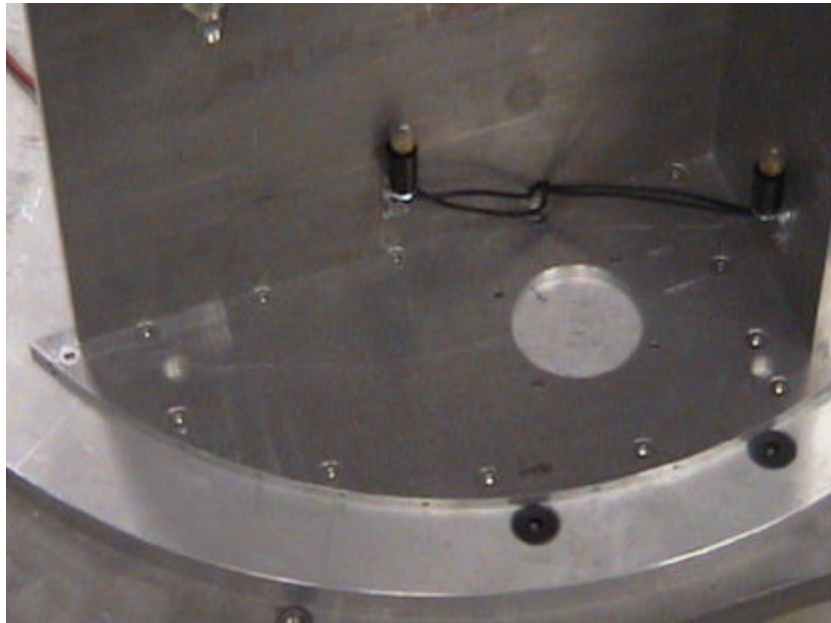


Figure 17. Quarter Structure Mounting Configuration to EMP

A frequency analysis was run on the quarter structure model in ABAQUS, and the first bending modes were examined. These values were then used to determine the locations



on the structure, where maximum displacements could be expected. These locations were used in the ping testing as accelerometer locations. The EMP was then fastened to the shaker head mount and the quarter structure bolted down onto the EMP.

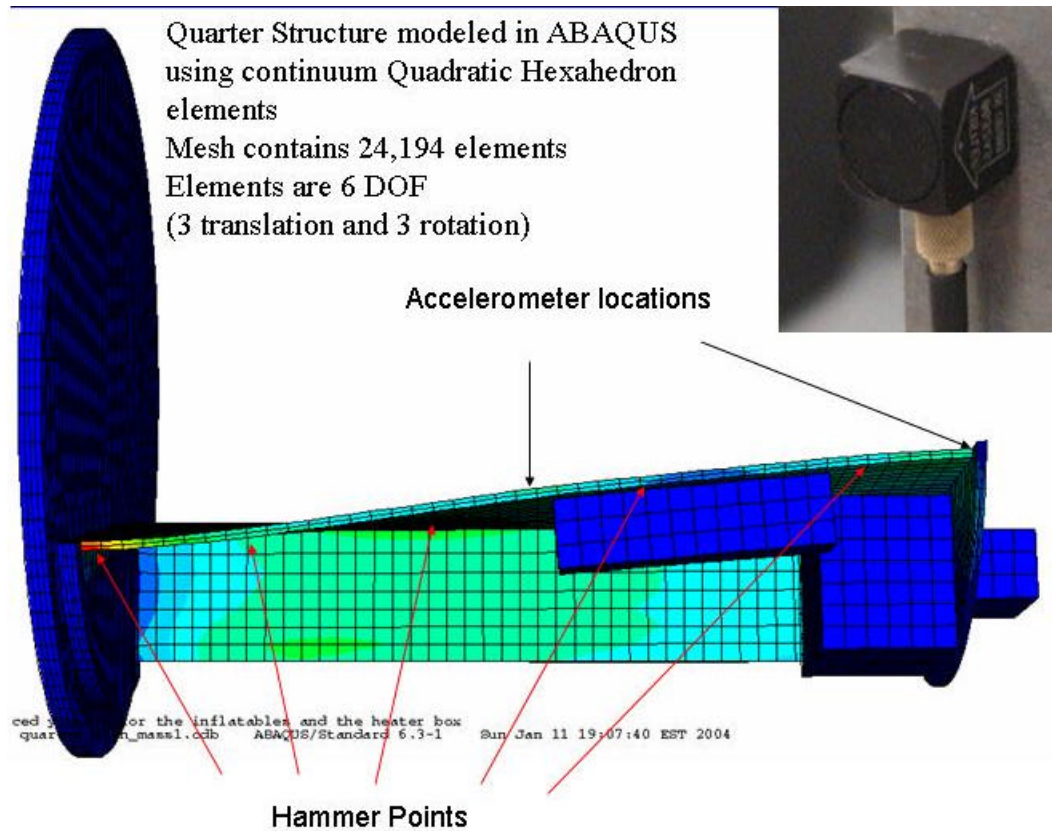


Figure 18. ABAQUS Bending Mode 1 for Quarter Structure

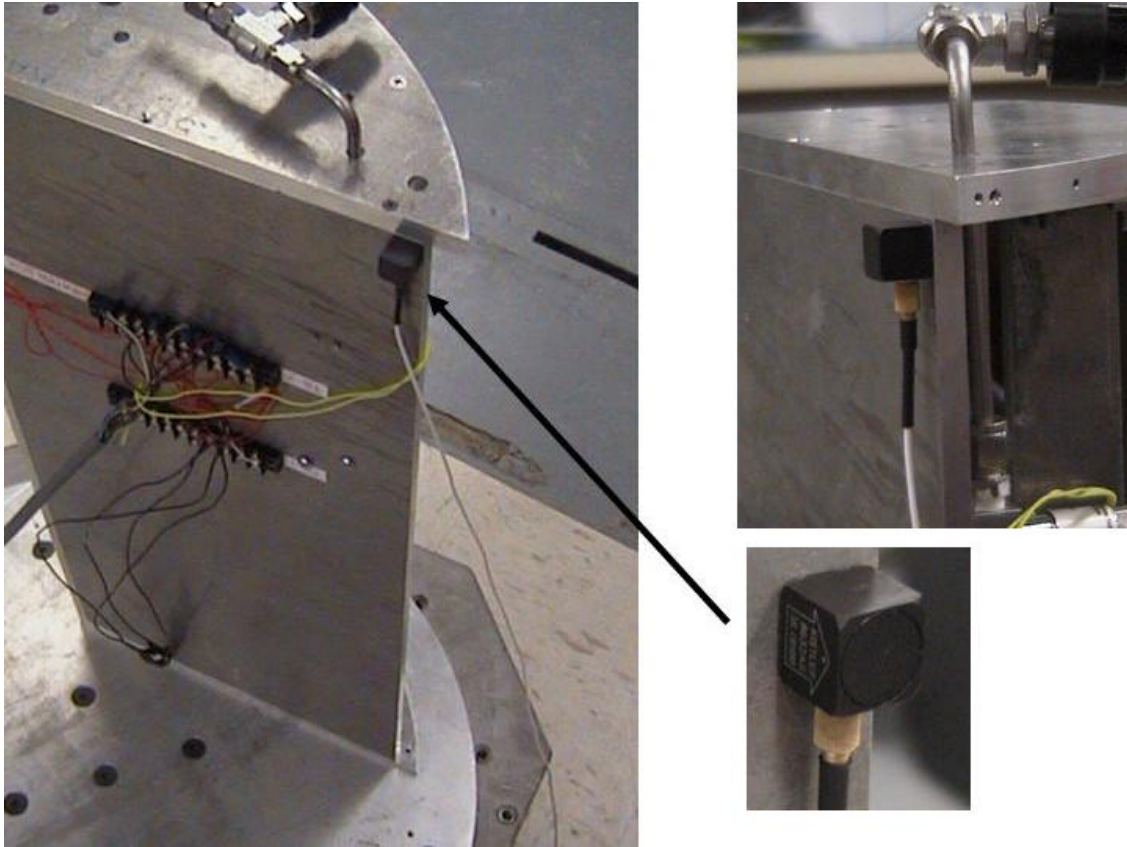


Figure 19. Accelerometer Tip Location on Quarter Structure

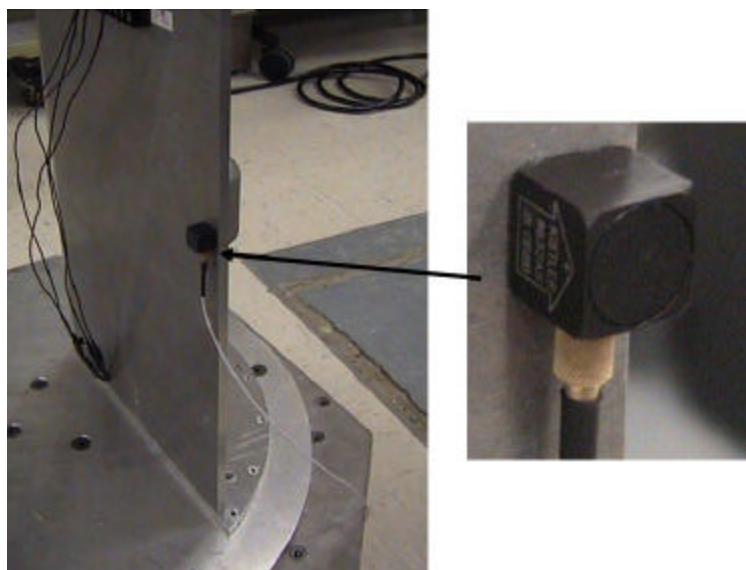


Figure 20. Accelerometer mid span location on quarter structure

In carrying out the ping test, the accelerometer was attached at the locations depicted in Figure 18 and the structure was struck in the locations marked as hammer points. The data was collected and transferred to MATLAB for processing. Figure 19 and Figure 20 elaborate on the accelerometer placement.

### **Full Structure Model**

The full scale ABAQUS structural model was first constructed of two-dimensional linear shell elements. As this model would be the most complex to date, it was decided to start off with a simple representation for three reasons: first a two-dimensional model would not require as much time to construct as a three-dimensional representation, second the time it would take for the software to converge to a solution would also be reduced as compared to a three-dimensional model, and lastly the structure design had not yet been finalized. This first attempt at analysis was intended to give a rough estimate on the natural frequency of the structure, to see if the design was even close to meeting the frequency requirement of 35 Hz for its fundamental frequency. Since the plate thickness (0.25 inch) is less than 1/15 the characteristic length of the plate (more on the order of 1/100), two-dimensional thin wall elements should be adequate for modeling the plates of the structure.

The entire structure will be modeled as one piece, as will the EMP. The two will then be joined by tying the nodes along a cylindrical section representing the bolt ring between the two parts. This will constitute the chief assumption in this model, as it is not yet practical to model each individual bolt connecting the EMP to the structure.



For the final ABAQUS model of the RIGEX structure, the actual three-dimensional part geometries used in the design and manufacturing of the structure were imported from PRO-Engineer as IGES files. This allowed the connection between the structure and the EMP to be modeled more realistically. On the down side, this model is three-dimensional and much more complicated geometry wise, thus the components had to be meshed using a variety of elements and meshing techniques.

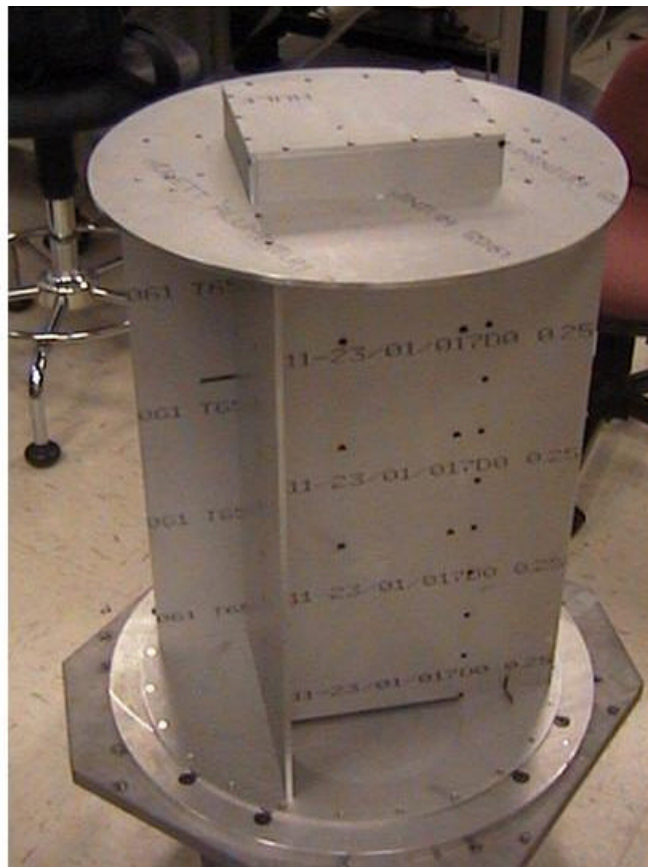


Figure 21. RIGEX Structure

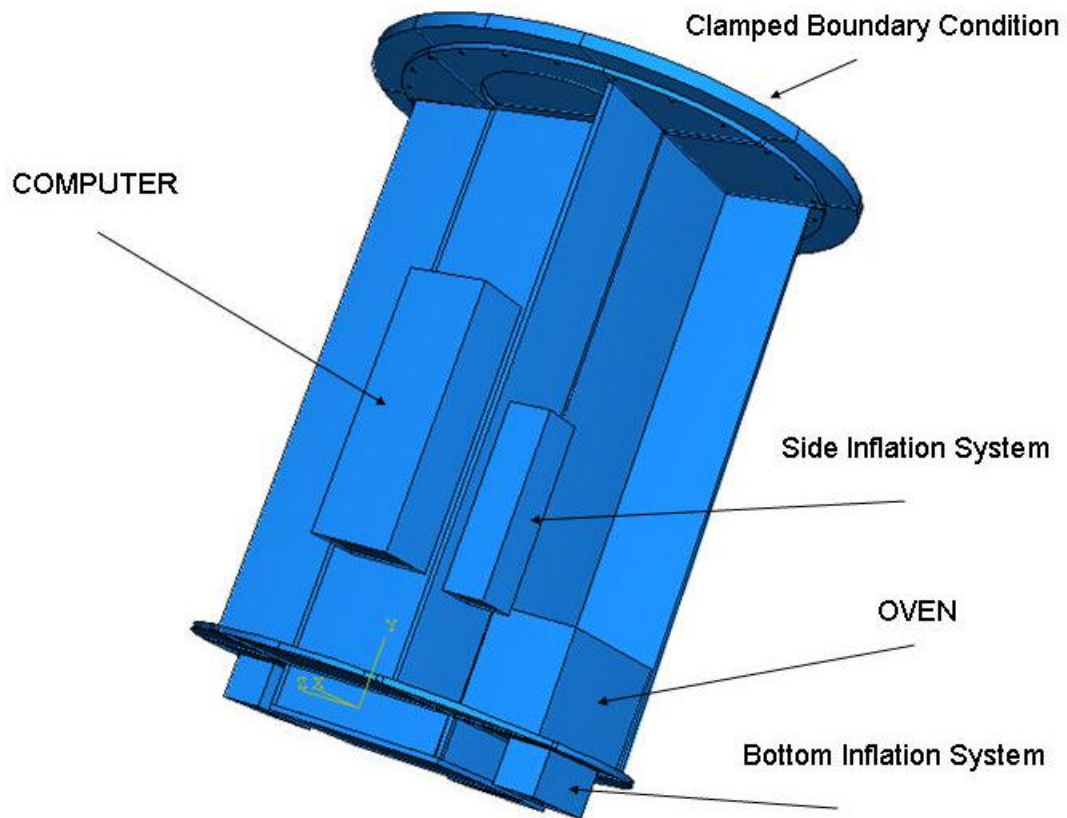


Figure 22. ABAQUS representation of RIGEX Structure

For the full structure, ping testing was accomplished by first attaching the structure to the EMP, using 24 stainless steel #10-32 screws. The laser vibrometer was then used to create a grid on the face of the 13 inch plate that runs across the computer access hole. A grid was also created on the overhang of the opposing 13 inch plate, as depicted in Figure 23. The ping hammer was used to strike the structure in the location indicated in Figure 24. The laser vibrometer would then measure the velocity of the plate at the current grid point location. This procedure was repeated until data was collected on all mapped grid points.

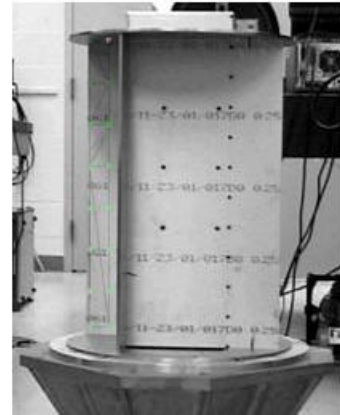
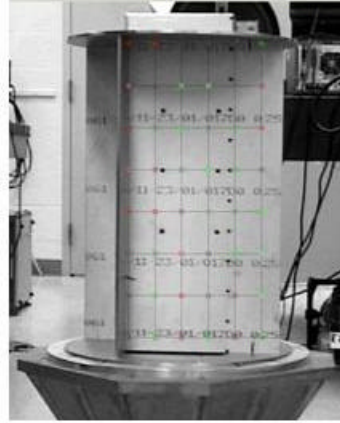


Figure 23. Laser Vibrometer and Meshed Plates

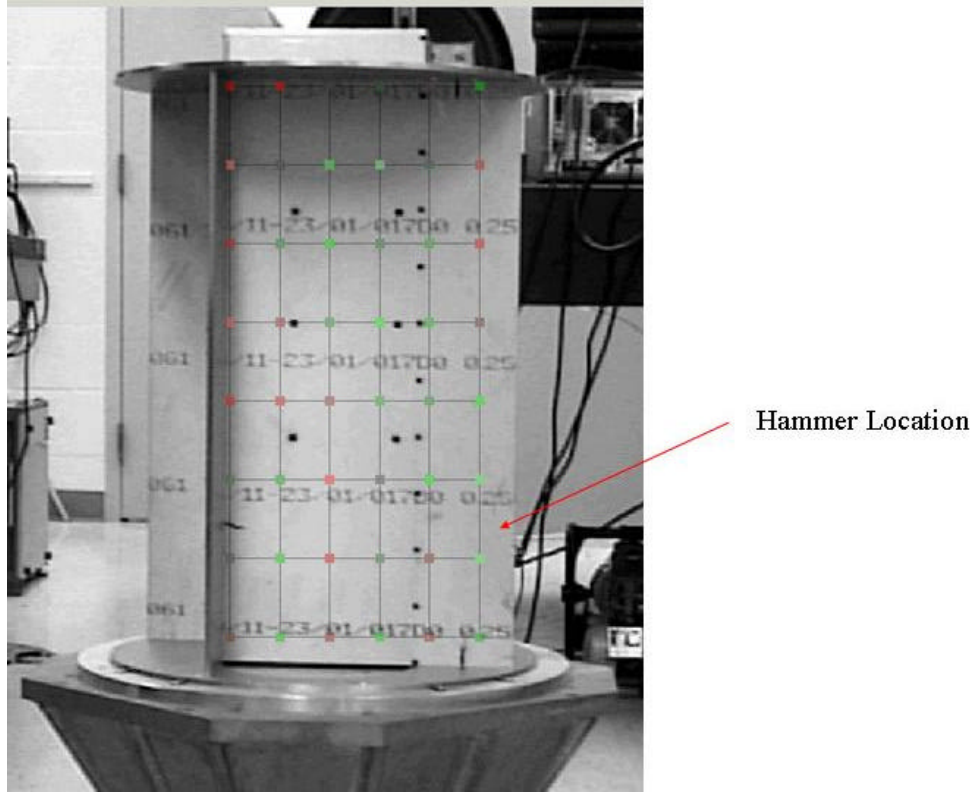


Figure 24. Ping Test Hammer Location

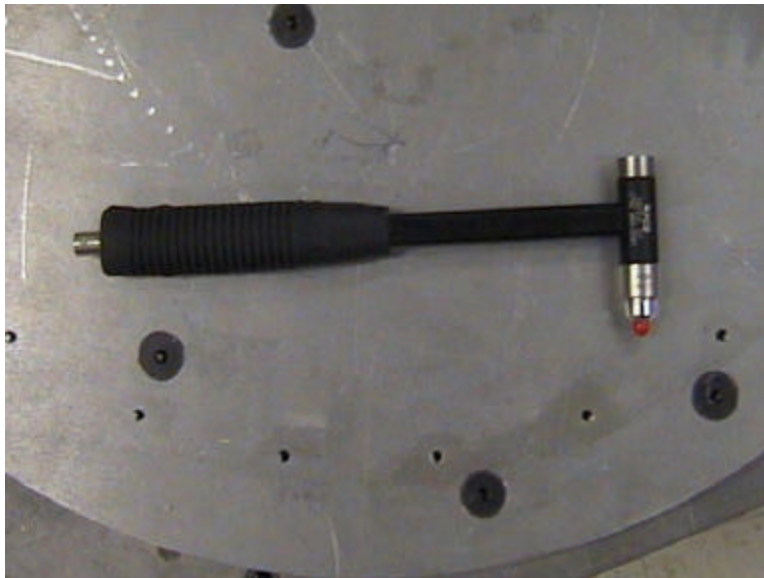


Figure 25. Ping Test Hammer

## **Dynamic Stress Analysis on Full Model**

The stress analysis was only conducted on the full scale model, and is intended to satisfy the NASA requirement for validating the structural integrity of the RIGEX structure under simulated flight limit loadings. To accomplish this, the two-dimensional shell model was modified to perform a dynamic stress analysis simulating a 15 G multi-axis body force on the structure. As NASA requires testing of worst-case scenarios for the application of the loading, the model was run with several different X,Y,Z axis loadings. These simulations were also used to help determine high stress areas that needed further investigation in the three-dimensional model to be built. They were also used to find a suitable material for construction of the final structure.

The three-dimensional model used for the stress analysis was again built from the PRO-Engineer solid modeling program, used to provide the manufacturing drawings used for the structures construction. All loading was applied in a similar fashion as with the two-dimensional model. The batteries, ovens, and inflation systems were all attached to the model to simulate the mass of these components on the structure. One major modification to the previous model was that stainless steel nubs were modeled in the place of bolts on the surface of the EMP. These nubs were then tied to the holes in the top plate of the RIGEX structure to simulate the fasteners. This would give a more accurate representation of the stress concentrations in these areas.

## **Design and Manufacturing**

The preliminary design called for a structure made from quarter inch aluminum plates welded together in a box-like fashion and capped at the bottom and top with half and quarter inch thick aluminum plates, respectively. An estimate for the weight of this structure put it around 58 pounds, which is slightly over a quarter of the weight allowance for the entire experiment. So, one of the first considerations was how to trim some weight from the structure, and yet have it maintain enough strength and rigidity to meet NASA standards for structural integrity. Having a preliminary design allowed for the creation of a stress analysis model in ABAQUS as mentioned above. This analysis gave locations of the maximum stress values for the preliminary design structure under NASA specified load conditions. The maximum stress encountered on the structure was on the top plate near where it intersected with the corner of a 13 inch vertical plate. The value of the stress in this location was determined to be around 36 Ksi tension. This value was considered high, due to stress concentrations where the sharp corners of the vertical plates mated to the top plate. It was assumed that welding of the plates would create a fillet in these areas, thus reducing the stress concentrations. With this value, a search for an appropriate structural material began. Two wrought aluminum alloys were considered for the structure, AL 2024-T4 and AL 6061-T6. Both materials possessed adequate yield and ultimate strength values of 47/68 Ksi for AL 2024-T4 and 40/45 Ksi for AL 6061-T6 based on values from the Metals handbook (3). AL 2024-T4 is difficult to weld and has poor Stress Corrosion Cracking (SCC) resistance, the latter places it in Table II of MSFC-SPEC-522B which requires special approval from NASA to use. AL 6061-T6 has

excellent weldability and SCC resistance, and thus was selected for use in the construction of the RIGEX structure.

As power requirements for the experiment increased, so did the need for more battery cells and battery cell volume within the structure. As the battery weight climbed from 53 to 70 lbs, the experiment exceeded the GAS weight limitation. In order to correct this, weight would have to be trimmed in other areas of the RIGEX project. With this in mind, the structural design was examined for areas of potential weight savings, and several design changes were made to incorporate the new battery cell while cutting structure weight. The first of the changes was to reduce the thickness of the bottom plate from half to quarter inch aluminum. This was done resulting in a ten pound weight savings. The second modification extended the battery box area through the bottom plate, effectively lengthening the battery compartment by two inches with no additional structure weight.

PRO-Engineer was used to create all the structural components and allow the parts to be fitted together as a three-dimensional assembly and to fit-check the entire structure as it was being pieced together. The parts and assemblies created in Pro-Engineer could also be turned into shop drawings for manufacturing, with a few clicks of the mouse. Pro-Engineer also assisted in the construction of ABAQUS models. Parts and assemblies created in Pro-Engineer were converted to IGES files and exported into ABAQUS where they were meshed out and used for stress and frequency analysis.

Another consideration in the construction of the structure was to use screws to fasten the structure together until all the subsystems and experimental components could be attached. This would allow the structure to be disassembled and modified for



component additions. When modifications are complete, the screws will provide a means for stabilizing the structure while it is being welded together.

Finally, bumpers for lateral stability of the cantilevered end of the structure must be manufactured. At least three are required and are to be equally spaced around the outside edge of the bottom plate. Each bumper is composed of four main parts: the Viton rubber facing, aluminum face plate, thread all (for adjusting the bumper) and mounting bracket. The bumper assembly is depicted in Figure 26.

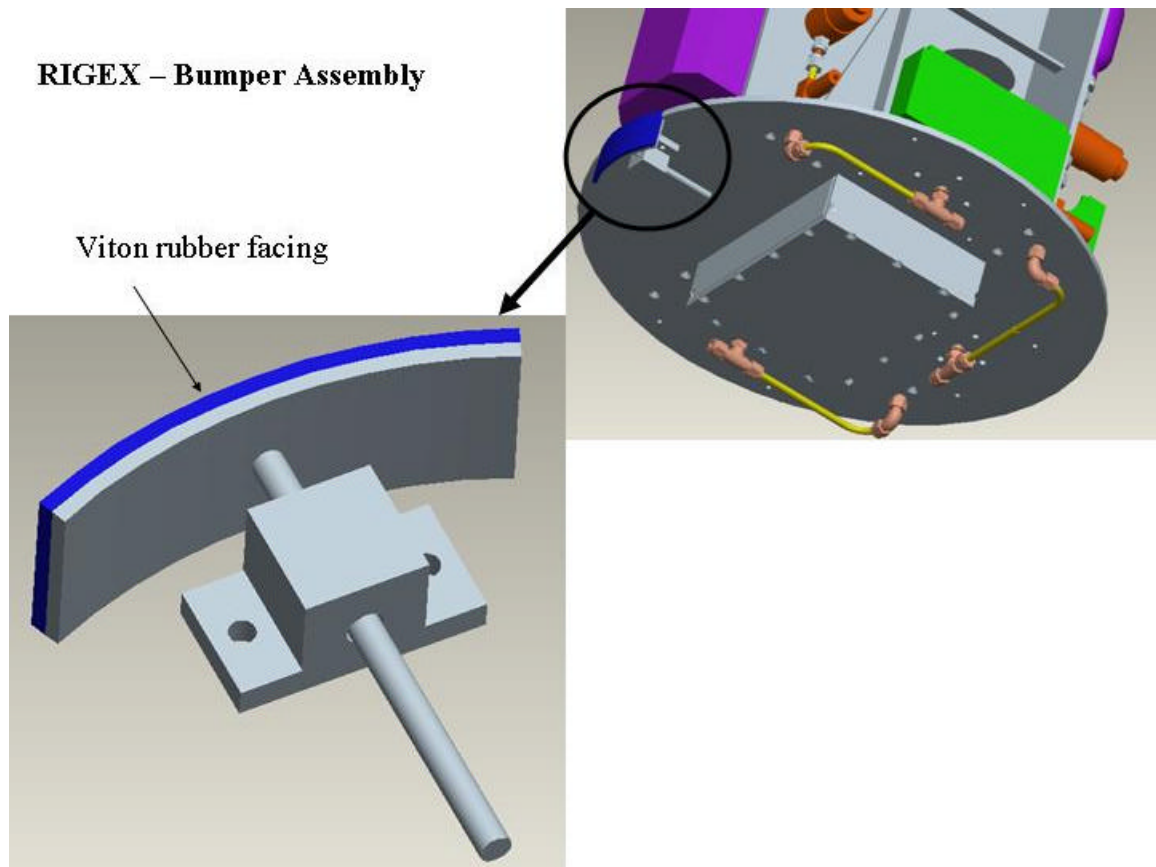


Figure 26. Bumper Assembly



## **IV: Results and Discussion**

### **Overview**

The results of the frequency analysis for the inflatable tube, quarter structure and full structure are presented in this chapter as well as the stress analysis for the full structure. The ABAQUS frequency model for the tube is developed first using Young's Modulus developed from the Fundamental Frequency Formula presented in the Literature Review. In the second section, an ABAQUS tube model is further developed by constructing it as a three-dimensional entity. Section three presents the frequency analysis results of the quarter structure modeled in ABAQUS. Finally, the frequency and stress analysis results for the full RIGEX support assembly are presented.

### **ABAQUS Vibration Results**

Frequency analysis using ABAQUS/FEA proceeds from a simple one-dimensional beam model through to the modeling of the entire RIGEX structure. Each successive model presented entailed an increasing degree of complexity regarding element type, component modeling and assembly techniques. As each successive model was constructed, the frequency results produced for the individual models were compared to results obtained from ping testing the actual assembly that had been modeled.

In all cases, the ABAQUS model provided good correlation with the results obtained from testing. This allowed for frequency validation of the entire RIGEX

structure before all components could actually be manufactured and assembled, with reasonable certainty that the results would compare favorably with those obtained once the structure was actually completed.

### **Rigidized Tube Model Results**

The frequency analysis of the RIGEX inflated and rigidized tube proceeded by developing ABAQUS models of the tube based on two and three-dimensional representations of the tube. The first considered was the two-dimensional beam or pipe model, which was modeled using the length between the flanges as the length of the tube and a point mass on the free end to simulate the top flange. The beam model was run using the ABAQUS Lanczos eigensolver which produced the plots in Figures (27 - 31). The bending modes produced from the ABAQUS model were compared with the experimental values determined in Philley's thesis (25), and were found to be in good agreement with the results presented for the inflated tube mounted to the table. The 2-D tube model incorporated the clamped end boundary condition from Figure 15.

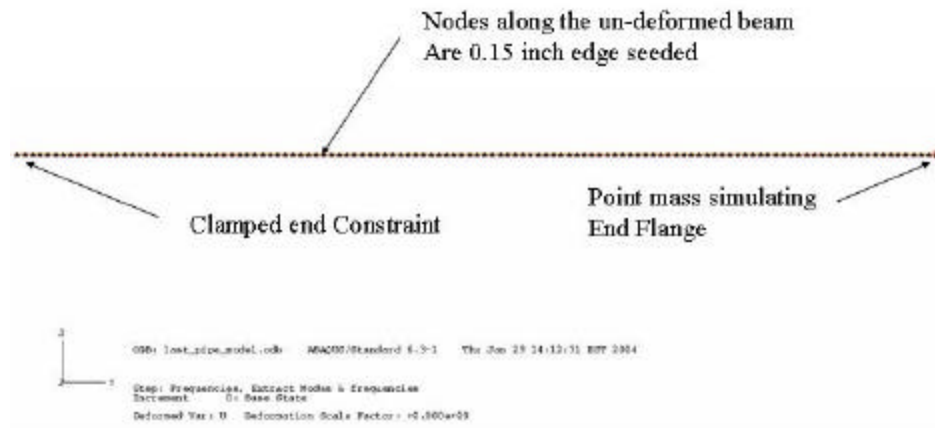


Figure 27. ABAQUS Beam Model

Figure 27 depicts the centerline of a tube whose cross-sectional properties were defined in ABAQUS using the inside and outside radius of the composite tube. The section was then broken down into elements using a 0.15 inch seeding along the length of the tube.

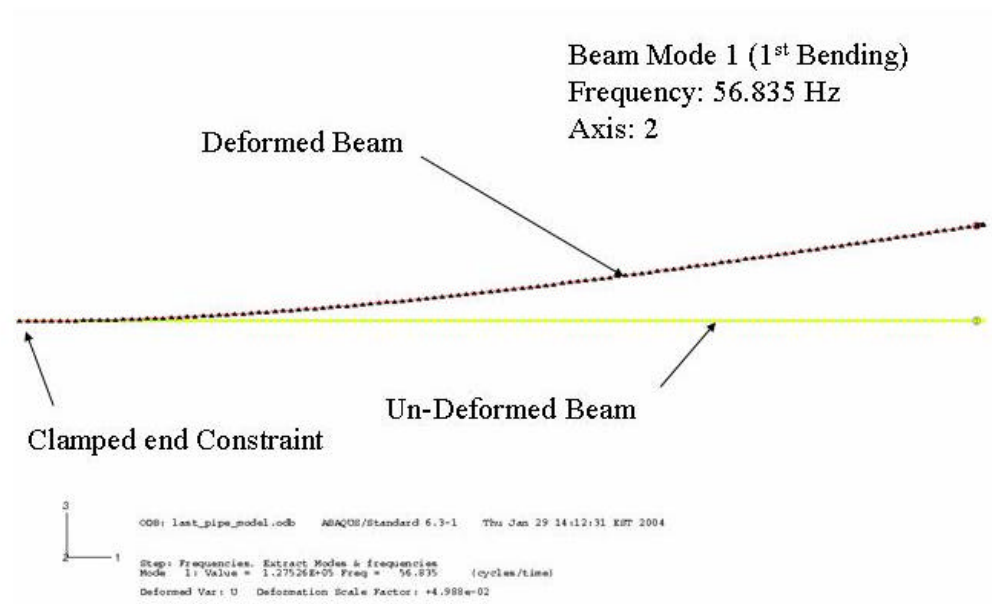
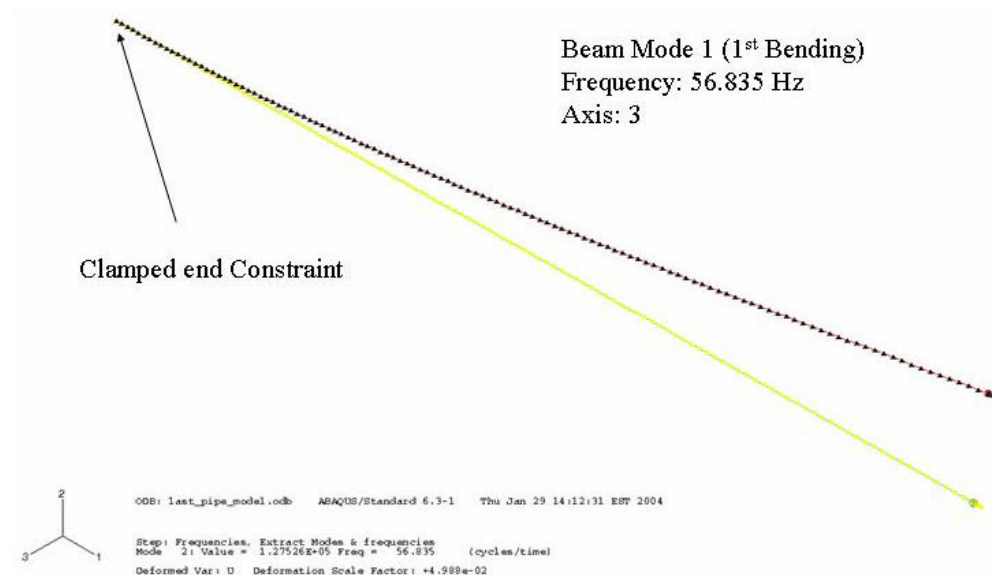


Figure 28. 1<sup>st</sup> Bending Mode of the Beam Model

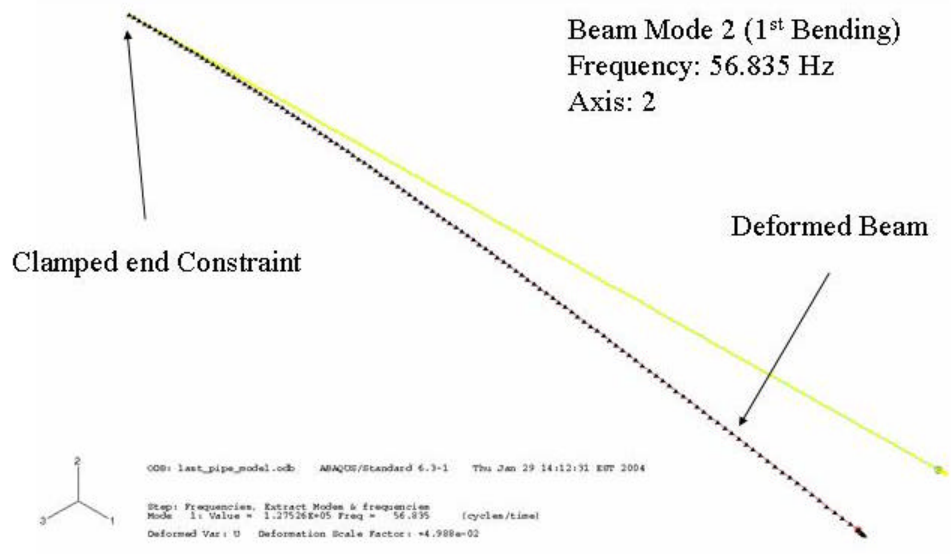
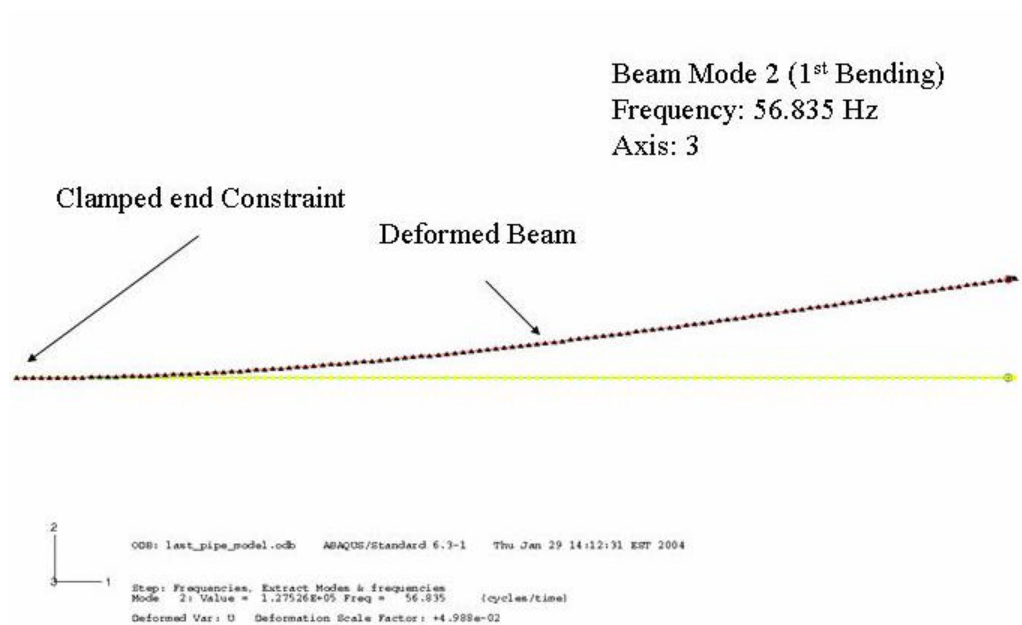


Figure 29. 1<sup>st</sup> Bending Mode of the Beam Model about Axis 2

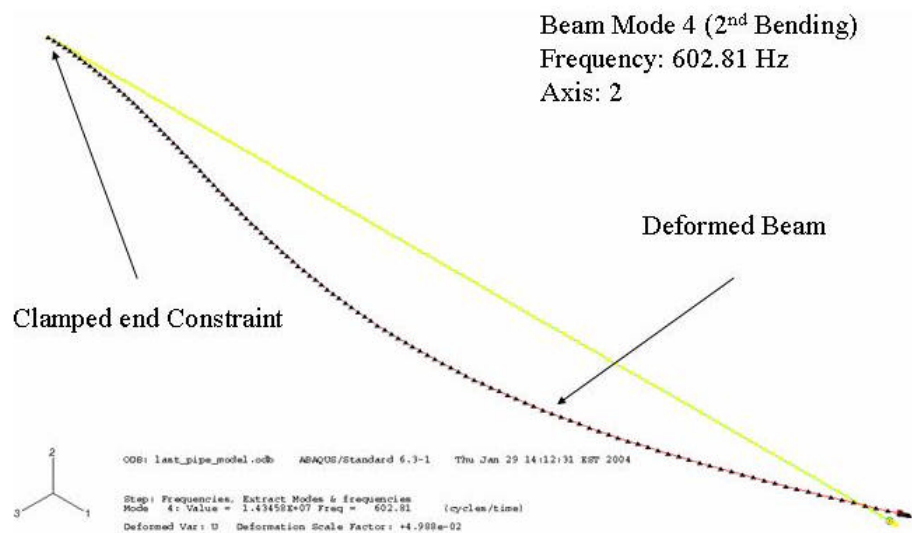
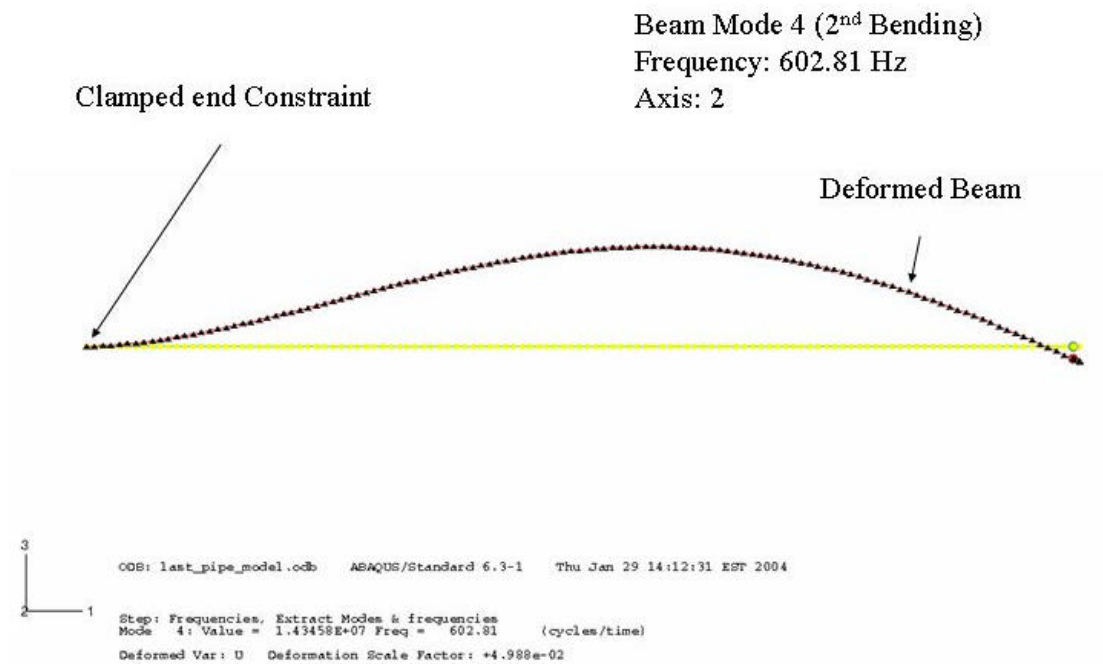


Figure 30. 2<sup>nd</sup> Bending Mode of the Beam Model about Axis 2

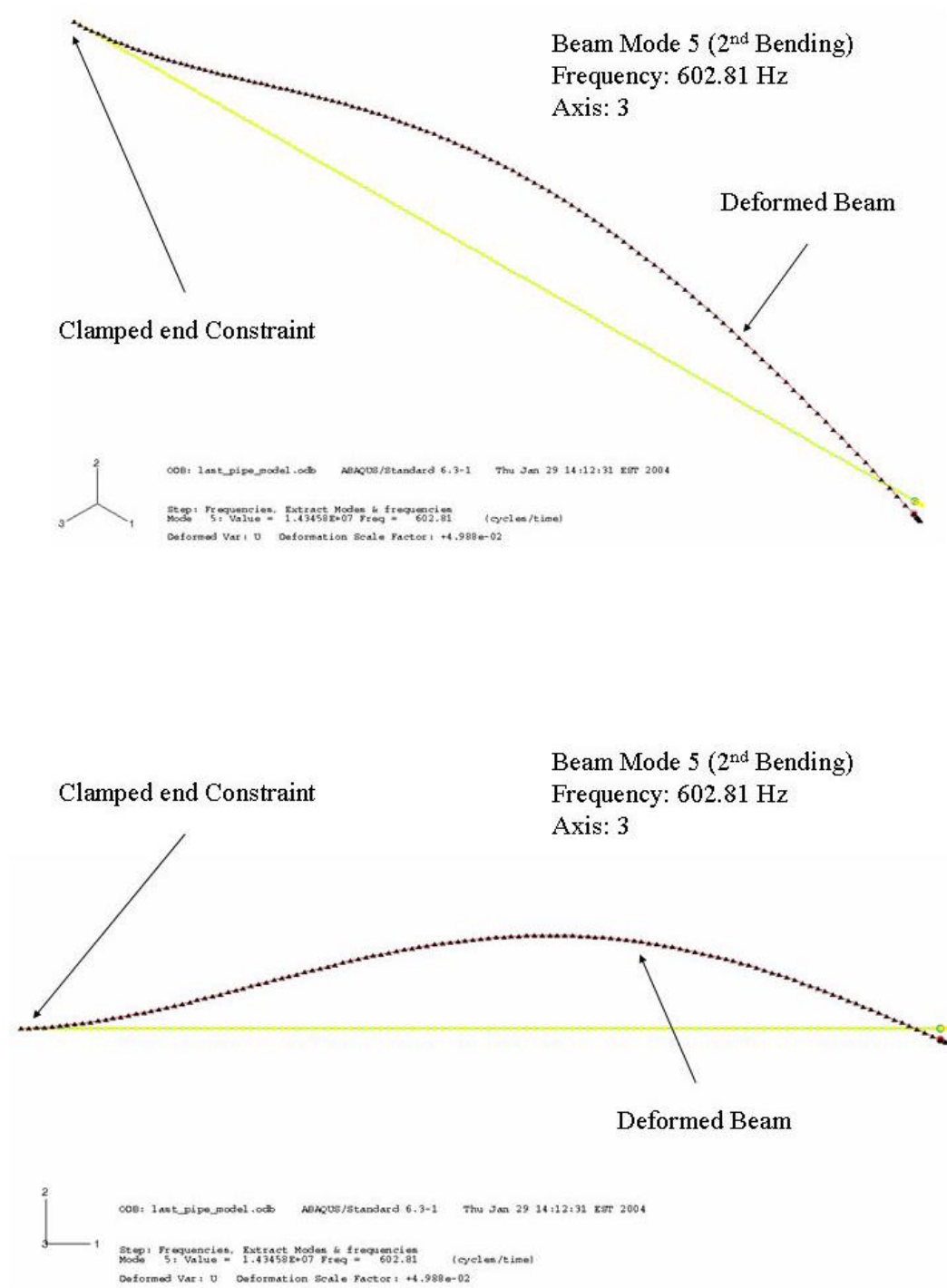


Figure 31. 2<sup>nd</sup> Bending Mode of the Beam Model about Axis 3

A second and more accurate three-dimensional representation of the tube was constructed using the actual dimensions for each component of the tube. This model was intended to verify the ability of ABAQUS to produce accurate results using three-dimensional continuum elements and assembled components to produce a representative model of the geometry to be analyzed. Again, the model was run using ABAQUS Lanczos natural frequency, and the results were compared to those obtained with the one-dimensional beam model and experimental values. The values produced by the three-dimensional model were also found to be in good agreement with those of the ABAQUS beam model and experimental values for the table mounted beam. In addition, for the three-dimensional model a mesh convergence study was conducted where the mesh density of the tube was reduced until the frequency results converged to within ten percent. Mesh reduction beyond this point was considered impractical due to the increase in the amount of time required for the model to produce a solution. Results for the first two bending modes and first torsional mode of the coarse and refined tube model are presented in Figures 32-35. The ping test frequency response plots for the tube can be found in Appendix C.1.





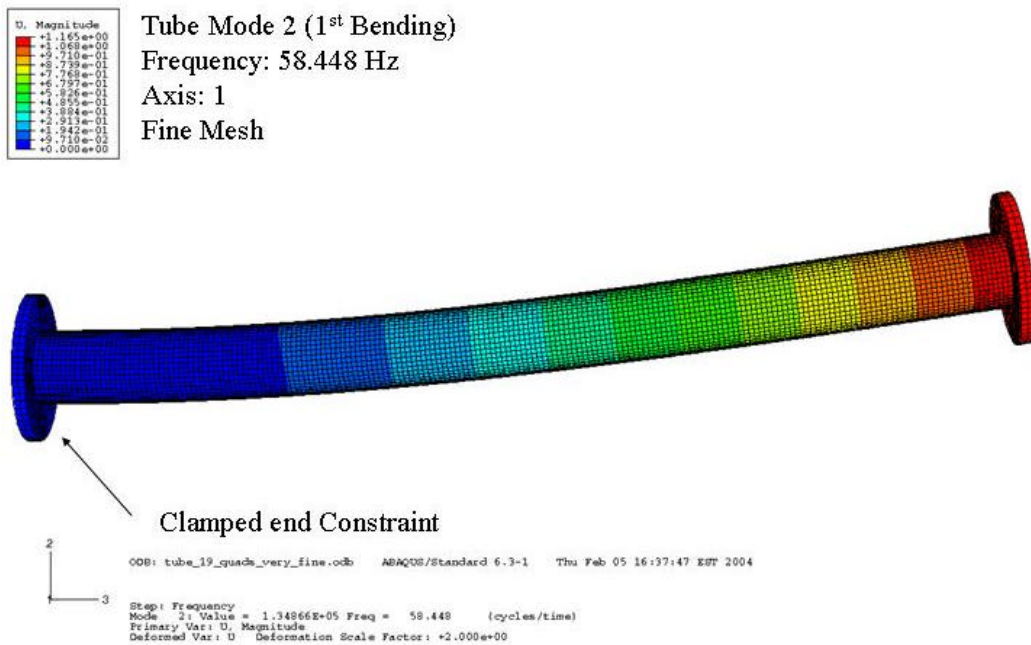
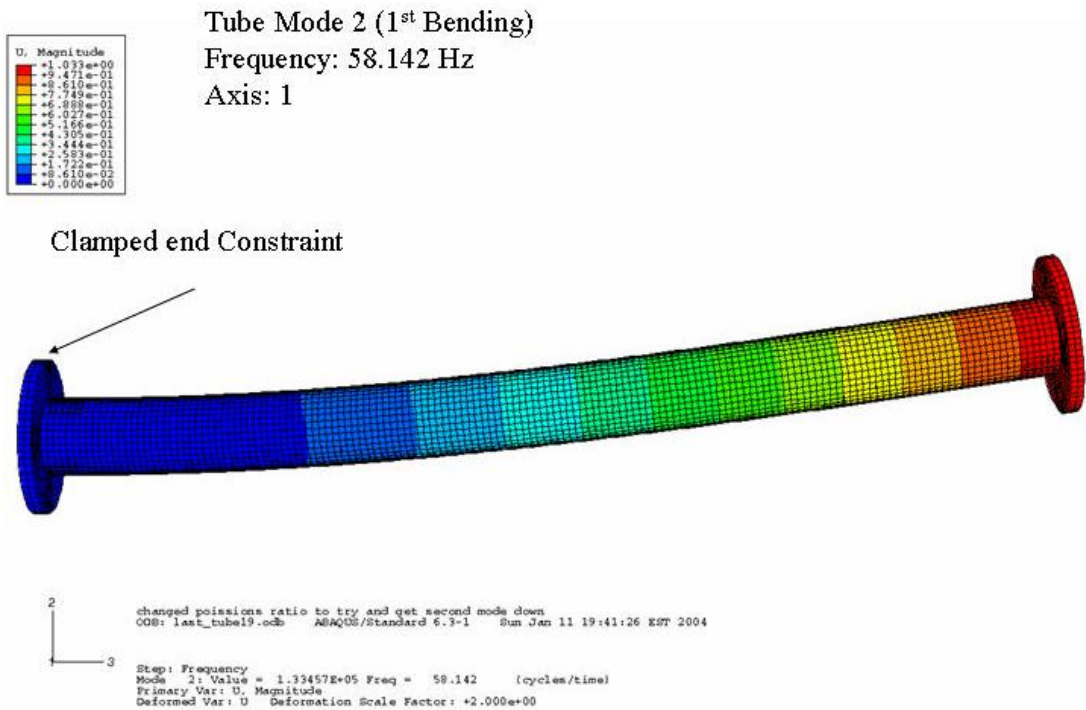


Figure 33. Coarse and Fine Mesh for 1<sup>st</sup> Bending Mode of Tube Model about Axis 1

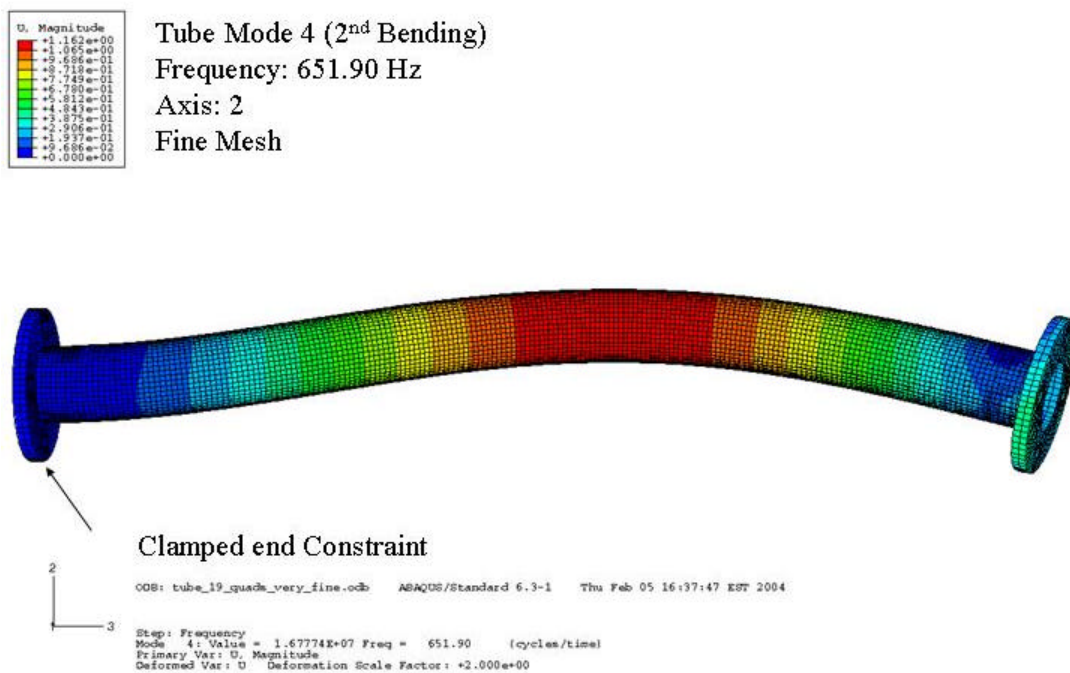
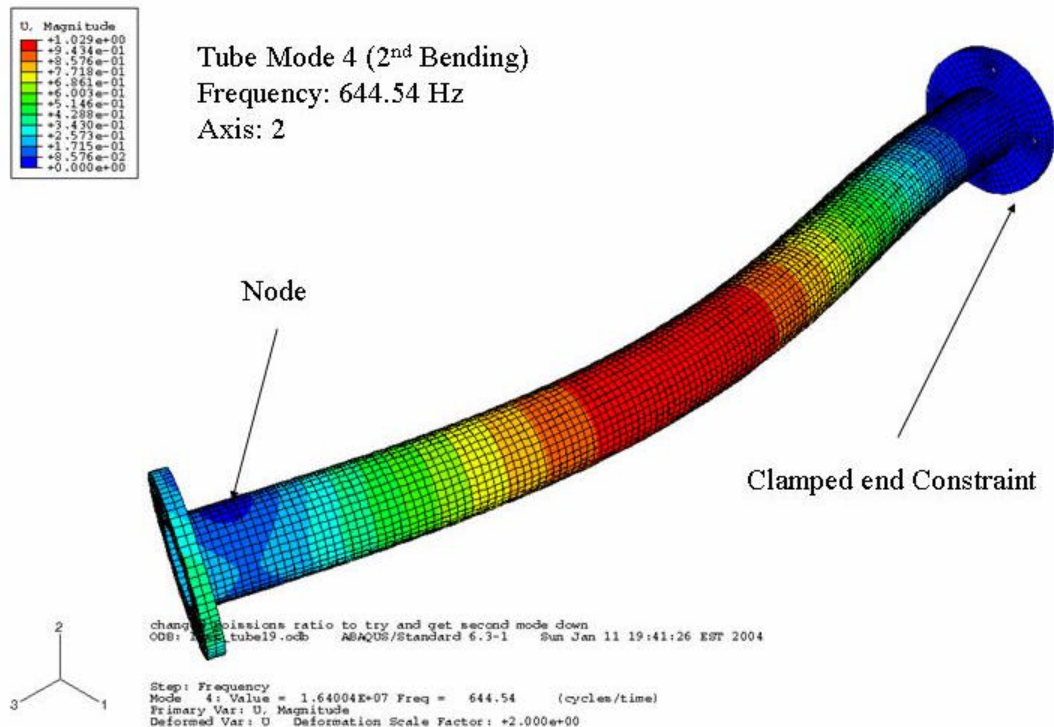


Figure 34. Coarse and Fine Mesh for 2<sup>nd</sup> Bending Mode of Tube Model about Axis 2

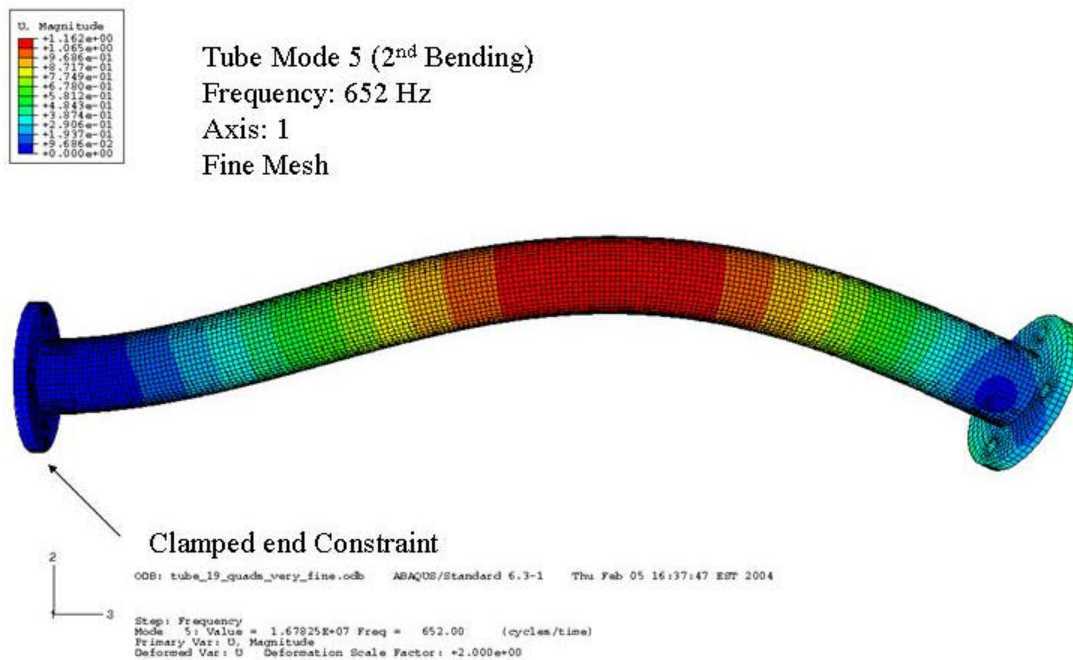
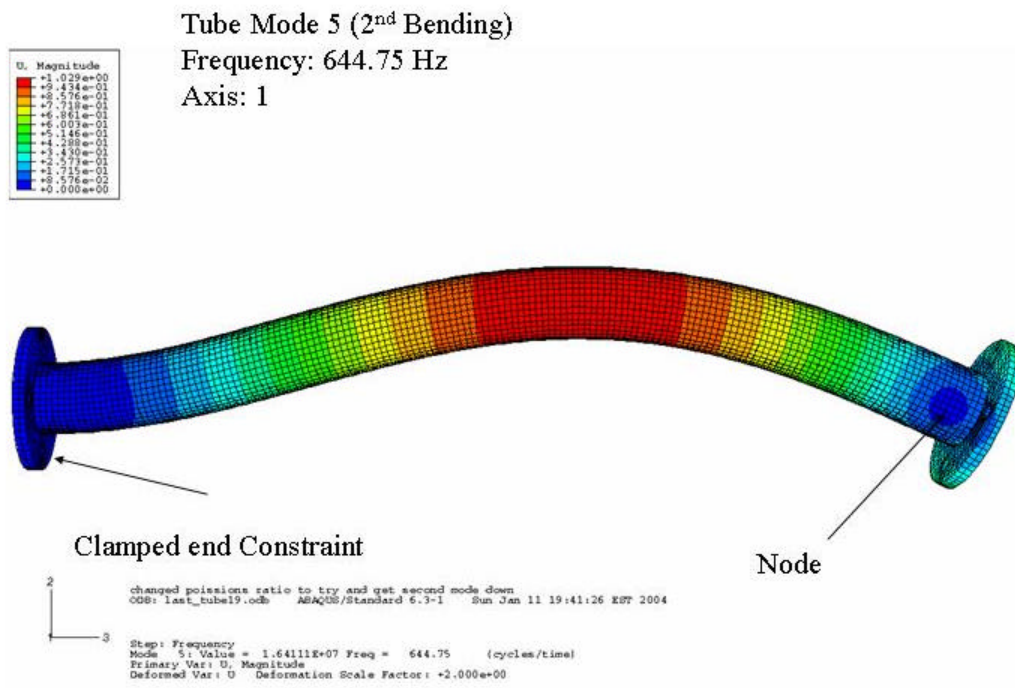


Figure 35. Coarse and Fine Mesh for 2<sup>nd</sup> Bending Mode of Tube Model about Axis 1

Results of the beam and three-dimensional tube model are depicted in Table 7. The figures for the simply supported and tube with 15 gram RIGEX experiment accelerometer can be found in Appendix C.1 and C.2. The simply supported model was constructed to determine the effect of using two bolts, instead of four, to secure the bottom flange to the table. This type of restraint represented more of a simply supported boundary condition along the axis where the bolts were removed. The effects on the frequency response of the tube can also be seen in Table 7.

Table 7. Results of the Beam and Three-Dimensional Tube Model

Model	Mesh Density	Frequency 1 <sup>st</sup> Bending (Hz)	Frequency 2 <sup>nd</sup> Bending (Hz)	Percent Difference 1 <sup>st</sup> Bending	Percent Difference 2 <sup>nd</sup> Bending
Test Results Philley's Thesis (25) Table Mount	-	59.688	660	-	-
ABAQUS 2-D Beam	0.15 inch	56.835	602.81	4.78	8.94
ABAQUS 3-D Tube Quadratic Hex	0.2 inch	58.12 58.142	644.54 644.75	2.62 2.59	2.34 2.31
ABAQUS 3-D Tube Quadratic Hex	0.1 inch	58.441 58.448	651.9 652.0	2.09 2.08	1.21 1.21
ABAQUS 3-D Tube Quadratic Hex Simply Supported	0.1 inch	57.056 50.919	562.21 629.60	4.41 14.69	4.61 14.81
ABAQUS 3-D Tube Quadratic Hex Accelerometer	0.1 inch	50.667 50.683	622.27 625.88	-	-

## **Quarter Structure Model Results**

To develop a more representative model of the RIGEX structure for verifying the ABAQUS frequency analysis technique, the quarter test structure was modeled and a frequency run performed. This model was constructed using techniques and elements to be used in the construction of the RIGEX full scale model, and could be done while the flight article was being manufactured. The quarter model provided a convenient test bed, as it was on hand and ping testing could be conducted to provide immediate verification of the results obtained through the ABAQUS frequency analysis of the model. The model was constructed using quadratic hexahedron elements and tied to a model of the EMP. Masses representing the oven and inflation system were tied to the structure and a frequency analysis run performed in ABAQUS. The first three mode shapes and frequencies were obtained for a coarse and fine meshed model of the structure. The fine mesh was again based on a ten percent mesh convergence criteria. The results for the first three modes of the quarter structure are depicted in Figures 36-38. The coarse mesh of 0.4 represents a 0.4 inch edge seeding, and the fine mesh of 0.2 represents a 0.2 inch edge seeding.



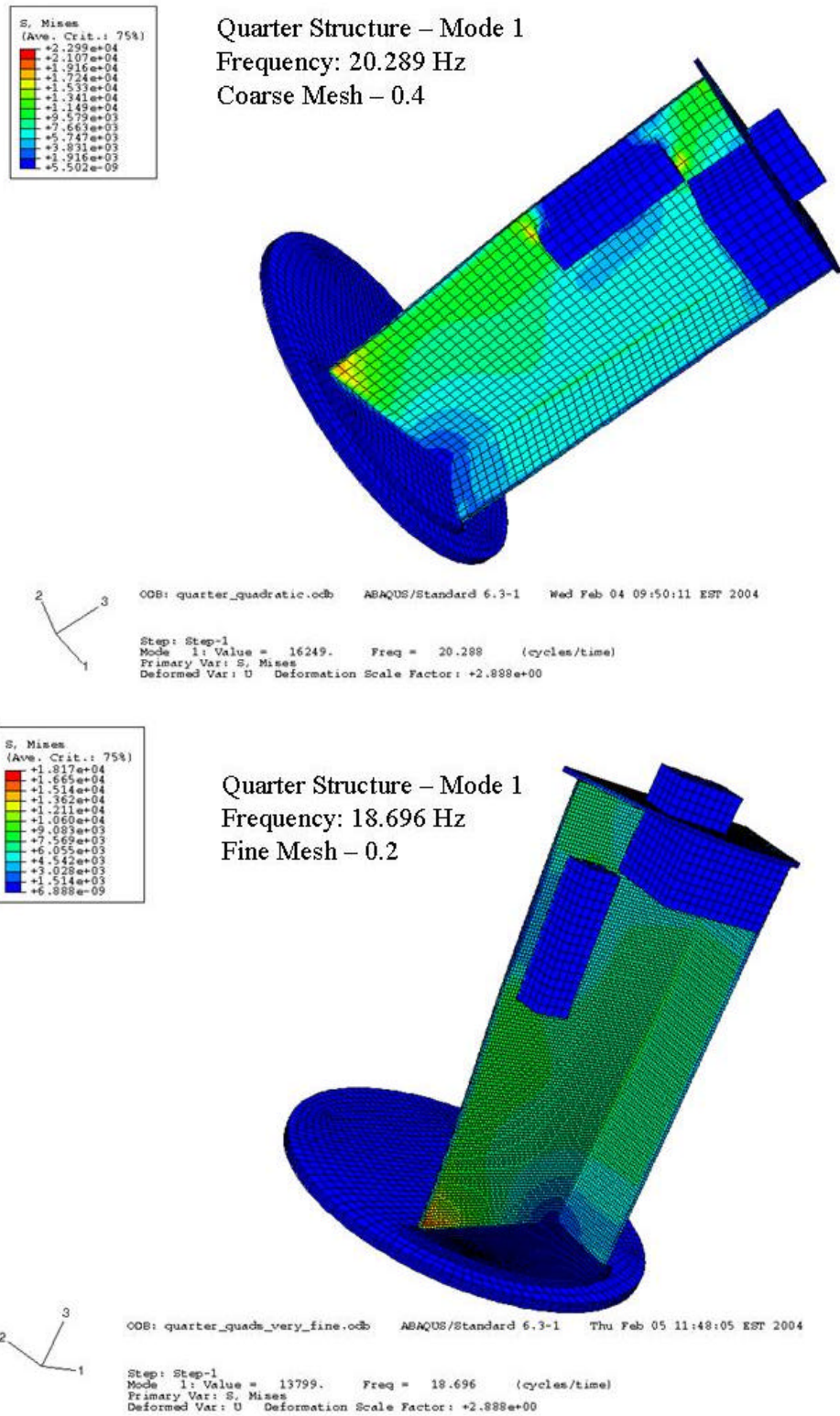
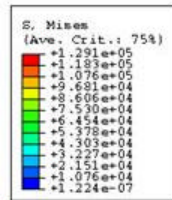
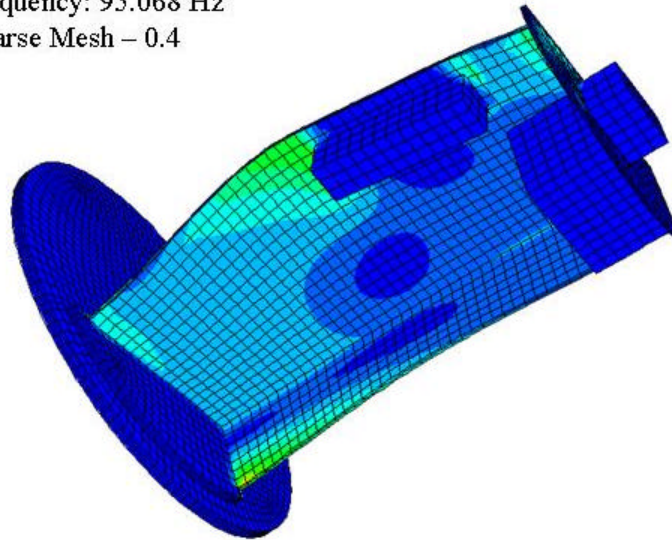


Figure 36. Coarse and Fine Mesh for Mode 1 of Quarter Structure

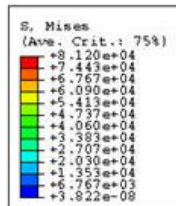


Quarter Structure – Mode 2  
Frequency: 95.068 Hz  
Coarse Mesh – 0.4

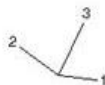
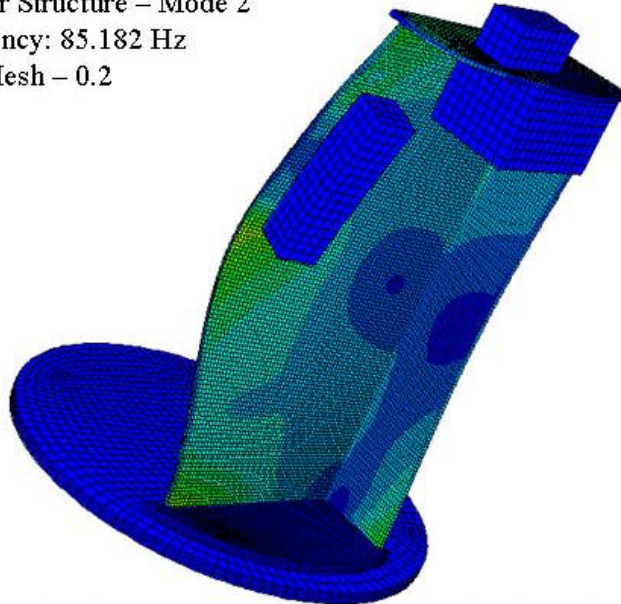


ODB: quarter\_quadratic.odb ABAQUS/Standard 6.3-1 Wed Feb 04 09:50:11 EST 2004

Step: Step-1  
Mode 2: Value = 3.56804E+05 Freq = 95.068 (cycles/time)  
Primary Var: S, Mises  
Deformed Var: U Deformation Scale Factor: +2.988e+00



Quarter Structure – Mode 2  
Frequency: 85.182 Hz  
Fine Mesh – 0.2

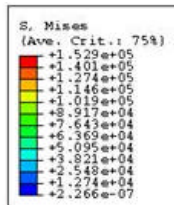


ODB: quarter\_quads\_very\_fine.odb ABAQUS/Standard 6.3-1 Thu Feb 05 11:48:05 EST 2004

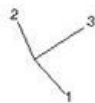
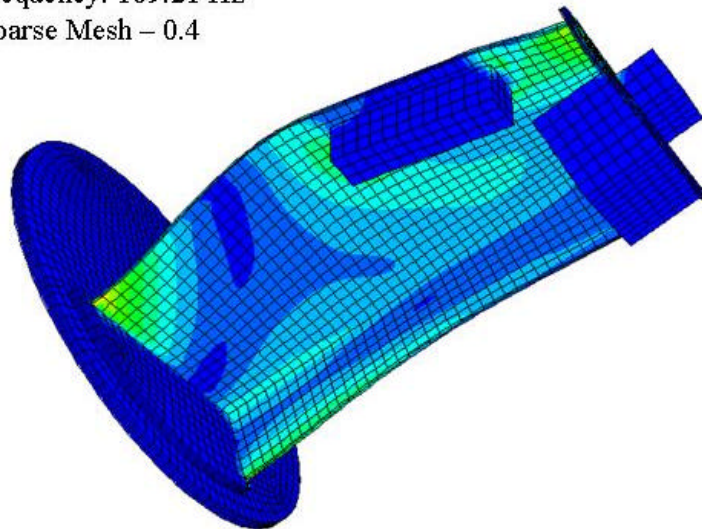
Step: Step-1  
Mode 2: Value = 2.86453E+05 Freq = 85.182 (cycles/time)  
Primary Var: S, Mises  
Deformed Var: U Deformation Scale Factor: +2.898e+00

Figure 37. Coarse and Fine Mesh for Mode 2 of Quarter Structure



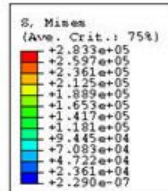


Quarter Structure – Mode 3  
Frequency: 109.21 Hz  
Coarse Mesh – 0.4

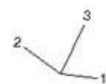
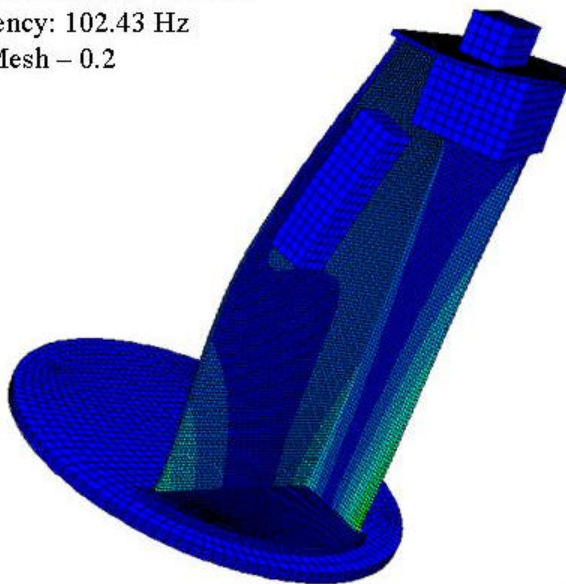


ODB: quarter\_quadratic.odb ABAQUS/Standard 6.3-1 Wed Feb 04 09:50:11 EST 2004

Step: Step-1  
Mode 3: Value = 4.70895E+05 Freq = 109.21 (cycles/time)  
Primary Var: S, Mises  
Deformed Var: U Deformation Scale Factor: +2.888e+00



Quarter Structure – Mode 3  
Frequency: 102.43 Hz  
Fine Mesh – 0.2



ODB: quarter\_quads\_very\_fine.odb ABAQUS/Standard 6.3-1 Thu Feb 05 11:48:05 EST 2004

Step: Step-1  
Mode 3: Value = 4.14189E+05 Freq = 102.43 (cycles/time)  
Primary Var: S, Mises  
Deformed Var: U Deformation Scale Factor: +2.888e+00

Figure 38. Coarse and Fine Mesh for Mode 3 of Quarter Structure

Table 8. Results of the Quarter Structure Frequency Analysis

Frequency analysis method	Mode 1 (Hz)	Mode 2 (Hz)	Mode 1 Percent difference form Ping testing	Mode 2 Percent difference form Ping testing
ABAQUS linear model coarse Mesh 0.4 inch seeding w/o masses	38.38	131.26	62.63	38.45
ABAQUS linear model coarse Mesh 0.4 inch seeding (massed)	23.179	96.08	1.78	1.35
ABAQUS model - Coarse Mesh 0.4 inch seed	20.289	95.068	14.03	0.28
ABAQUS model - Fine Mesh 0.2 inch seed	18.696	85.182	20.78	10.15
Ping Testing	23.6 Hz	94.8 Hz		

Comparison of the ping test results to those obtained from the ABAQUS frequency analysis show that the results from the linear model were the most accurate. This result can be attributed to the manner in which the side inflation masses were modeled to the quarter structure. The theoretically less accurate model modeled with linear elements happened to produce better results because the side inflation masses were modeled as a lumped mass lower on the structure than they should have been. As it happened, the mass placement produced very good results on the first frequency analysis of the linear model, and was therefore considered an acceptable baseline for further model refinement. The assumption that an accurate model of the quarter structure had been obtained, led to subsequent refinements in the model that led to results that diverged

from the actual modes of the structure instead of converging. However, the lumped mass locations were not modeled too far from their actual locations, as the model tended to settle within 20% of the expected value for the first natural frequency and 10% of the second. Ping test frequency response plots for the quarter structure are located in Appendix D.2

### **Full Structure Model Results**

Having completed the frequency analysis on the tube and quarter structure the structural verification of the full RIGEX assembly could begin. It was decided to start with the frequency analysis portion of the analysis, as these results would be verifiable through ping testing. After obtaining acceptable results for the frequency analysis, the stress analysis could be performed using a modified version of the ABAQUS model used in the frequency analysis. With this methodology, parts modeled in Pro-Engineer for manufacturing the structure were imported into ABAQUS, assigned material properties based on MIL-HBK-5 and assembled as a structure. Due to time constraints and progress on assembling experimental components onto the structure, ping testing was conducted on the empty structure. These results were compared to the values obtained from the frequency analysis run on the structure modeled without experimental components. Once satisfied with the results for the empty model, the component masses were added and another frequency run was performed to determine if the entire structure met the NASA requirement that the RIGEX experiments first natural frequency be above 35 Hz. Once the frequency verification was complete, the final segment of the RIGEX structural verification was undertaken. The ABAQUS model from the frequency analysis was

modified to perform a stress analysis on the structure and to ensure that the stresses resulting from the application of 15 and 20 G loads would not exceed the yield strength for the 15 G case or the ultimate strength of the structural material for the 20 G case. Figure 39 depicts the type and number elements used to mesh out the three-dimensional ABAQUS model of the empty RIGEX structure.

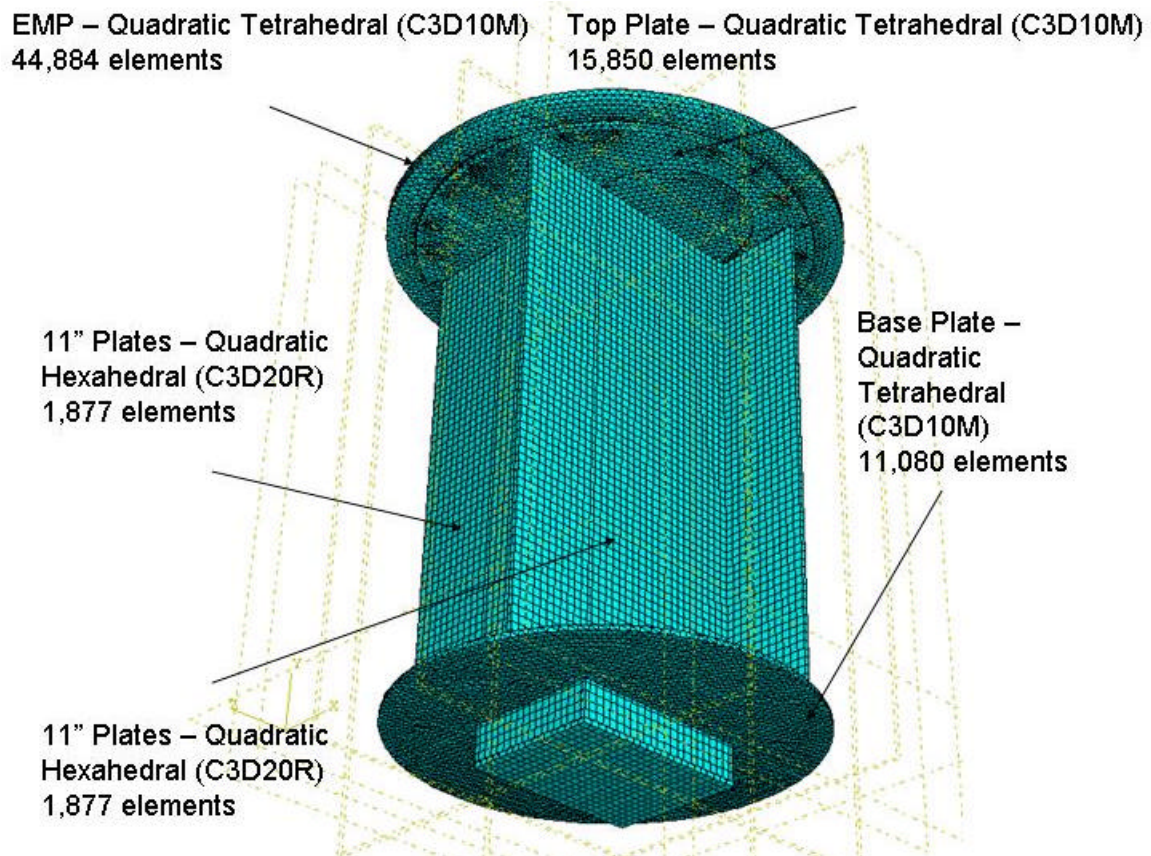


Figure 39. Three-Dimensional ABAQUS Full Structure Model

The first model constructed for the frequency analysis of the full structure used linear plate elements and a band of elements partitioned in the region of the bolt ring to approximate the boundary condition between the EMP and the structure. Subsequent changes in structure design called for several model iterations to incorporate the changes.

The two-dimensional model was also run with quadratic plate elements to further refine the model. The refined plate model frequency results are shown for the first two modes in Figures 40 and 41. The results for the quadratic three-dimensional model are presented in Figures 42-45.

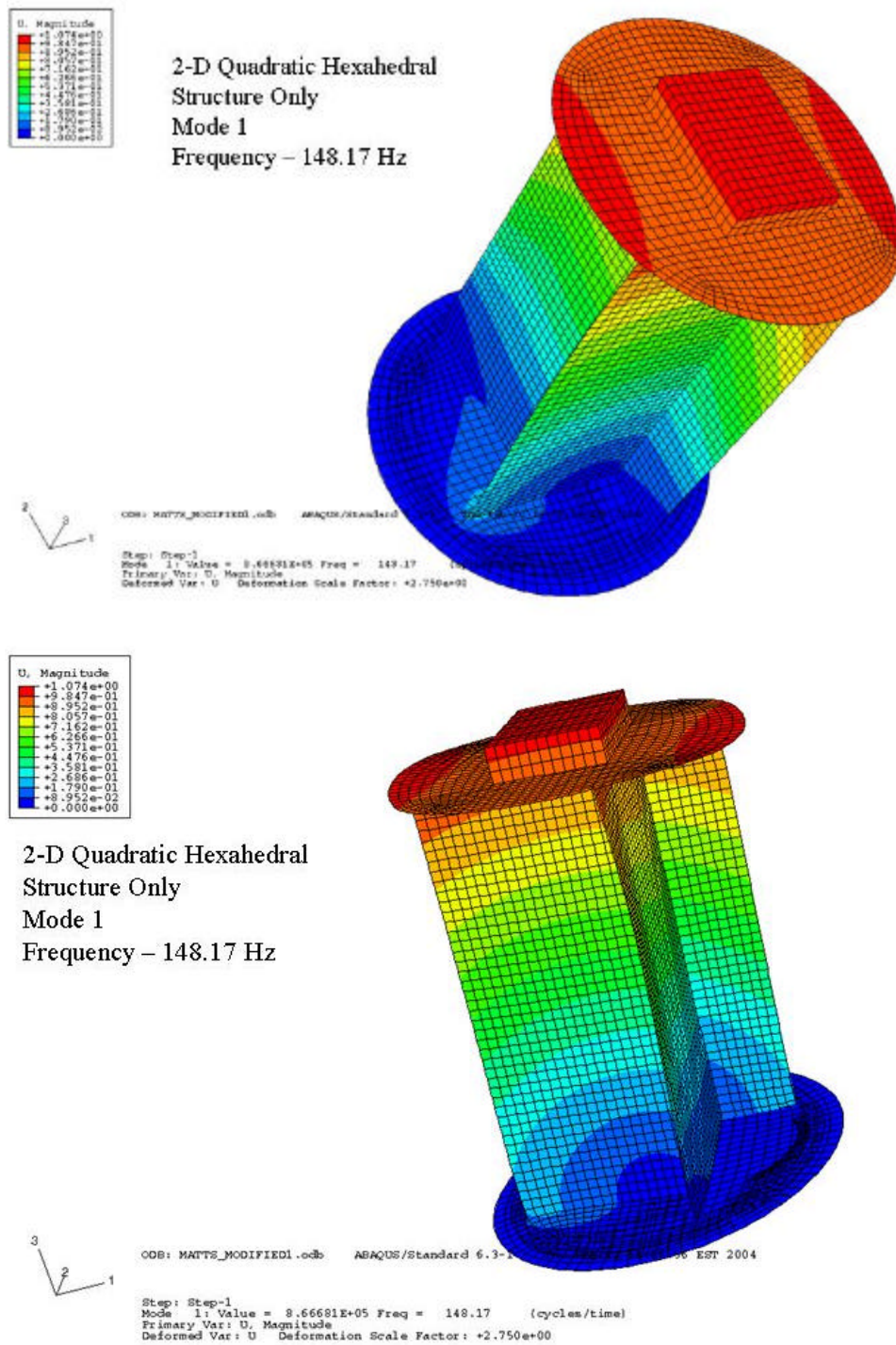
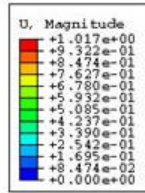
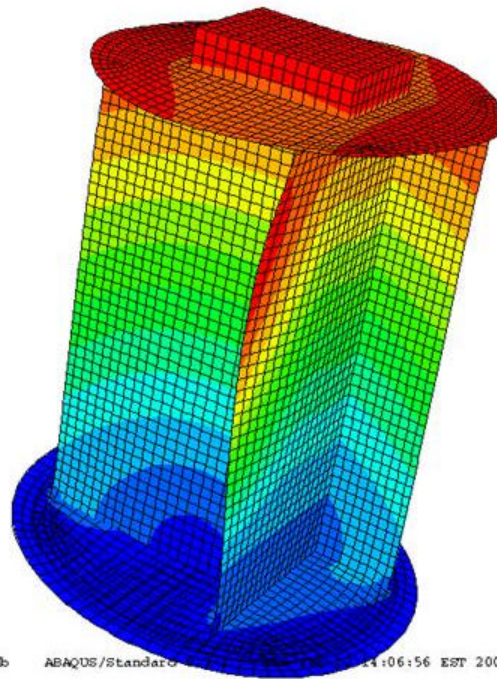


Figure 40. Mode 1 for the Two-Dimensional Model of the RIGEX Structure



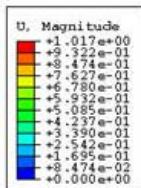


2-D Quadratic Hexahedral  
Structure Only  
Mode 2  
Frequency – 192.69 Hz

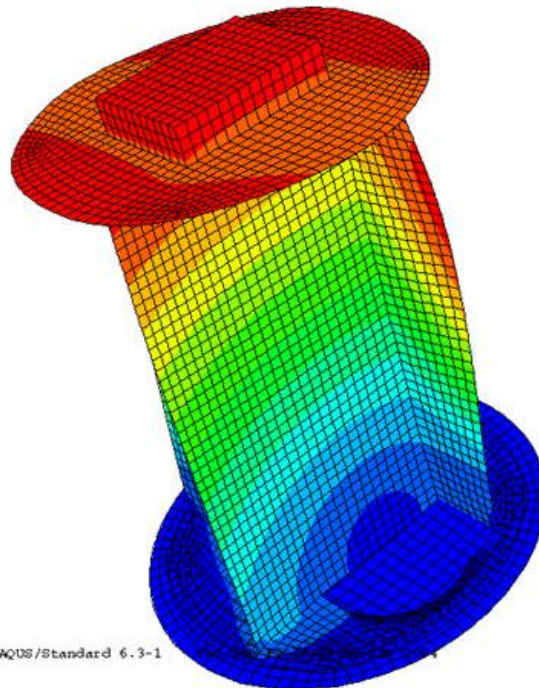


ODB: MATTS\_MODIFIED1.odb ABAQUS/Standard 6.3-1 11:06:56 EST 2004

Step: Step-1  
Mode 2: Value = 1.46576E+06 Freq = 192.69 (cycles/time)  
Primary Var: U, Magnitude  
Deformed Var: U Deformation Scale Factor: +2.750e+00



2-D Quadratic Hexahedral  
Structure Only  
Mode 2  
Frequency – 192.69 Hz



ODB: MATTS\_MODIFIED1.odb ABAQUS/Standard 6.3-1 11:06:56 EST 2004

Step: Step-1  
Mode 2: Value = 1.46576E+06 Freq = 192.69 (cycles/time)  
Primary Var: U, Magnitude  
Deformed Var: U Deformation Scale Factor: +2.750e+00

Figure 41. Mode 2 for the Two-Dimensional Model of the RIGEX Structure

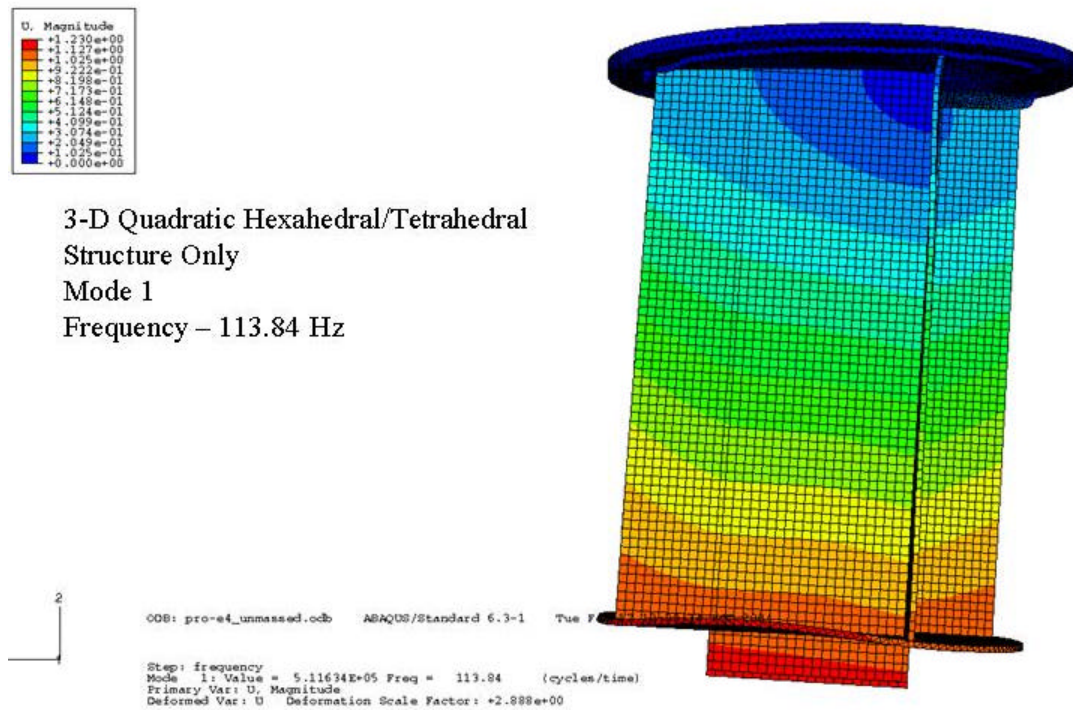
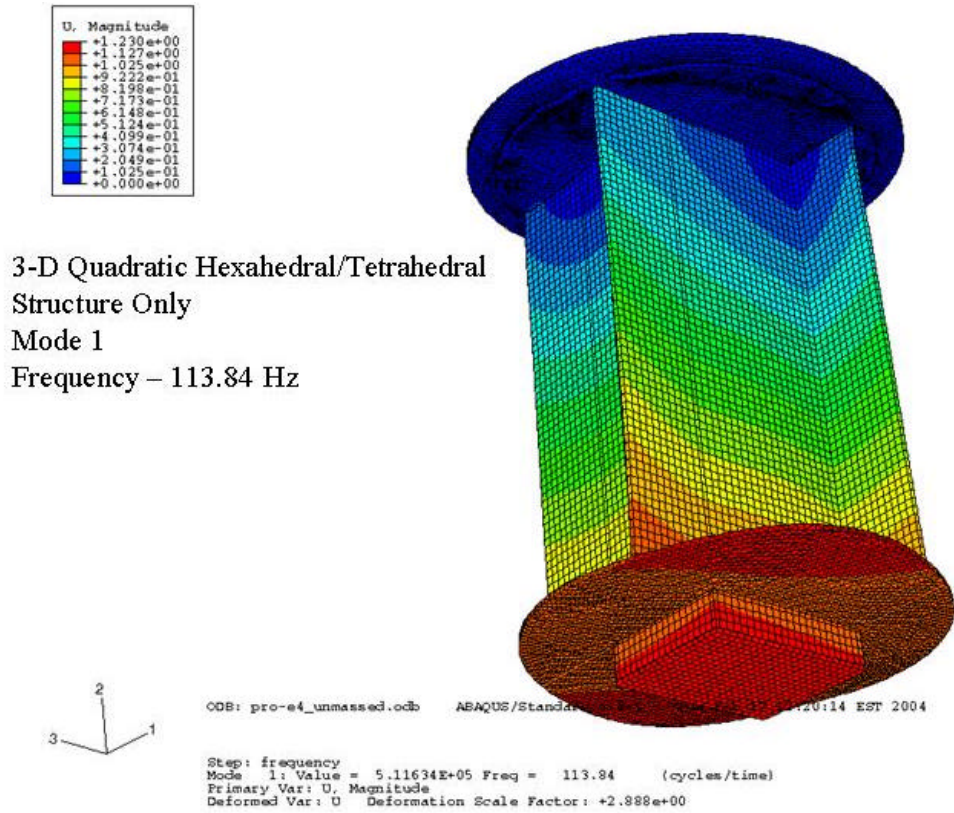


Figure 42. Mode 1 for the Three-Dimensional Model of the RIGEX Structure



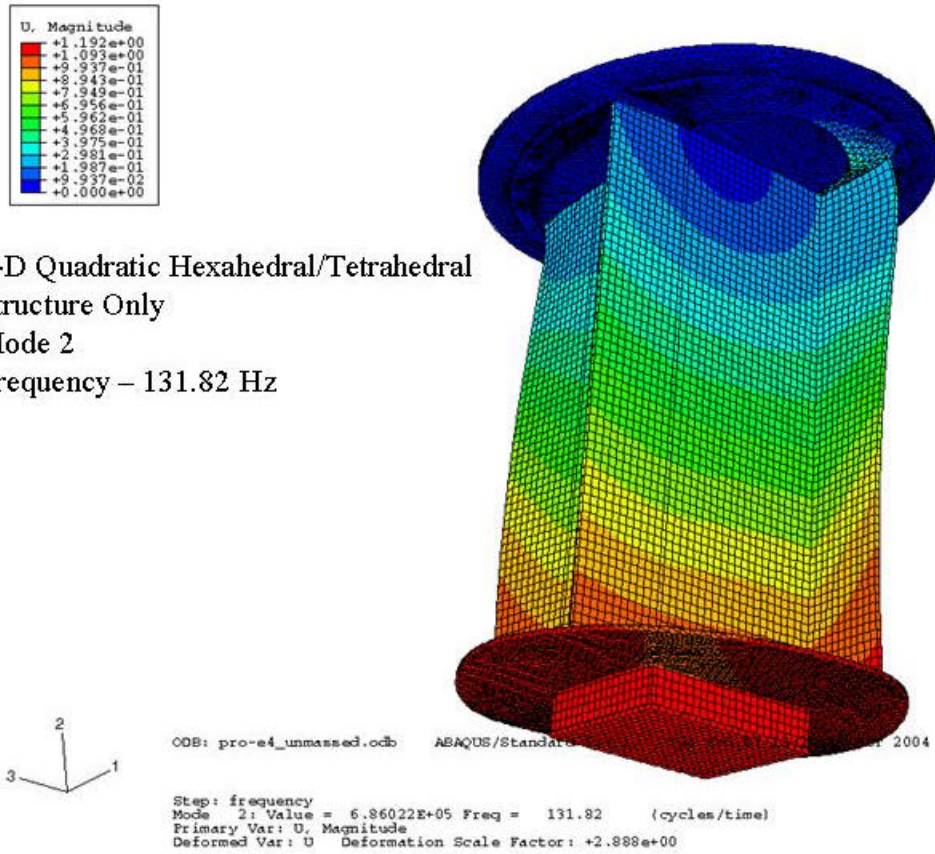


Figure 43. Mode 2 for the Three-Dimensional Model of the RIGEX Structure

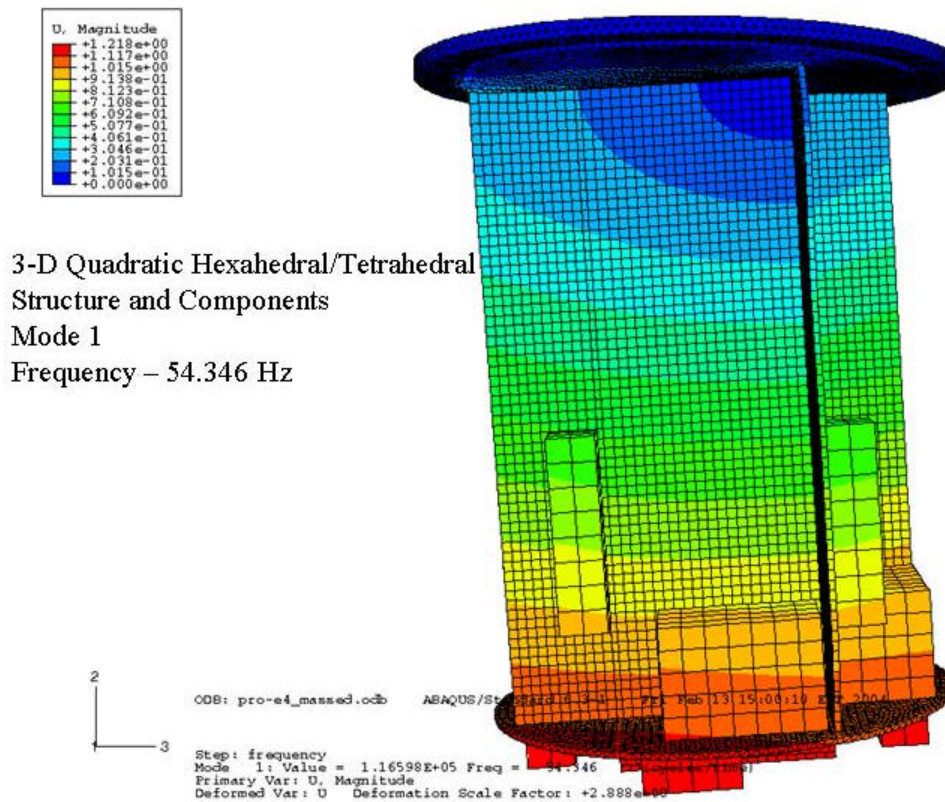
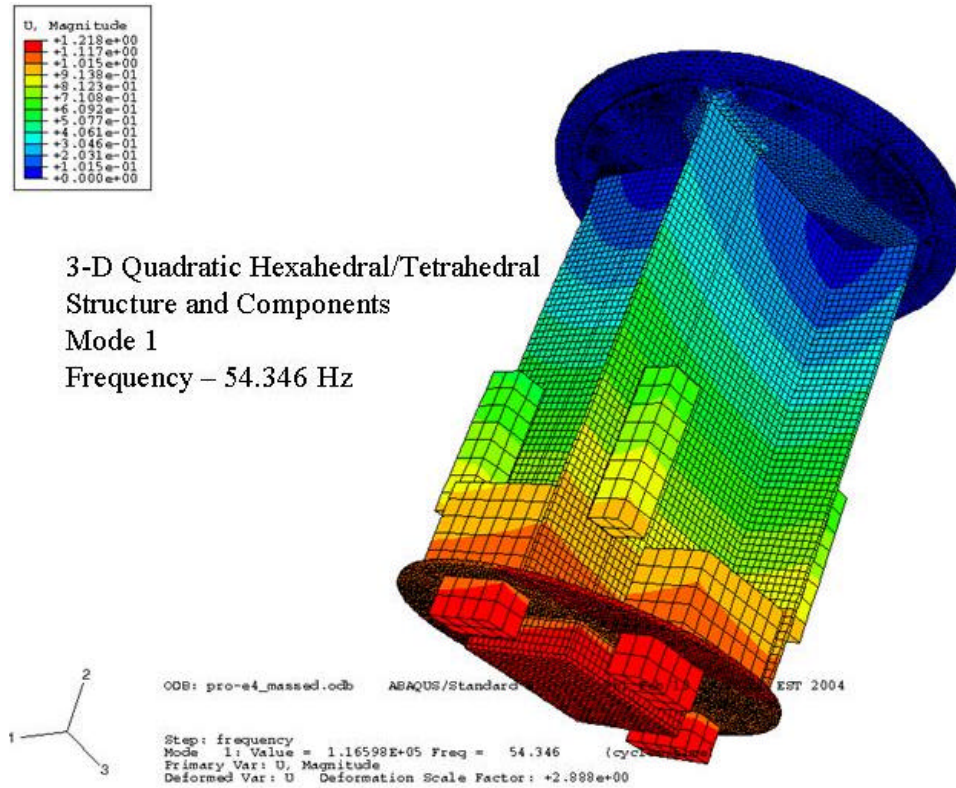
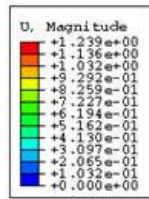


Figure 44. Mode 1 for the Massed Three-Dimensional Model of the RIGEX Structure



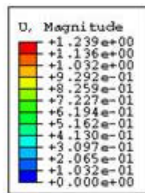
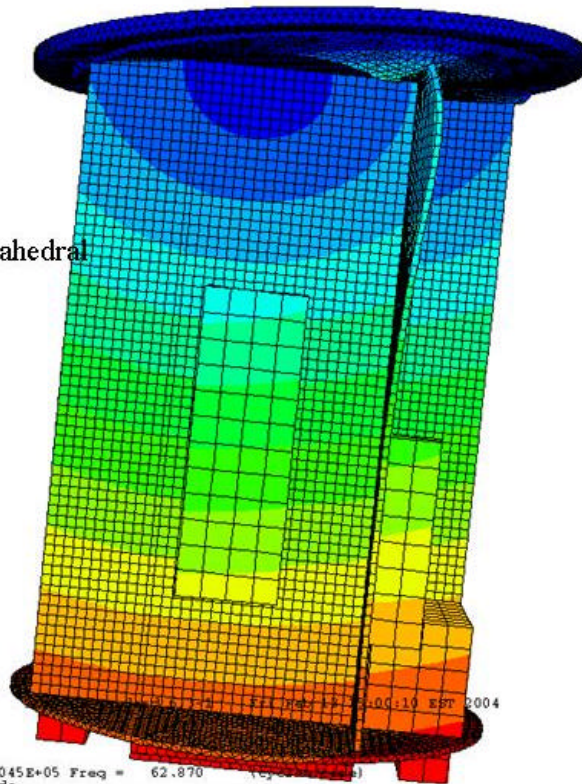


3-D Quadratic Hexahedral/Tetrahedral  
Structure and Components  
Mode 2  
Frequency – 62.870 Hz



ODB: pro-e4\_massed.odb

Step: frequency  
Mode 2: Value = 1.56045E+05 Freq = 62.870 (Hz)  
Primary Var: U, Magnitude  
Deformed Var: U Deformation Scale Factor: +2.888e+00



3-D Quadratic Hexahedral/Tetrahedral  
Structure and Components  
Mode 2  
Frequency – 62.870 Hz



ODB: pro-e4\_massed.odb

Step: frequency  
Mode 2: Value = 1.56045E+05 Freq = 62.870 (Hz)  
Primary Var: U, Magnitude  
Deformed Var: U Deformation Scale Factor: +2.888e+00

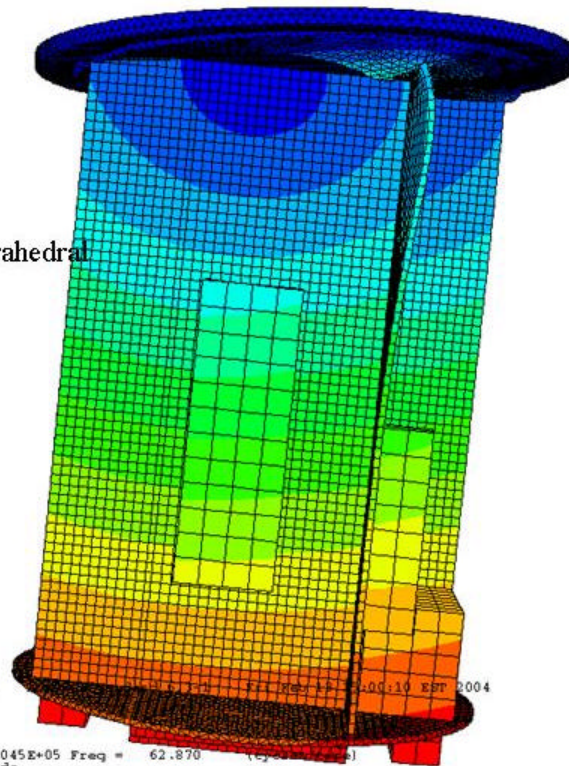


Figure 45. Mode 2 for the Massed Three-Dimensional Model of the RIGEX Structure

Results of the frequency analysis on the plate and three-dimensional model are presented with ping test results for the full structure in Table 9. See Appendix D-2 for frequency response function curves from ping testing.

Table 9. Results of the Full Structure Frequency Analysis

Frequency analysis method	Mode 1 (Hz)	Mode 1 Percent difference form Ping testing
ABAQUS linear Plate model coarse Mesh 0.4 inch seeding (un - massed)s	178	89.4
ABAQUS quadratic Plate model coarse Mesh 0.4 inch seeding (un - massed)	148.17	58.2
ABAQUS 3-D quadratic model - Coarse Mesh 0.2 inch seed (un- massed)	113.84	21.11
ABAQUS 3-D quadratic model - Fine Mesh 0.2 inch seed (massed)	54.35	N/A
Ping Testing Empty structure only	94 Hz	

The results of the frequency analysis of the RIGEX structure progressed as expected with the linear two-dimensional elements performing the least satisfactorily. The results obtained from the two-dimensional model cannot entirely be attributed to the element selection. Changing the elements in the two-dimensional model from linear to

quadratic did improve the results, but not sufficiently to claim element selection as the major contributor to the discrepancy between model results and those obtained from ping testing. In ping testing the full structure for the first time, several screws attaching the structure to the EMP were found loose; this had a significant impact on the ping test results. With the screws loose, the structures first natural frequency was found to be around 57 Hz. After all of the screws were tightened down, that frequency moved up to 94 Hz. This is significant in regards to the two-dimensional model because of how the connection between the EMP and structure top plate were modeled. The screw holes are spaced approximately 2.5 inches apart on the actual structure, but were modeled as a continuous ring of tie nodes in the model. This would make the two-dimensional model stiffer than the structure it was intended to represent. The three-dimensional model provided for a more realistic representation in this area, which should explain the large discrepancy in results between the two-dimensional and three-dimensional models.

### **Dynamic Stress Analysis of the Full Structure**

The stress analysis of the RIGEX structure was undertaken in a similar fashion to the full structure frequency analysis. The two-dimensional linear model was reconfigured to perform the stress analysis by adding 15 G loads in all three axes, and in different combinations to determine which case would produce the maximum stress on the structure. The worst case loading was determined by changing the loading configurations and running a stress analysis for each case. This worst case was used in subsequent models to produce the worst case stress predictions for the three-dimensional model. The same assumption was made for the connection of the EMP to the top plate of

the structure. A ring was partitioned in the area where the bolt ring exists, and the nodes in this region on both the top plate and the EMP were tied together. The result of the worst case loading is depicted in Figure 46. This model was produced before some of the design modifications were made, and so it has the entire inflation system modeled on the lower side of the bottom plate.

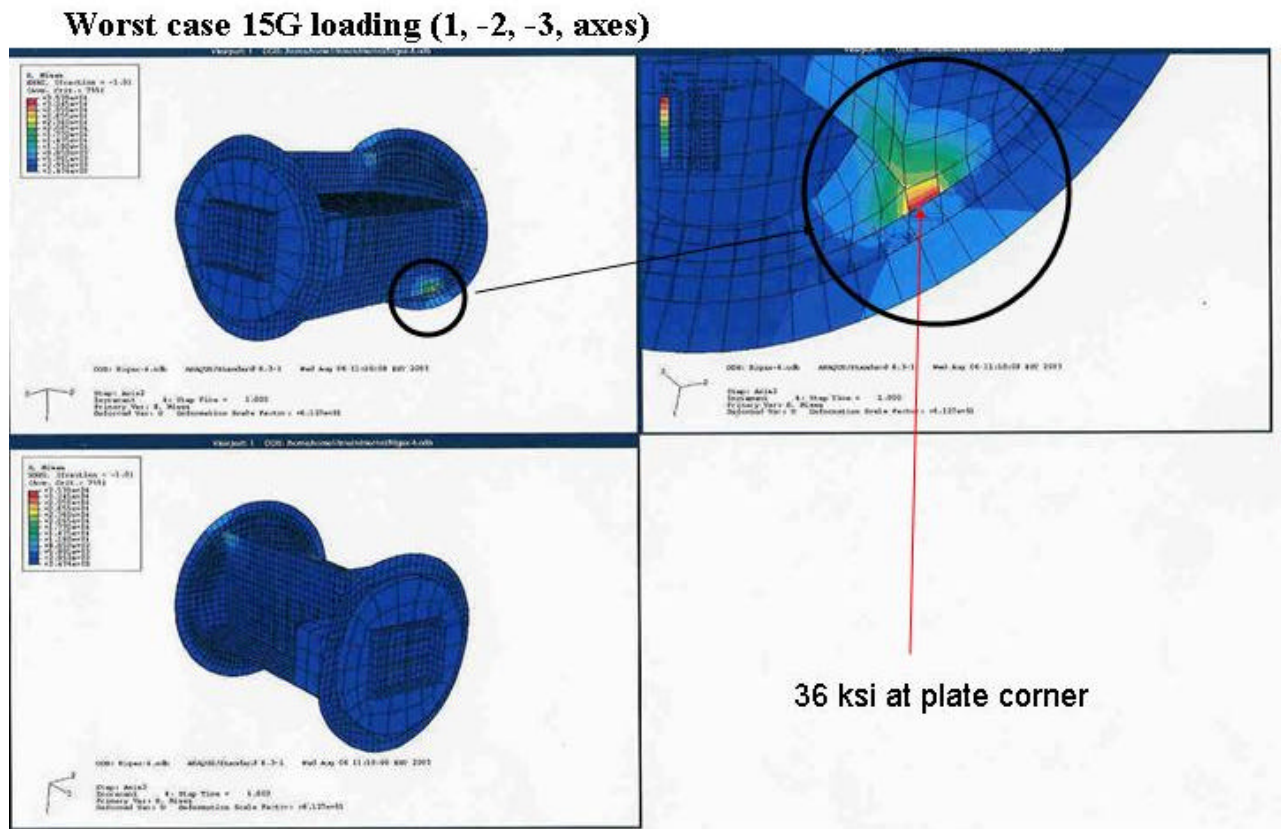


Figure 46. 15G Loading on Two-Dimensional Model

Following the finalization of the structural design modifications, the full structure was modeled as a three-dimensional assembly, as in the case of the frequency analysis model and the same worst case loading applied. In addition, the three-dimensional

structure was loaded with a 20G configuration to meet NASA requirements on ultimate strength verification. Both the 15 and 20G loads are meant to represent a 10G loading on the structure with a 1.5 and 2.0 factor of safety for yield and ultimate strength built into the simulation. Once built, the simulations were run producing the plot depicted in Figures 47-54.

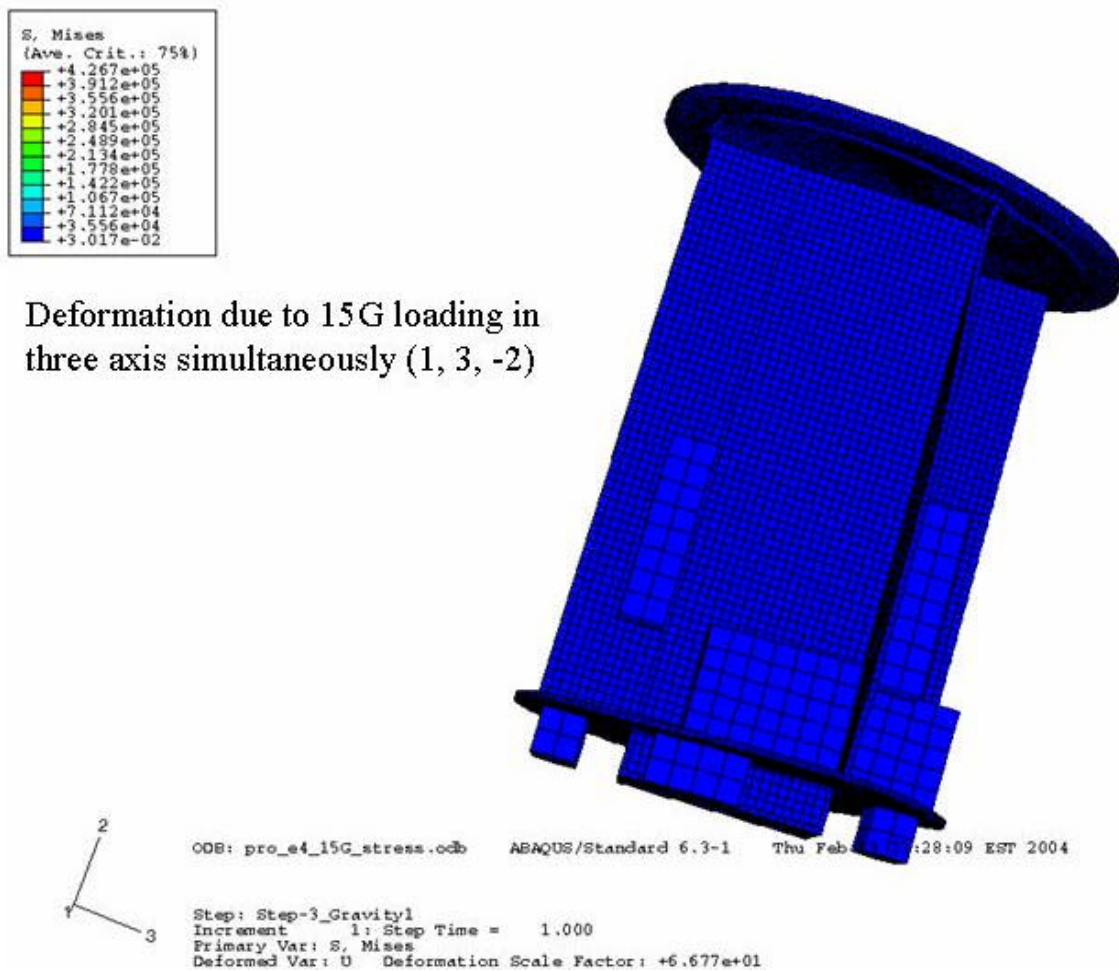


Figure 47. Deformed Structure under 15G Load



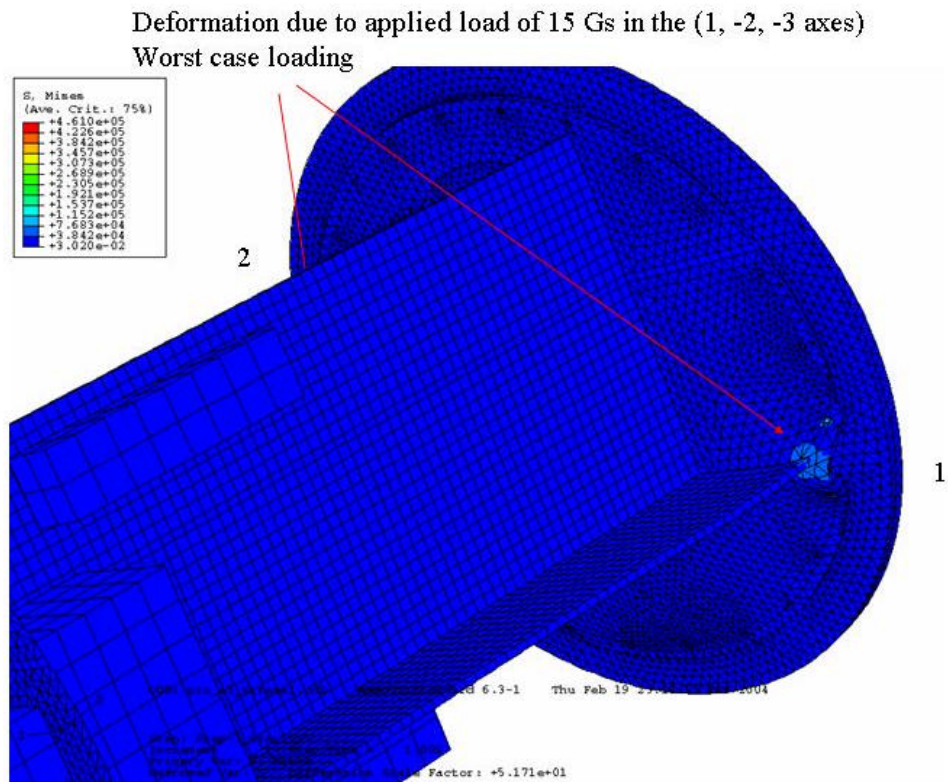


Figure 48. Worst Case Loading for 15G Load



Detail 1 due to 15 G worst case loading

38.5 ksi around bolt hole  
And around discontinuity at corner

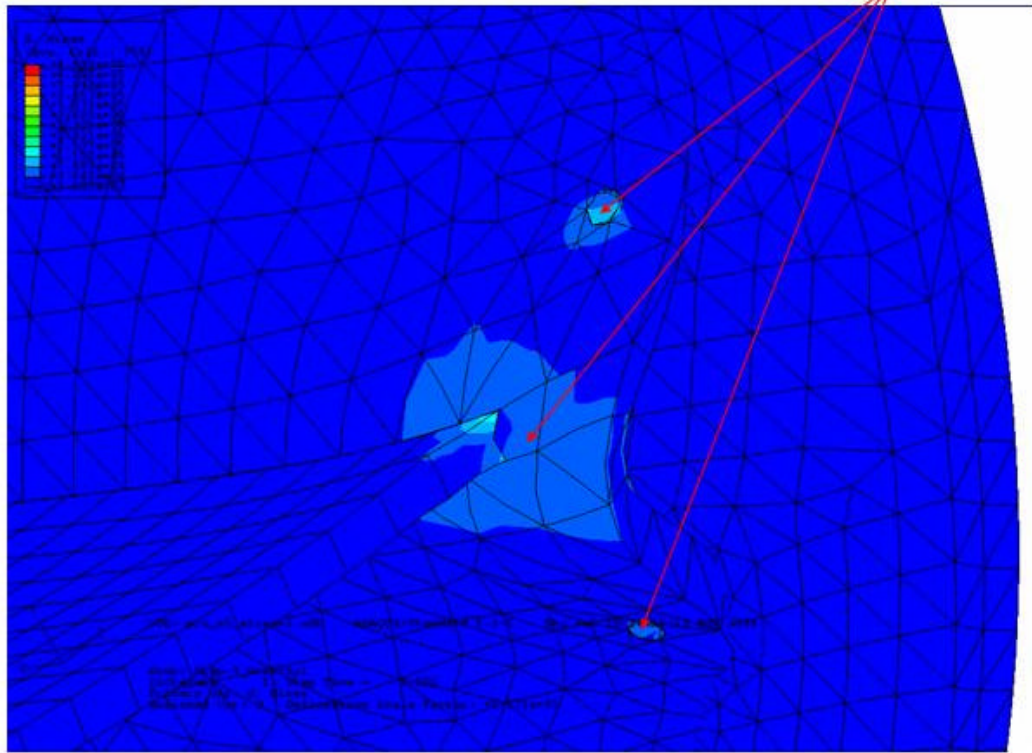


Figure 49. Detail 1 of Worst Case Loading for 15G Load

Detail 2 due to 15 G worst case loading

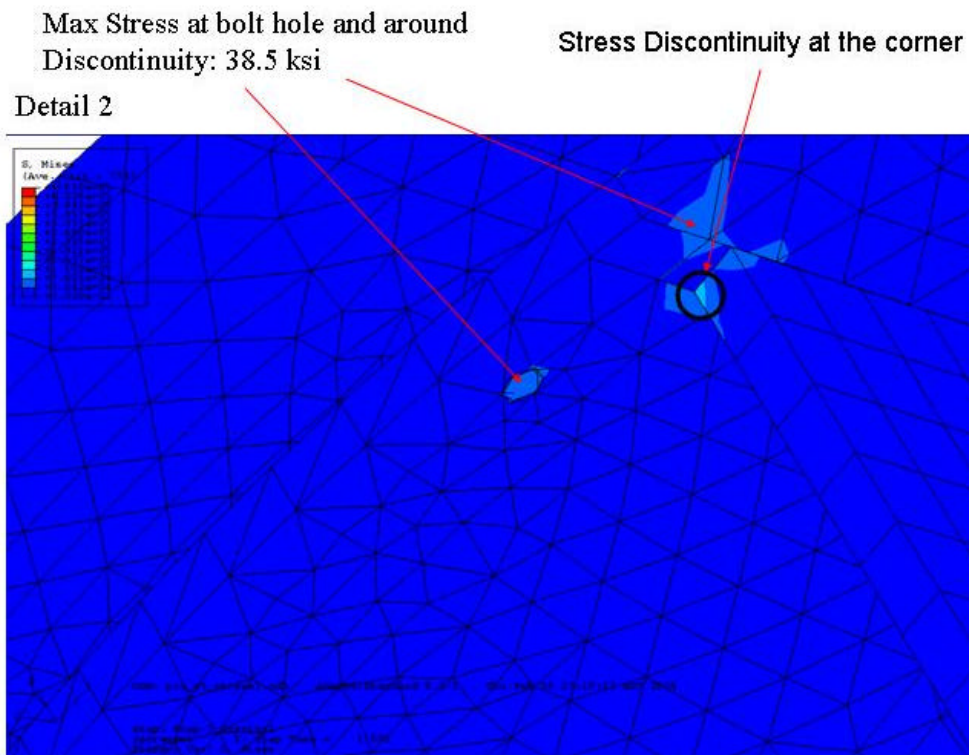
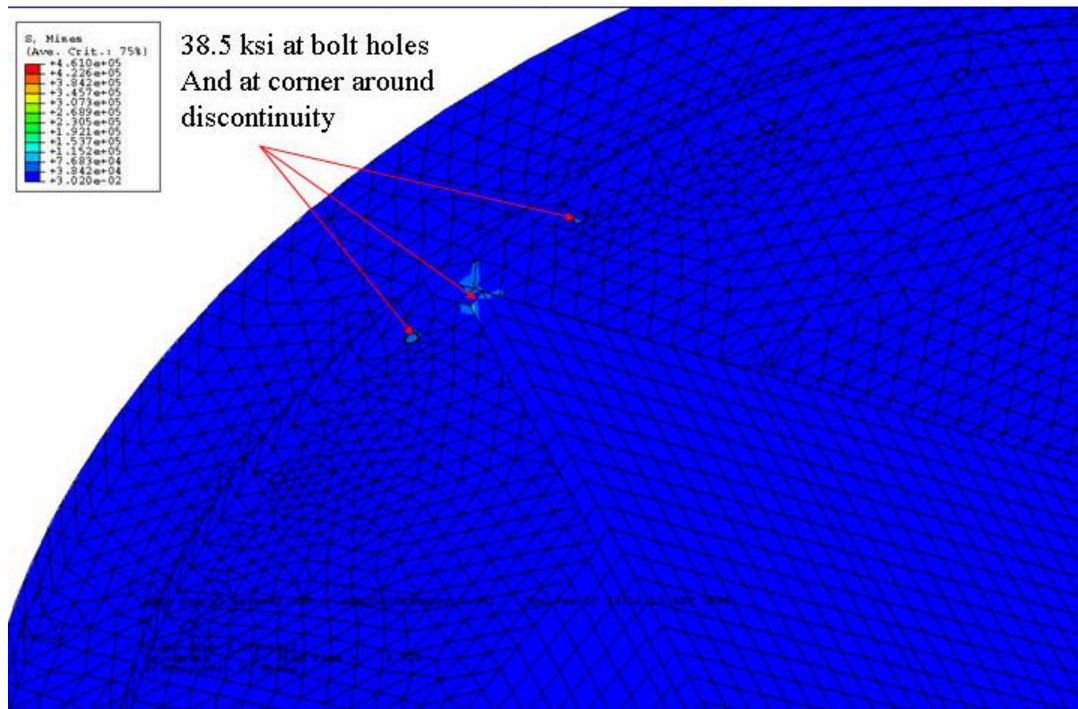


Figure 50. Detail 2 of Worst Case Loading for 15G Load

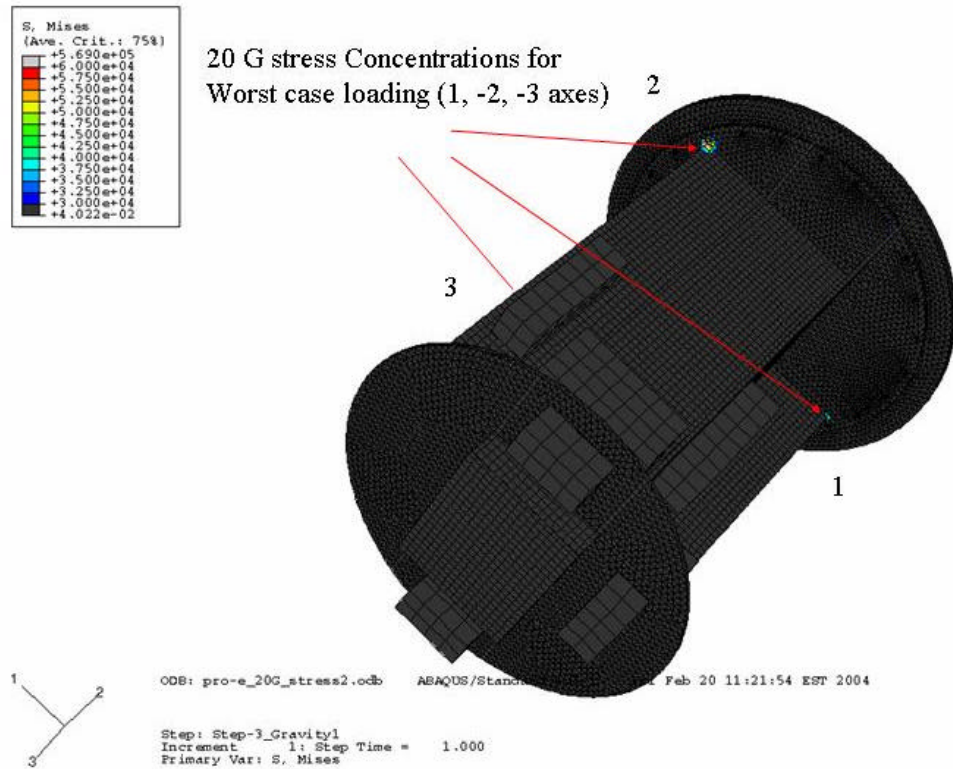


Figure 51. Worst Case Loading for 20G Load

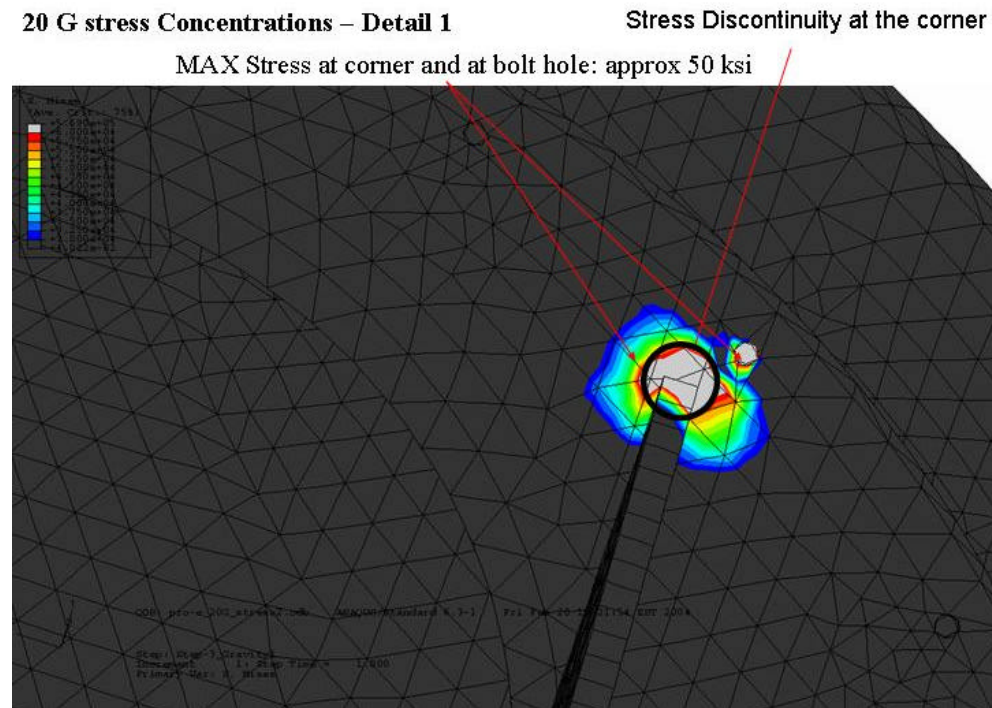


Figure 52. Detail 1 of Worst Case Loading for 20G Load



### 20 G stress Concentrations – Detail 2

Stress Discontinuity at the corner

MAX Stress at corner and at bolt hole: approx 45 ksi

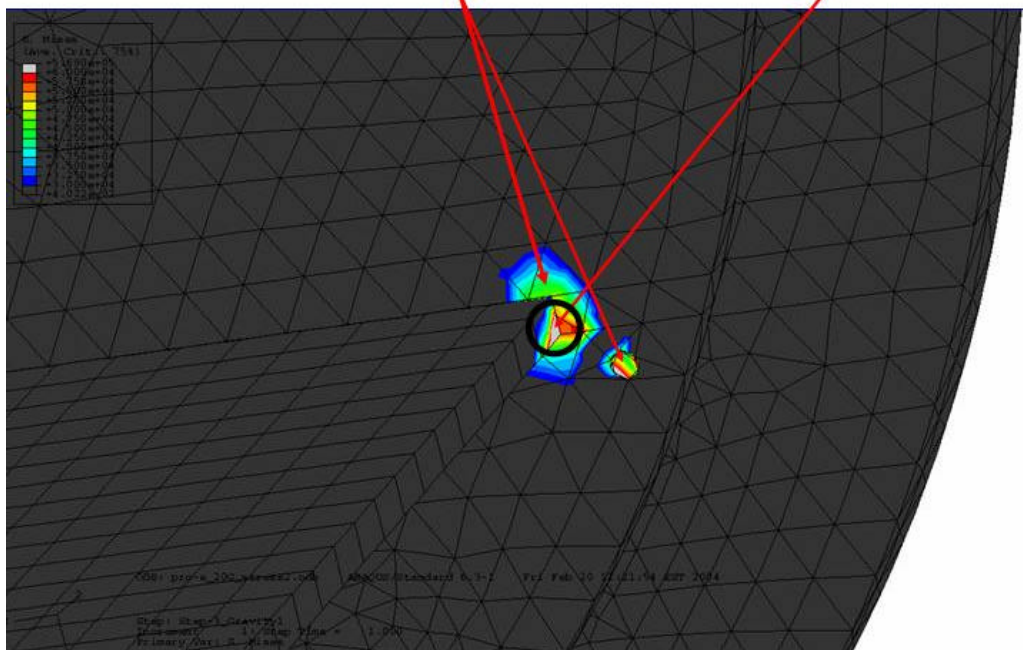


Figure 53. Detail 2 of Worst Case Loading for 20G Load

### 20 G stress Concentrations – Detail 3

Stress Discontinuity at the corner

MAX Stress at corner approx: 45 ksi and at bolt hole: approx 50 ksi

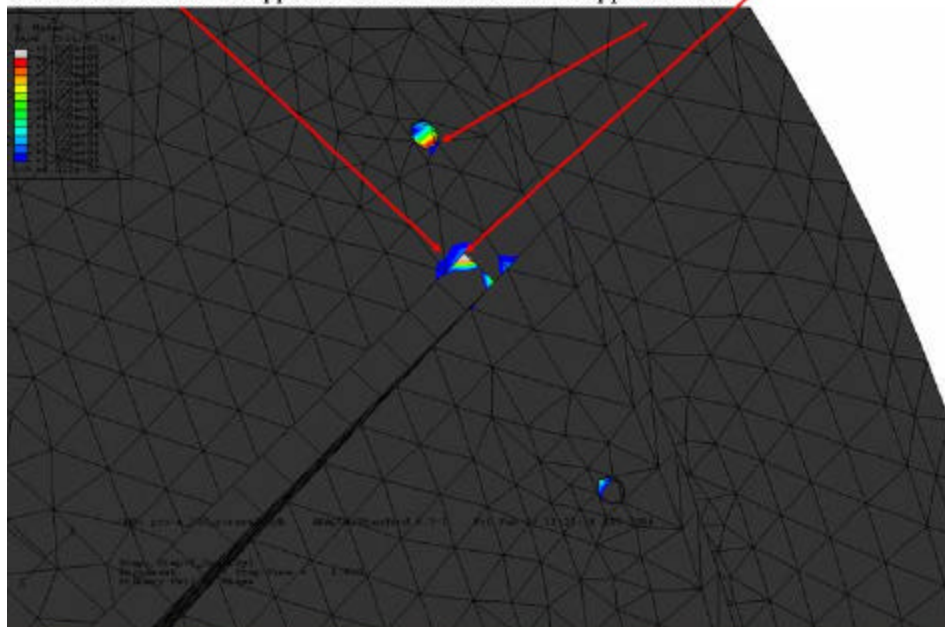


Figure 54. Detail 3 of Worst Case Loading for 20G Load

The results of the stress analysis run are summed up in Table 10.

Table 10. Stress Analysis Results

Model	Max Stress for 15 G worst case loading (Yield Strength)	Max Stress for 20 G worst case loading (Ultimate strength)	Yield/Ultimate strength for AL-6061 T-6 Metals Hand Book	Yield/Ultimate strength for AL-6061 T-6 MIL-HDBK-5
2-D linear plate	36 ksi	N/A	40/45 ksi	36/42 ksi
3-D quadratic	38.5 ksi	50 ksi	40/45 ksi	36/42 ksi

The results of the stress analysis run show that the stresses encountered in the 15G worst case loading exceed the yield strength of the structural material AL-6061 T-6 as presented in MIL-HDBK-5 (8). One of the decisions early on in the design of the structure was material selection. Al 6061 T-6 was chosen based on information out of the metals handbook (3), it wasn't discovered until later in the design that values for material properties used in the structural analysis must come from MIL-HDBK-5. The values for the yield strength of AL-6061 T-6 vary by 4 ksi from the metals handbook to MIL-HDBK-5. Instead of having 4 ksi of leeway, the analysis was begun at the limit of the materials yield strength.

Early assumptions as to the NASA test requirements and ambiguity in the GAS handbook led to discounting the 2.0G loading case in the early stages of the analysis. The case was considered again after its mention in the structural verification section in the GAS Experimenter's Guide to the STS Safety Review Process and Data Package Preparation (22). In any event, the ultimate strength of the structural material was also exceeded for the worst case 20G loading.

## **V: Conclusions and Recommendations**

### **ABAQUS Frequency Evaluation**

The modeling and simulation of the RIGEX rigidized tube assembly, quarter structure and full structure proceeded as expected and provided good correlation with test results. The use of the fundamental frequency for determining the material properties of the inflatable tube proved successful. Young's modulus was back-calculated from the fundamental frequency formula developed in the literature review and using the experimental value for the first bending mode of the tube mounted on the table. The tube model was then run using this value for Young's modulus and the second bending mode was compare to the experimental value. The tube model using the calculated material properties was found to be within 2-3 percent of the experimental value for the second bending mode. The results of the beam and tube analysis showed that ABAQUS could accurately model the thin shell of composite material that makes up the inflatable tube. The difference in boundary conditions was also explored for the tube model, simulating clamped and simply supported conditions. The result of this study showed significant difference in the response of the tube along the axis where the bolts were removed for the simply supported case. The fist bending mode of the simply supported case lost 6 db on the axis were the bolts were removed and 32 db from the second bending mode. The true condition is somewhere between these two.

The frequency results obtained from the ABAQUS models for the quarter and full structure tended to be a little on the high side, but this can be attributed to the

assumptions made in modeling of these structures. As was seen in modeling the tube, boundary conditions play an important role in the frequency analysis of an assembly modeled in ABAQUS. Thus as the sophistication of the model increases the difficulty in accurately modeling the proper boundary condition will also increase. This difference between the ping test results and the ABAQUS frequency analysis results for the full structure can in large part be attributed to this difficulty in modeling the proper boundary conditions. However, the end goal of verifying the natural frequency of the full RIGEX structure was accomplished, and the results show that the NASA requirement for keeping the fundamental frequency above 35 Hz for the structure with experimental components has been met.

### **ABAQUS Stress Evaluation**

The stress analysis of the RIGEX support structure did not provide results to back validation of the NASA requirements for structural verification, based on worst case loadings of 15 and 20G loadings. The stresses developed in the structure exceeded the Yield strength of the aluminum for the 15G loading and the Ultimate strength for the 20G loading. These failures can be attributed to several factors in the ABAQUS model. First, there are large stress concentrations present, due to the way in which the model was constructed. The plates were assembled in ABAQUS using the tie command to secure the parts together; this left sharp edges where the plates were joined. These areas are where the stress concentrations/discontinuities were encountered and would not be as prevalent in the actual structure where the plates are welded together, which creates a

fillet between the joined plates. The second, was a design issue where a structural material was chosen based on information obtained early in the design and before all the actual test to documentation had been acquired. Finally, an assumption was made early on to test to the 10G load with margin of safety of 1.5 on Yield strength only. When it was determined that there was a need for a second case, testing to 10Gs with a margin of safety of 2.0 on Ultimate strength, that case was run but could not hope to meet the requirement with the chosen structural material and structure design. The good news is that the structure was designed to be screwed together before welding and that all of the stress hot spots are located on the top plate of the structure. This means that the top plate can be removed and its design can be modified without having to rebuild the entire structure.

## **Recommendations**

In order to resolve stress concentration issues encountered in the top plate of the RIGEX structure, several design modifications can be incorporated. The first would be the removal of the computer access port machined out of the top plate. This will increase the overall weight of the structure, but not significantly. Deformations seen in the structure were largely due to the gap created between the top plate and one of the vertical side plates by this feature. Removal of this feature, in conjunction with a change to the mounting of the bolts connecting the computer, will still allow access to the computer box after assembly while increasing the overall stiffness of the support structure. The increased rigidity of the structure should redistribute some of the stresses encountered at the plate tips to the inner wall of the structure and eliminate some of the stress



concentrations at the aforementioned locations. The second modification would be to add a second row of restraining bolts to the top plate that mate up with holes provided in the EMP. This too would draw some of the load away from the outer bolt ring and reduce the stress concentrations present in the current configuration. This was not done in the original design because the second bolt ring would cut across the computer access hole in the top plate. Another modification, which could be used to reduce the amount of stress at critical locations on the top plate, would be to increase the overall thickness of the top plate from quarter-inch to half-inch aluminum, in conjunction with the addition of the second bolt ring and removal of the computer access hole. This is not as attractive as the two previously mentioned modifications because of the increase in weight that it would cause, but might become a viable alternative if the stress cannot be brought down by other design modifications. Least attractive of all the design modification options would be to remanufacture the structure with a material that has a higher Yield and Ultimate strength such as Al 2024. This however will lead to more problems in joining the pieces together (2024 is difficult to weld) and NASA would have to sign-off on the Stress Corrosion Cracking issues involved with this material.

## Appendix A. Fundamental Frequency Calculations

To construct a model in ABAQUS that would provide an accurate frequency analysis tool, the correct material properties for the tube had to be determined and used in the system model. The Fundamental Frequency Formula was used in determination of Young's Modulus for the composite material, using the spring constant for the lateral vibration and 62 Hz (obtained for testing) as the first natural frequency in bending.

$$f = .159 \sqrt{\frac{k}{(m + am_b)}}$$

	<b>k</b>	<b>a</b>
Axial Vibration	EA/L	1/3
Lateral Vibration	EI/L <sup>3</sup>	1/4

where  $m$  = lumped mass  
 $m_b$  = beam mass  
 $k$  = spring constant  
 $a$  = parameter

where

$$I = \frac{P}{64}(d_0^4 - d^4) = 9.04299\text{e-}9 \text{ m}^4$$

$$m = 0.074 \text{ kg}, m_b = .040 \text{ kg}, L = 0.507\text{m}$$

$$62\text{Hz} = .159 \sqrt{\frac{3EI}{L^3(0.074 + .25(0.40))}}$$

$$E = 61,740,461,021 \text{ N/m}^4 \text{ or } 8,954,696 \text{ psi}$$

## Appendix B. RIGEX Structural Drawings

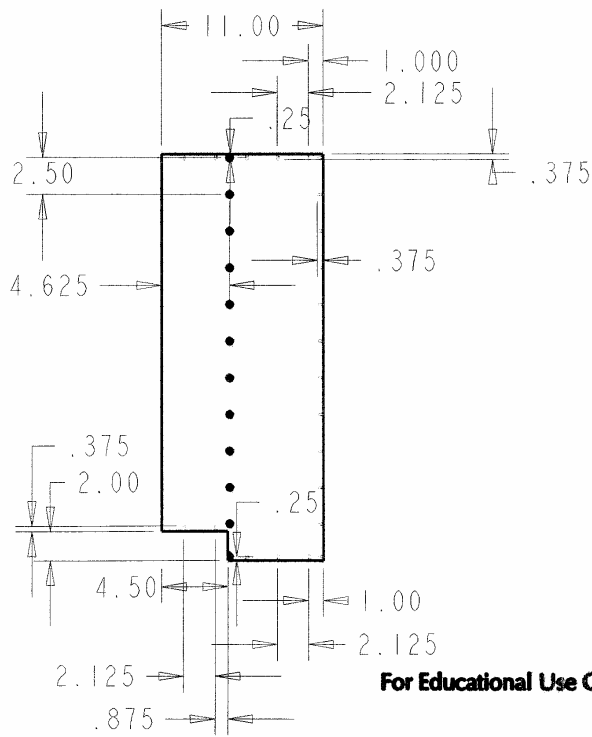
### B.1 Eleven-Inch Plate

For Educational Use Only

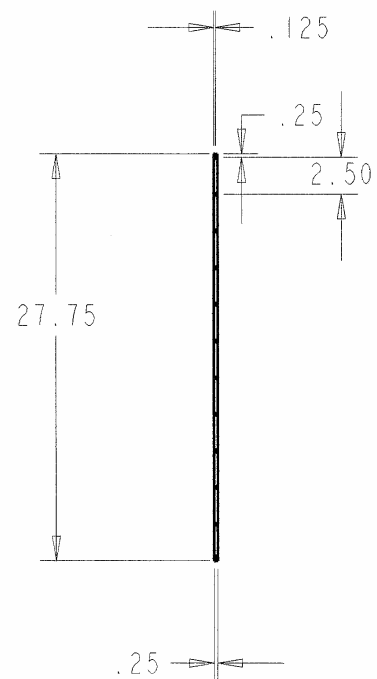
NOTE: All blind holes are drilled to accomodate #6-32 screws to a depth of 0.375 inch.  
All through holes are 9/64 " inch DIA and counterst



For Educational Use Only



For Educational Use Only

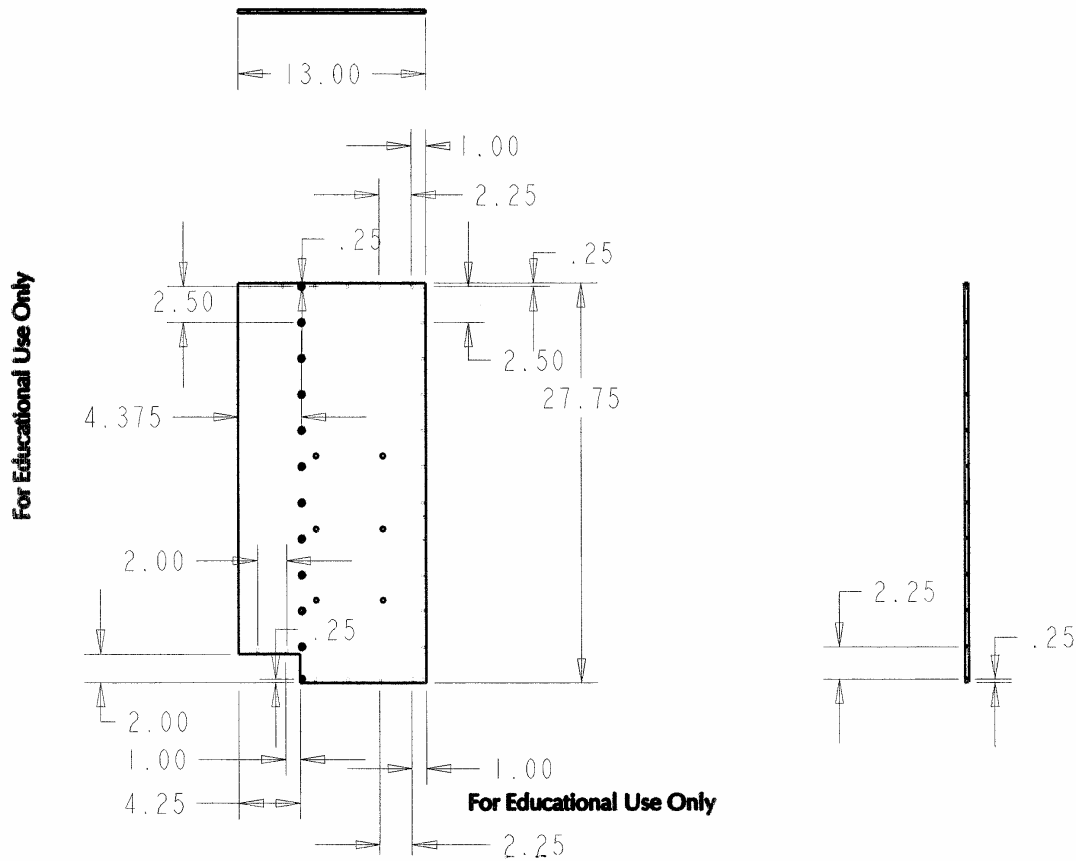


For Educational Use Only

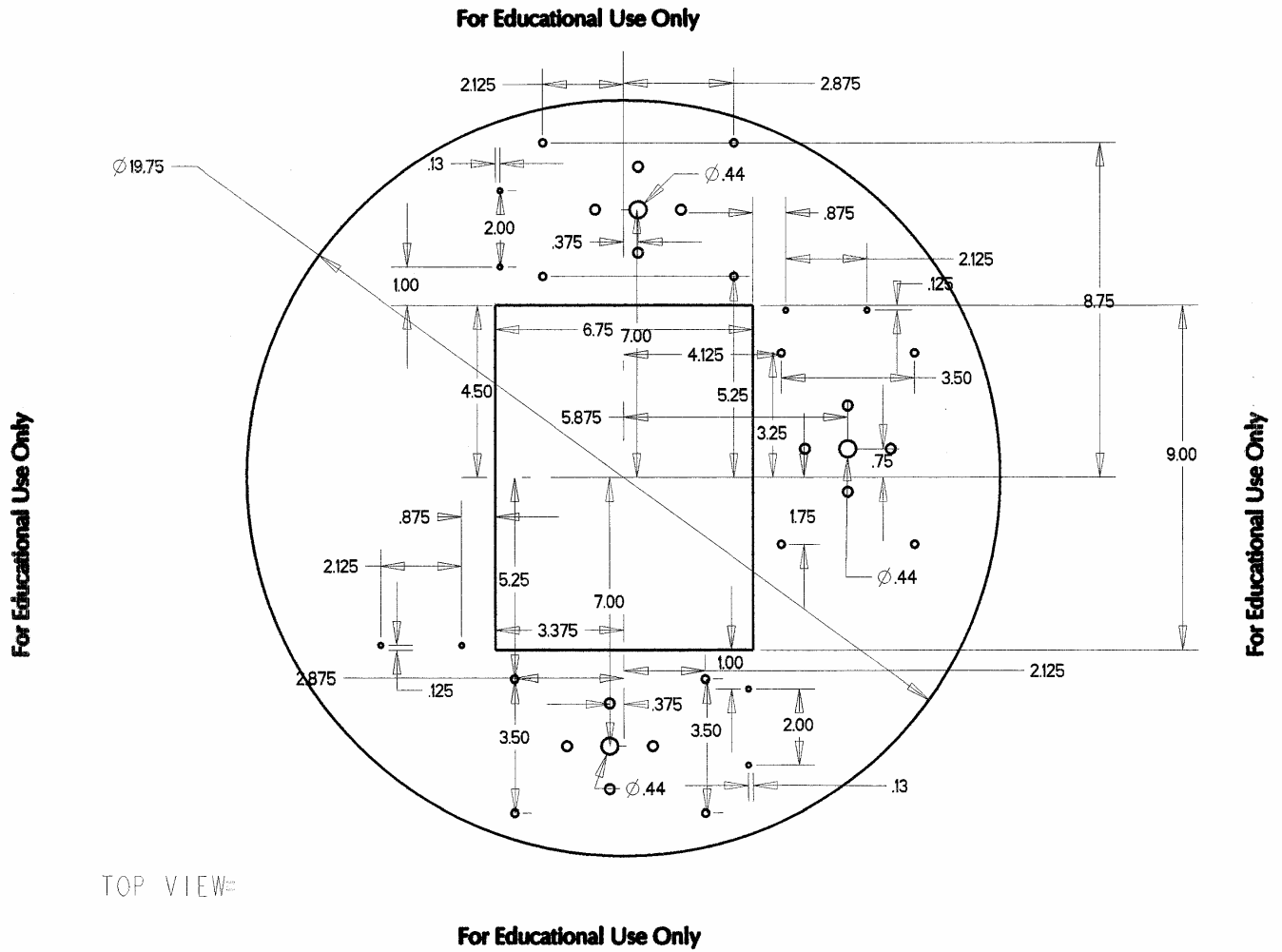
## B.2 Thirteen-Inch Plate

**For Educational Use Only**

NOTE: All blind holes are drilled to accomodate #6-32 screws to a depth of 0.375 inch. All through holes are 9/64" DIA and countersunk.

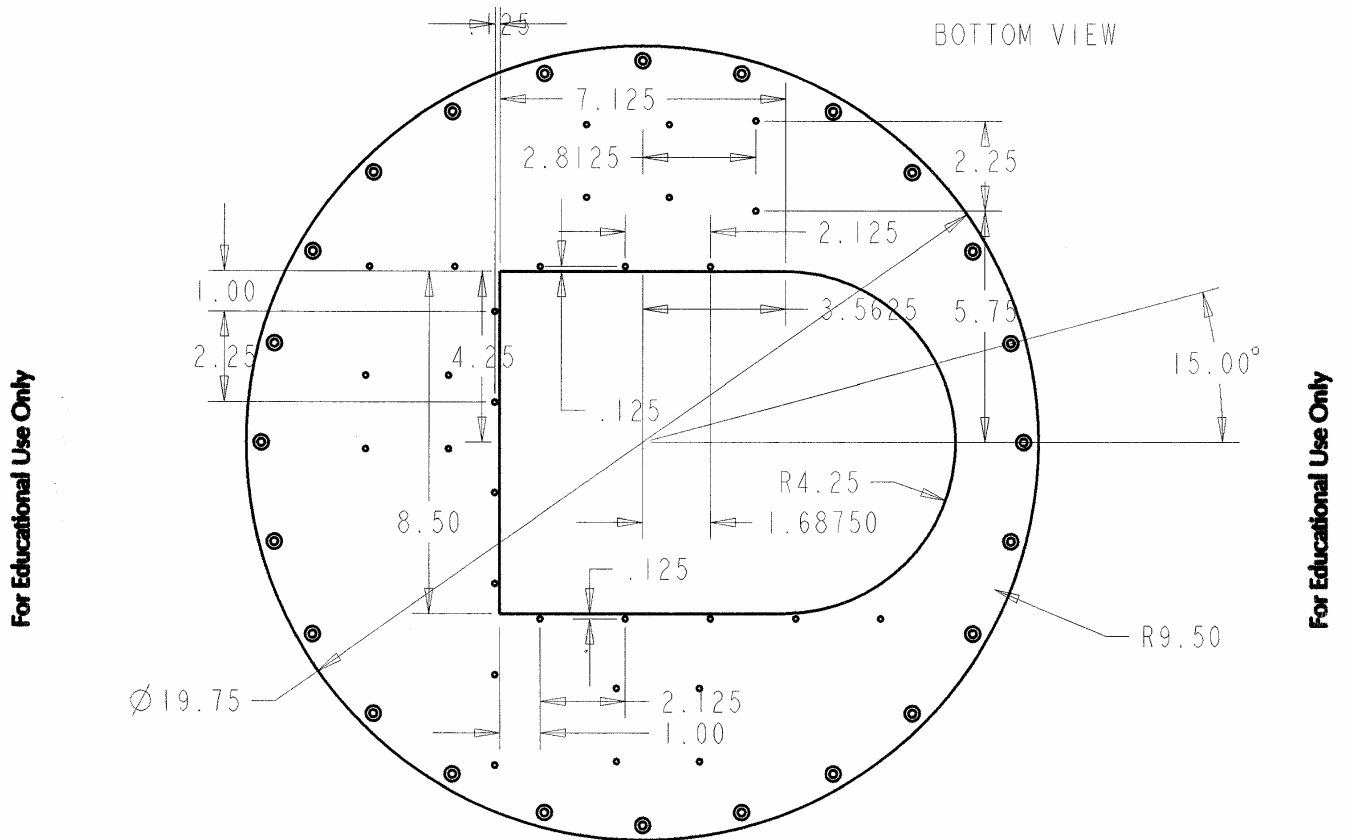


### B.3 Bottom Plate



## B.4 Top Plate

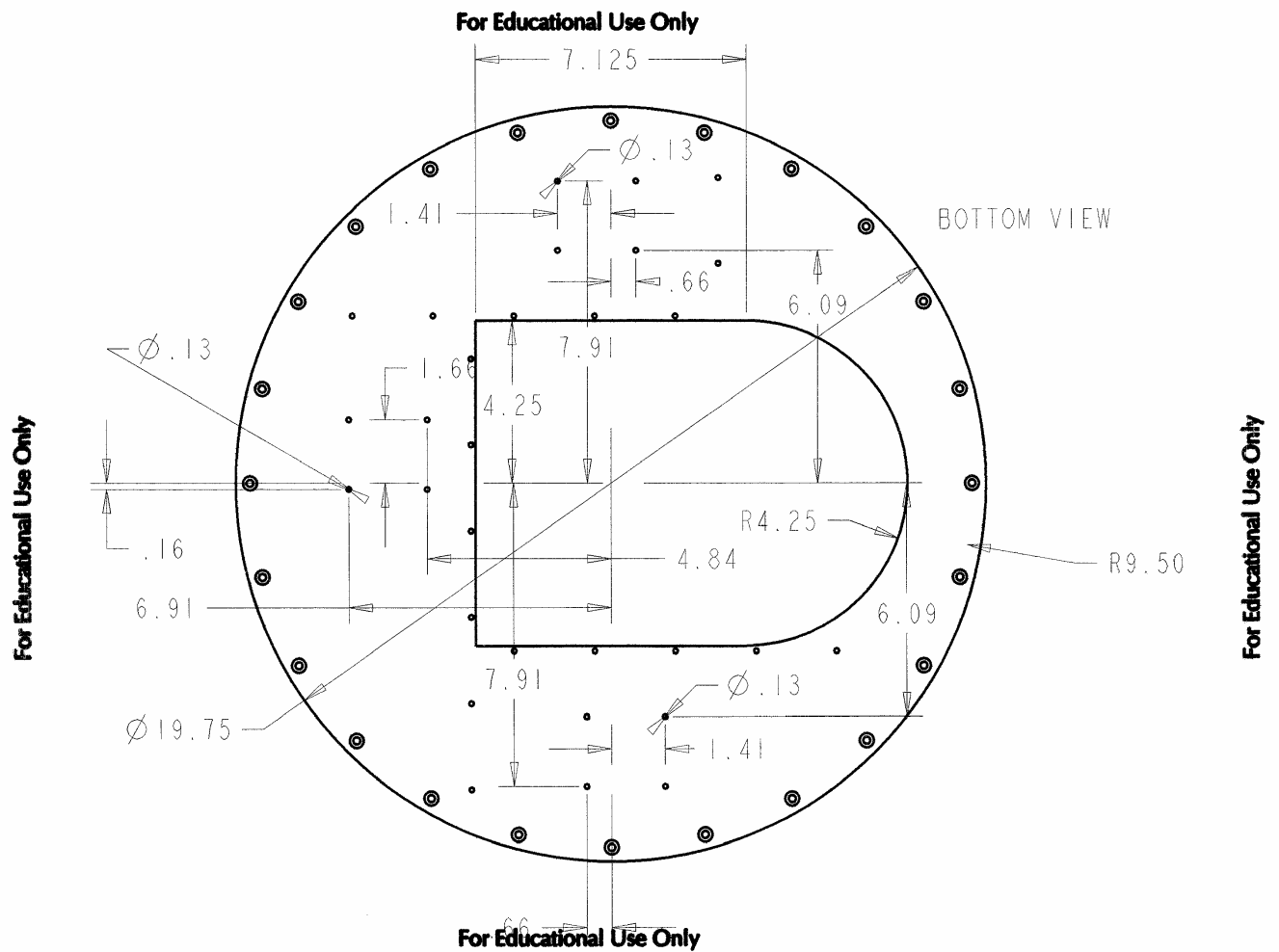
For Educational Use Only



NOTE: 24x #10-32 Through Holes on back side at R9.50.  
 NOTE: All other through holes are 9/64 inch DIA and countersunk.

For Educational Use Only

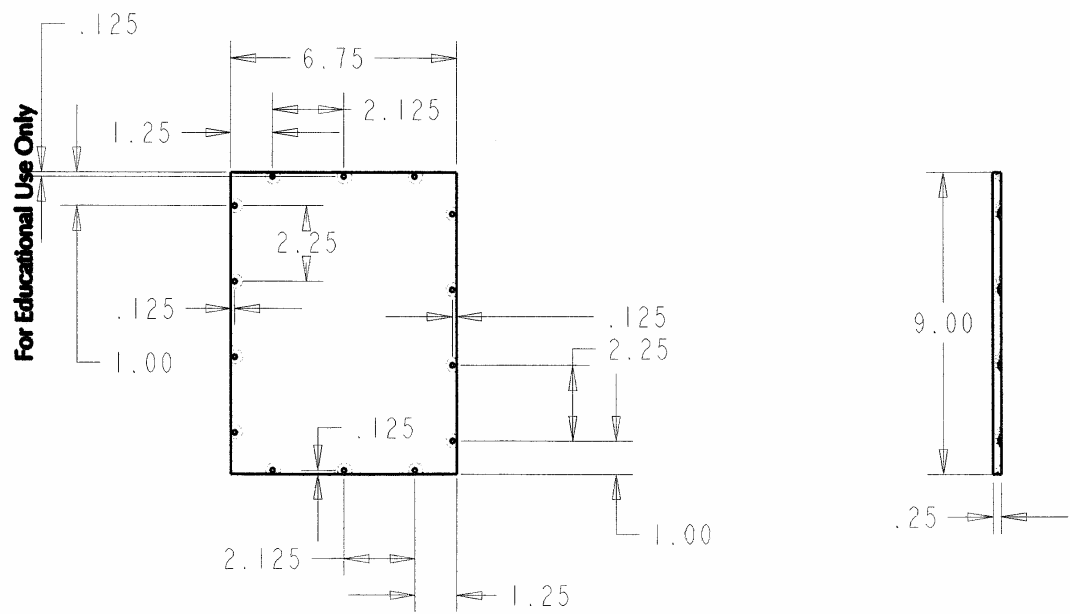
## B.5 Top Plate (Camera Mount Hole Detail)



B.6 Battery Plate

For Educational Use Only

NOTE: Through holes are  
9/64 inch DIA and countersunk



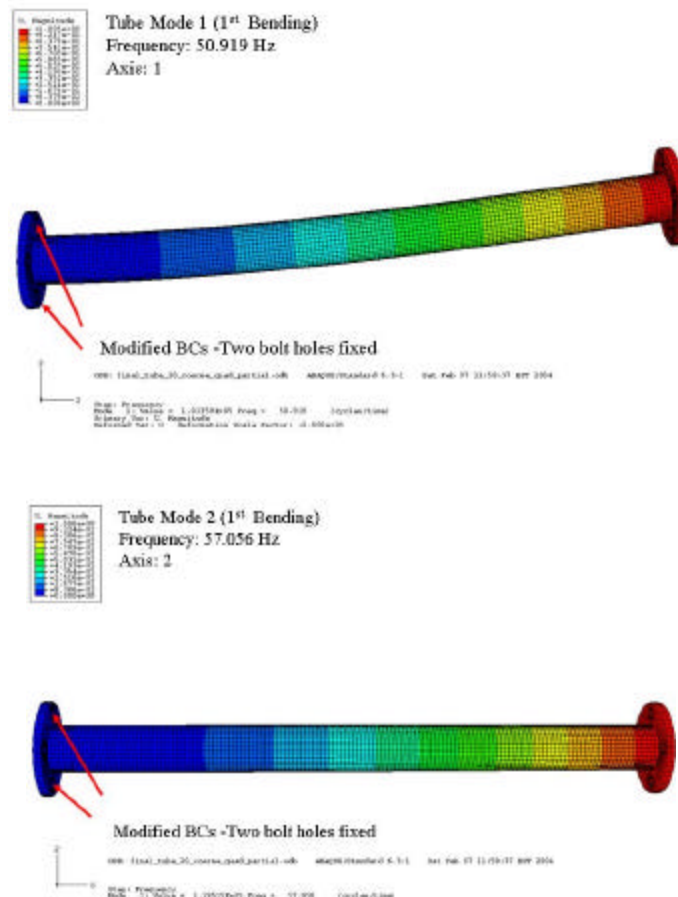
For Educational Use Only



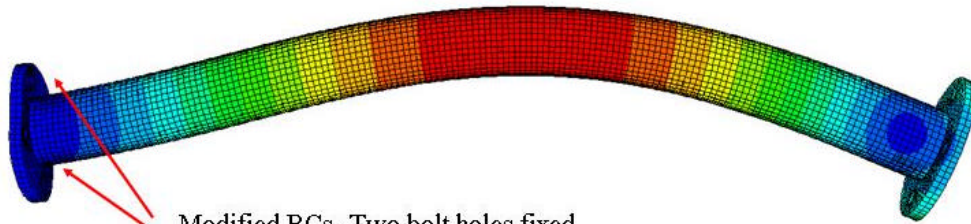
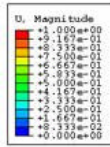
## Appendix C. Additional Tube Models

### C.1 Tube with two bolt boundary condition

The Tubes presented here are based on the fine mesh (0.2 inch edge seeding) quadratic hexahedral tubes. The only change from the tubes presented in chapter four was the boundary condition. The tubes in chapter four were run with a clamped end constrain (see Figure 15), while the tubes presented here are simply supported (see figure 14). The results from the simply supported tube are compared to the clamped tube in Table 7.



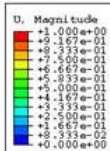
Tube Mode 4 (2<sup>nd</sup> Bending)  
Frequency: 562.21 Hz  
Axis: 1



Modified BCs -Two bolt holes fixed

2  
3  
ODB: final\_tube\_20\_coarse\_quad\_partial.odb ABAQUS/Standard 6.3-1 Sat Feb 07 11:59:37 EST 2004  
Step: Frequency  
Mode 4: Value = 1.24784E+07 Freq = 562.21 (cycles/time)  
Primary Var: U, Magnitude  
Deformed Var: U Deformation Scale Factor: +2.000e+00

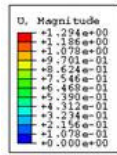
Tube Mode 4 (2<sup>nd</sup> Bending)  
Frequency: 629.6 Hz  
Axis: 2



Modified BCs -Two bolt holes fixed

3  
2  
1  
ODB: final\_tube\_20\_coarse\_quad\_partial.odb ABAQUS/Standard 6.3-1 Sat Feb 07 11:59:37 EST 2004  
Step: Frequency  
Mode 5: Value = 1.56491E+07 Freq = 629.60 (cycles/time)  
Primary Var: U, Magnitude  
Deformed Var: U Deformation Scale Factor: +2.000e+00

## C.2 Tube with 35 gram accelerometer

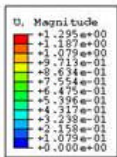
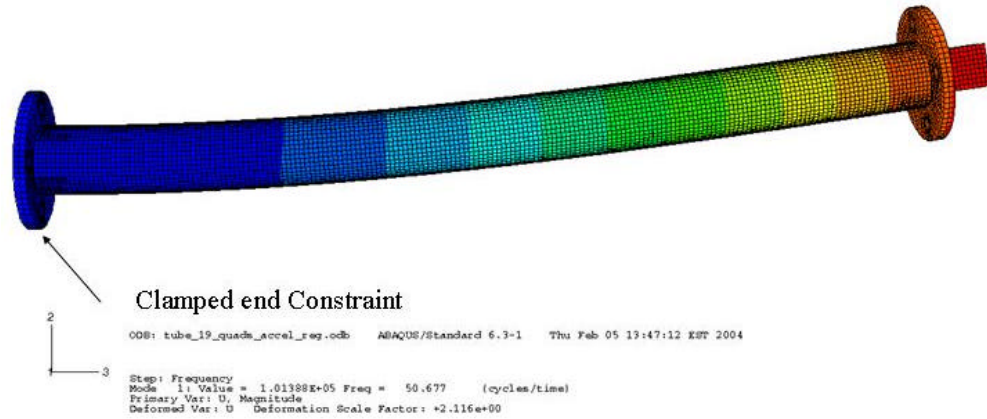


Tube Mode 1 (1<sup>st</sup> Bending)

Frequency: 50.677 Hz

Axis: 1

Fine Mesh - accelerometer

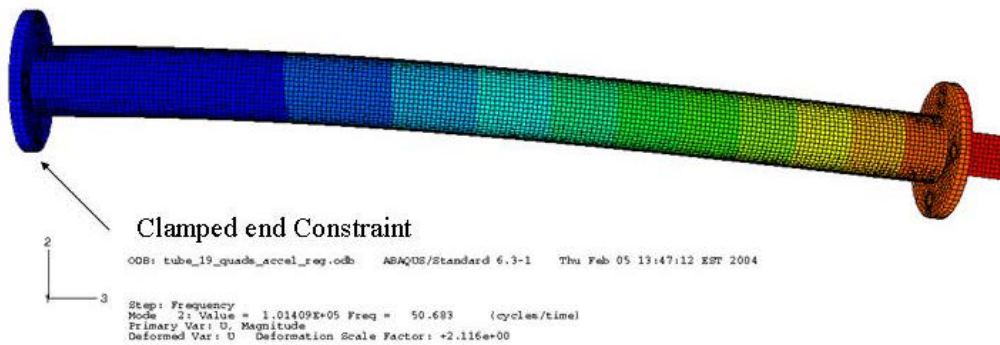


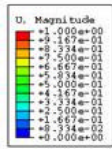
Tube Mode 2 (1<sup>st</sup> Bending)

Frequency: 50.683 Hz

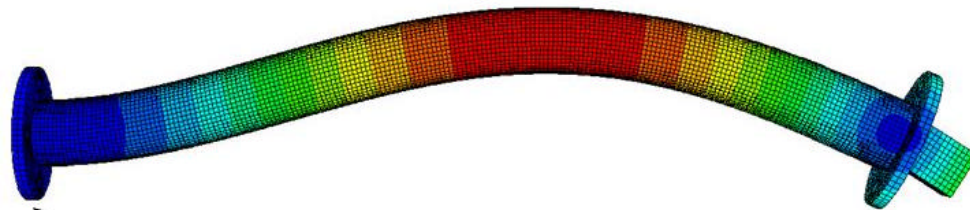
Axis: 1

Fine Mesh - accelerometer





Tube Mode 4 (2<sup>nd</sup> Bending)  
Frequency: 622.27 Hz  
Axis: 1  
Fine Mesh - accelerometer

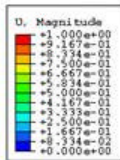


Clamped end Constraint

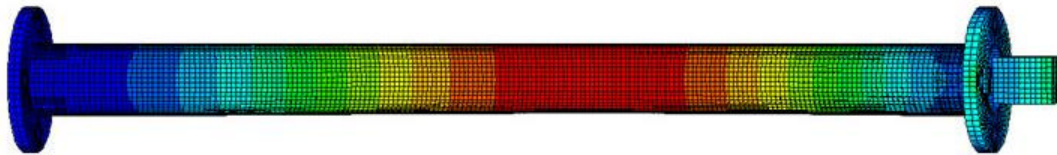


ODB: tube\_19\_quads\_accel\_req.odb ABAQUS/Standard 6.3-1 Thu Feb 05 13:47:12 EST 2004

Step: Frequency  
Node 4: Value = 1.52868E+07 Freq = 622.27 (cycles/time)  
Primary Var: U, Magnitude  
Deformed Var: U Deformation Scale Factor: +2.116e+00



Tube Mode 5 (2<sup>nd</sup> Bending)  
Frequency: 50.683 Hz  
Axis: 2  
Fine Mesh - accelerometer



Clamped end Constraint

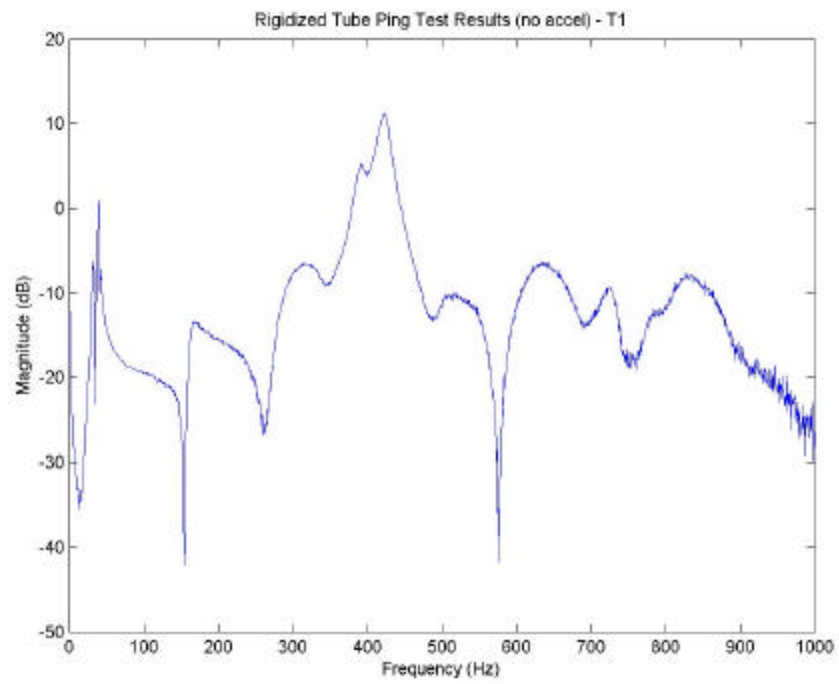


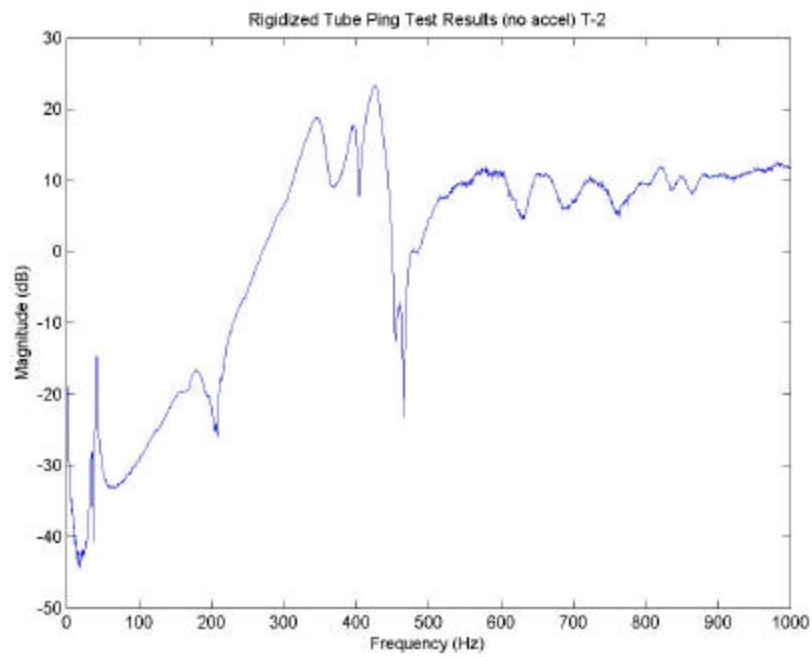
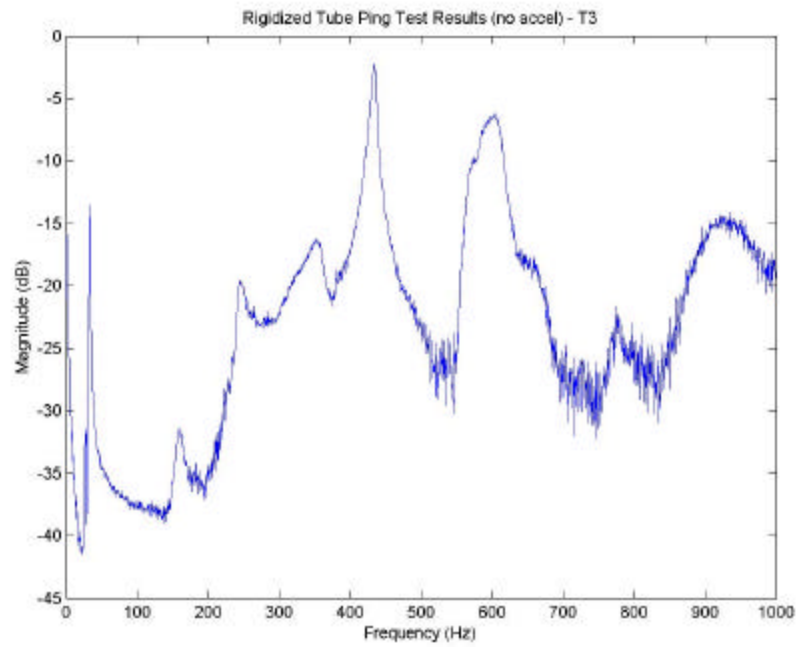
ODB: tube\_19\_quads\_accel\_req.odb ABAQUS/Standard 6.3-1 Thu Feb 05 13:47:12 EST 2004

Step: Frequency  
Node 5: Value = 1.54646E+07 Freq = 625.88 (cycles/time)  
Primary Var: U, Magnitude  
Deformed Var: U Deformation Scale Factor: +2.116e+00

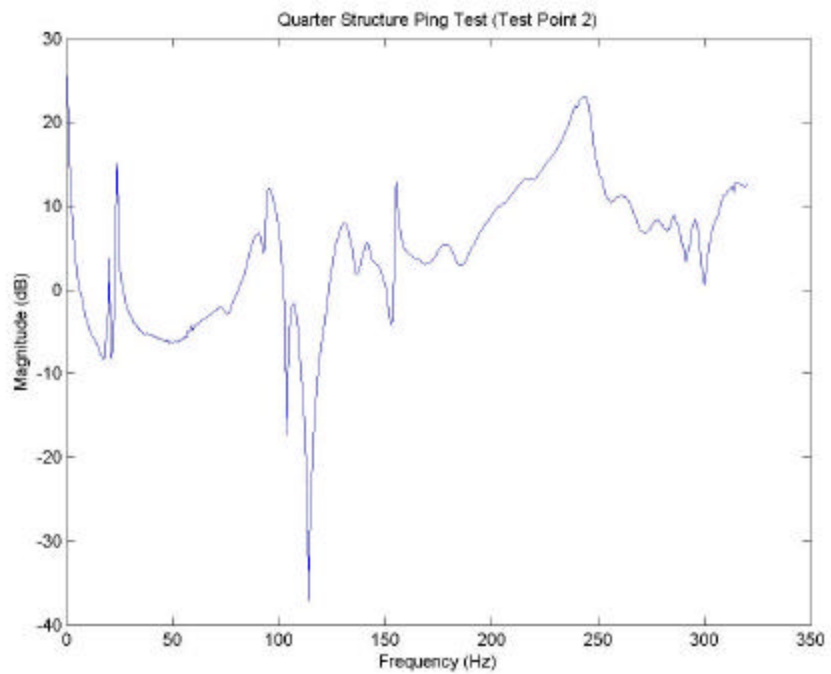
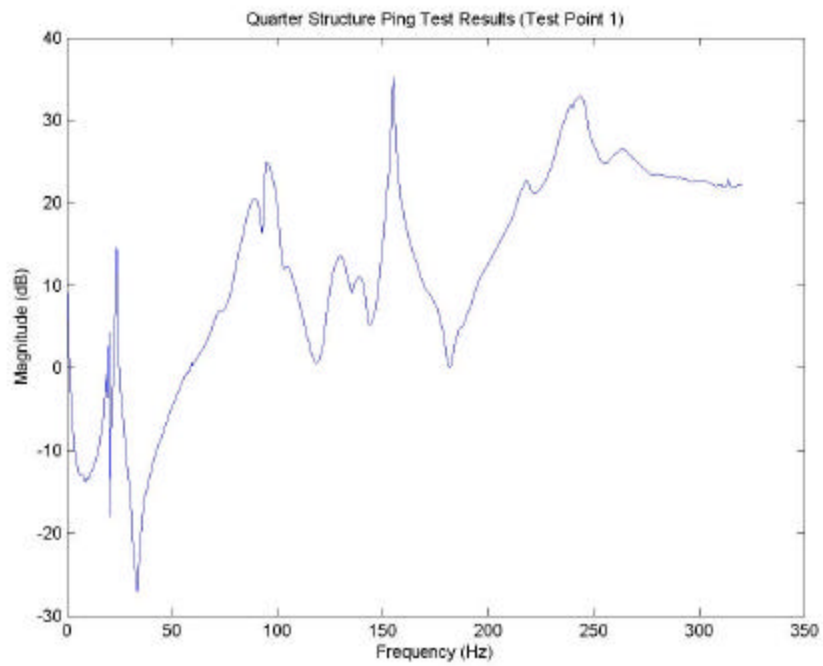
## Appendix D. Ping Test Results

### D.1 Ping Test Results for Rigidized Tube

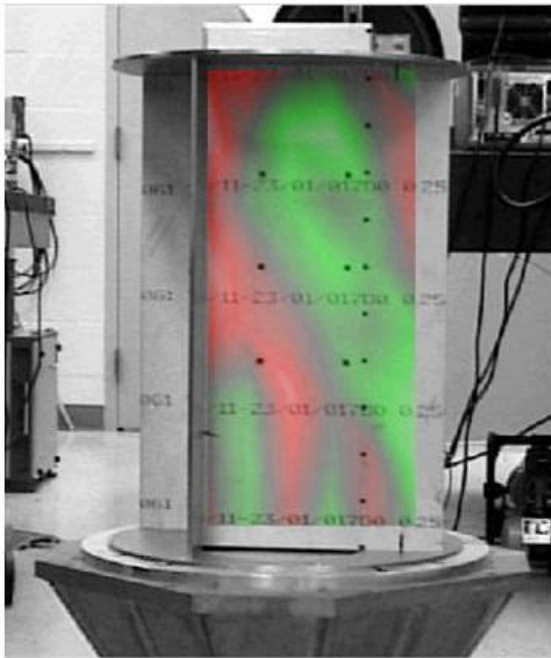




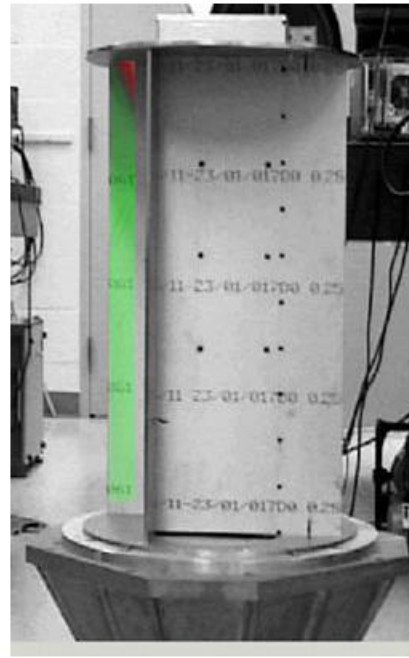
## D.2 Ping Test Results for Quarter Structure



### D.3 Ping Test Results for Full Structure (Empty)



92 Hz



94 Hz



## Bibliography

1. ABAQUS Central, Inc. *Introduction to ABAQUS*. Indiana. 2003.
2. AC Engineering, Inc. *A First Course in Using ABAQUS with an Introduction to ABAQUS/Explicit/CAE/Viewer*. Indiana. 2000.
3. ASM International Handbook Committee, *Metals Handbook, Volume 2: Properties and Selection: Nonferrous Alloys and Special-Purpose Materials* (Tenth Edition). USA: ASM International, 1990.
4. Barra, R.J. *Geo-Metric Vibration Analysis* (First Edition). Maryland: RMS Publishing Company, 1977.
5. Bezine, G. "On a Method of Comparison for Plate Elements in Finite Element Engineering Software Programs," Elsevier - Mechanics Research Communications 29, 35-43 (2002).
6. Bong, Duane. "Finite Element Analysis," VisionEngineer – Finite Element Analysis. 27 January 2004 [http://www.visionengineer.com/mech/tools\\_fea.shtml](http://www.visionengineer.com/mech/tools_fea.shtml).
7. Cook, Robert D, David S. Malkus, Michael E. Plesha, and Robert J. Witt. *Concepts and Applications of Finite Element Analysis* (Fourth Edition). USA: John Wiley & Sons, Inc, 2002.
8. Department of Defense. *Military Handbook, Metallic Materials and Elements for Aerospace Vehicle Structures*. MIL-HDBK-5CD-ROM 31 May 1997 based on MIL-HDBK-5G, CN2 1 December 1996.
9. De Silva, Clarence W. *Vibration: Fundamentals and Practice*. USA: CRC Press LLC, 2000.

10. Disebastian III, John D. *RIGEX: Preliminary Design of a Rigidized Inflatable Get-Away-Special Experiment*. Master's Thesis, Air Force Institute of Technology, Dayton, OH, March 2001.
11. Dornheim, Michael A. *Inflatable Structures Taking to Flight*. Aviation Week & Space Technology – 21<sup>st</sup> Century Satellite Technology, 31 January 2004  
<http://www.lgarde.com/programs/iaearticle/awarticle.html>.
12. “EN175: Advanced Mechanics of Solids,” Division of Engineering, Brown University – Finite Element Overview. 27 January 2004  
<http://www.engin.brown.edu/courses/EN175/fem/fem.htm>.
13. “Far Ultraviolet Spectroscopic Explorer (FUSE),” Johns Hopkins University – Instrument Development Group, Projects. 27 January 2004  
<http://idg.pha.jhu.edu/projects.html>.
14. Hibbitt, Karlsson & Sorensen, Inc. *ABAQUS/CAE User's Manual* (Version 6.2). USA, 2001.
15. -----, *ABAQUS/CAE User's Manual* (Version 6.3). USA, 2002.
16. -----, *ABAQUS/Standard User's Manual* (Volume 2, Version 6.3). USA. 2002.
17. -----, *Getting Started with ABAQUS/Standard* (Interactive Version, Version 6.3). USA. 2002.
18. McConnell, Kenneth G. *Vibration Testing: Theory & Practice*. USA: John Wiley & Sons, Inc, 1995.
19. McEwan, M.I., J.R. Wright, J.E. Cooper, and A.Y.T. Leung. “A Combined Modal/Finite Element Analysis Technique for the Dynamic Response of a Non-Linear Beam to Harmonic Excitation,” *Journal of Sound and Vibration*, 234 (4), 601-624 (2001).

20. Meirovitch, Leonard. *Elements of Vibration Analysis* (Second Edition). USA: McGraw Hill, 1986.
21. “Modern Practice in Stress and Vibration Analysis,” Trans Tech Publications, Inc – Finite Element Torsional Buckling Analysis and Prediction for Plain Shafts. 27 January 2004 <http://www.ttp.net/0-87849-928-8/455.htm>.
22. National Aeronautics and Space Administration Goddard Space Flight Center. *Gas Experimenter’s Guide to the STS Safety Review Process and Data Package Preparation*. Maryland. September 1993.
23. -----, *Shuttle Small Payloads Project Office Carrier Capabilites*. Maryland. 1999.
24. National Aeronautics and Space Administration Lyndon B. Johnson Space Center. *Safety Policy and Requirements For Payloads Using the Space Transportation System*. Texas. January 1989.
25. Philley Jr., Thomas L. *Development, Fabrication, and Ground Test of an Inflatable Structure Space-Flight Experiment*. Master’s Thesis, Air Force Institute of Technology, Dayton, OH, March 2003.
26. Single, Thomas G. *Experimental Vibration Analysis of Inflatable Beams for an AFIT Space Shuttle Experiment*. Master’s Thesis, Air Force Institute of Technology, Dayton, OH, March 2002.
27. “Spartan 207 Mission,” L’Garde - Special Payloads Division, Code 740. 31 January 2004. <http://www.lgarde.com/gsfc/sp207inf.html>.
28. Thilmany, Jean. “Smooth Operator,” *Mechanical Engineering*, Vol 124/No. 7 (July 2002).

## **Vita**

Captain Raymond G. Holstein III graduated from Floyd E. Kellam High School in Virginia Beach, Virginia. He enlisted in the Air Force and served as an Intelligence Operations Specialist for the 33<sup>rd</sup> Fighter Wing at Eglin AFB, FL. Upon completing his term of enlistment, he entered undergraduate studies at Auburn University in Auburn, Alabama where he graduated with a Bachelor of Science degree in Mechanical Engineering in December 1999. He was commissioned through the Detachment 005 AFROTC at Auburn University.

His first assignment was at Wright-Patterson AFB, OH as a System Safety Engineer. In August 2002, he entered the Graduate School of Engineering and Management, Air Force Institute of Technology. Upon graduation, he will be assigned to the Directed Energy Directorate at Kirtland AFB, NM.

REPORT DOCUMENTATION PAGE				Form Approved OMB No. 074-0188	
<p>The public reporting burden for this collection of information is estimated to average 1 hour per response, including the time for reviewing instructions, searching existing data sources, gathering and maintaining the data needed, and completing and reviewing the collection of information. Send comments regarding this burden estimate or any other aspect of the collection of information, including suggestions for reducing this burden to Department of Defense, Washington Headquarters Services, Directorate for Information Operations and Reports (0704-0188), 1215 Jefferson Davis Highway, Suite 1204, Arlington, VA 22202-4302. Respondents should be aware that notwithstanding any other provision of law, no person shall be subject to a penalty for failing to comply with a collection of information if it does not display a currently valid OMB control number.</p> <p><b>PLEASE DO NOT RETURN YOUR FORM TO THE ABOVE ADDRESS.</b></p>					
1. REPORT DATE (DD-MM-YYYY) 13 03 04		2. REPORT TYPE Master's Thesis		3. DATES COVERED (From – To) 9 SEPT 03 – 23 MAR 04	
4. TITLE AND SUBTITLE  STRUCTURAL DESIGN AND ANALYSIS OF A RIGIDIZABLE SPACE SHUTTLE EXPERIMENT				5a. CONTRACT NUMBER	
				5b. GRANT NUMBER	
				5c. PROGRAM ELEMENT NUMBER	
6. AUTHOR(S)  Holstein, Raymond G.III, Captain, USAF				5d. PROJECT NUMBER	
				5e. TASK NUMBER	
				5f. WORK UNIT NUMBER	
7. PERFORMING ORGANIZATION NAMES(S) AND ADDRESS(S) Air Force Institute of Technology Graduate School of Engineering and Management (AFIT/EN) 2950 Hobson Way WPAFB OH 45433-7765				8. PERFORMING ORGANIZATION REPORT NUMBER  AFIT/GAE/ENY/04-M08	
9. SPONSORING/MONITORING AGENCY NAME(S) AND ADDRESS(ES) IMINT/RNTS Attn: Maj. Dave Lee 14675 Lee Road Chantilly, VA 20151 DSN: 898-3084				10. SPONSOR/MONITOR'S ACRONYM(S)	
				11. SPONSOR/MONITOR'S REPORT NUMBER(S)	
12. DISTRIBUTION/AVAILABILITY STATEMENT APPROVED FOR PUBLIC RELEASE; DISTRIBUTION UNLIMITED.					
13. SUPPLEMENTARY NOTES					
14. ABSTRACT <p>AFIT is in the process of designing a Space Shuttle experiment designated as the Rigidized Inflatable Get-Away-Special Experiment (RIGEX) to study the effects of microgravity on the deployment of rigidizable composite structures. Once in space, the experiment will inflate and rigidize three composite structures and perform a vibration analysis on each by exciting the tubes using piezoelectric patches and collecting data via an accelerometer.</p> <p>This paper presents the structural and vibration analysis of the RIGEX assembly and inflatable composite tubes using ABAQUS Finite Element Analysis (FEA) software. Comparison of the analysis has been carried out with Eigenvalue/Eigenvector experimentation by means of ping testing. This FEA analysis has been used to verify the natural frequency and structural integrity of the RIGEX support assemblies. The ABAQUS FEA results correlated to within 20% of experimental values.</p>					
15. SUBJECT TERMS RIGEX, GAS, Inflatable Structure, ABAQUS, Finite Element Analysis					
16. SECURITY CLASSIFICATION OF:			17. LIMITATION OF ABSTRACT  UU	18. NUMBER OF PAGES 124	19a. NAME OF RESPONSIBLE PERSON ANTHONY N. PALAZOTTO
REPORT U	ABSTRACT U	c. THIS PAGE U			19b. TELEPHONE NUMBER (Include area code) (937) 255-6565, e-mail: ANTHONY.PALAZOTTO@afit.edu